Control system response for seed placement accuracy on row crop planters

by

Sylvester Alfredo Badua

B.S., Central Luzon State University, 2008
M.S., Central Luzon State University, 2011

AN ABSTRACT OF A DISSERTATION

submitted in partial fulfillment of the requirements for the degree

DOCTOR OF PHILOSOPHY

Department of Biological and Agricultural Engineering
College of Engineering

KANSAS STATE UNIVERSITY
Manhattan, Kansas

2020

Abstract

Planting is one of the most critical field operations that can highly influence early season vigor, final plant density and ultimately potential crop yield. It is the opportunity to place seeds at a uniform depth and spacing providing them the ideal environment for proper growth and development. However, inherent field spatial variability could influence seed placement and requires proper implementation of planter settings to prevent shallow seeding depth, sidewall compaction and uneven spacing. The overall goal of this research is to evaluate the response of the planter and crop to downforce control system implementation across a wide range of machine and field operating conditions. Planting operations were performed in corn production fields using a Horsch row-crop planter with 12 row units equipped with a hydraulic downforce system capable of implementing fixed and active downforce settings. A custom-made data acquisition system was developed to record sensor data at 10 Hz sampling frequency.

From this study, the following conclusions were drawn. First, soil texture and soil compaction due to tractor tires influenced real-time gauge wheel load (GWL). Implementing a fixed downforce setting with target GWL set at 35 kg showed that 25% of the total planting time GWL was less than 0 suggesting areas planted with uncertain seeding depth due to potential loss of ground contact of the gauge wheels. Likewise, fewer row units per section could provide lower variability in GWL indicating the need for an automatic section control to maintain target GWL within an acceptable range for all row units. Second, implementing an active downforce setting showed no significant difference between downforce A (63 kg) and downforce B (100 kg) on plant spacing, although downforce setting B resulted to higher plant spacing accuracy. Higher variability in spacing

was observed when ground speed is over 12 kph. To achieve desired seeding depth, downforce greater than 100 kg is needed when ground speed is over 7.2 kph on no-till field and when ground speed is over 12 kph on strip-tilled field. Third, response of row units segregated in sections revealed that row unit acceleration on wing, track and non-track sections increases with speed. Strip-tilled soil exhibited lower row unit acceleration by 18% compared to no-till soil. Finally, a proof-of-concept sensing and measurement (SAM) system was developed to calculate seed spacing, depth and geo-location of corn. This system could provide real-time feedback on seed spacing and depth allowing appropriate downforce control system management for more consistent seed placement during planting.

In summary, advances in planter technology paved the way for the addition of more row units across on the planter to increase planting productivity. With increasing width of planter toolbar, each row unit may need different downforce control to varying field and machine operating conditions. Appropriate downforce control management should be implemented to compensate for increased dynamics of planter row units across a highly variable field conditions to achieve the desired seed placement accuracy.

Control system response for seed placement accuracy on row crop planters

by

Sylvester Alfredo Badua

B.S., Central Luzon State University, 2008
M.S., Central Luzon State University, 2011

A DISSERTATION

submitted in partial fulfillment of the requirements for the degree

DOCTOR OF PHILOSOPHY

Department of Biological and Agricultural Engineering
College of Engineering

KANSAS STATE UNIVERSITY
Manhattan, Kansas

2020

Approved by:
Major Professor
Ajay Sharda

Copyright

Abstract

Planting is one of the most critical field operation that can highly influence early season vigor, final plant density and ultimately potential crop yield. It is the opportunity to place seeds at a uniform depth and spacing providing them the ideal environment for proper growth and development. However, inherent field spatial variability could influence seed placement and requires proper implementation of planter settings to prevent shallow seeding depth, sidewall compaction and uneven spacing. The overall goal of this research is to evaluate the response of the planter and crop to downforce control system implementation across a wide range of machine and field operating conditions. Planting operations were performed in corn production fields using a Horsch row-crop planter with 12 row units equipped with a hydraulic downforce system capable of implementing fixed and active downforce settings. A custom made data acquisition system was developed to record sensor data at 10 Hz sampling frequency.

From this study, the following conclusions were drawn. First, soil texture and soil compaction due to tractor tires influenced real-time gauge wheel load (GWL). Implementing a fixed downforce setting with target GWL set at 35 kg showed that 25% of the total planting time GWL was less than 0 suggesting areas planted with uncertain seeding depth due to potential loss of ground contact of the gauge wheels. Likewise, fewer row units per section could provide lower variability in GWL indicating the need for an automatic section control to maintain target GWL within an acceptable range for all row units. Second, implementing an active downforce setting showed no significant difference between downforce A (63 kg) and downforce B (100 kg) on plant spacing, although downforce setting B resulted to higher plant spacing accuracy. Higher variability in spacing

was observed when ground speed is over 12 kph. To achieve desired seeding depth, downforce greater than 100 kg is needed when ground speed is over 7.2 kph on no-till field and when ground speed is over 12 kph on strip-tilled field. Third, response of row units segregated in sections revealed that row unit acceleration on wing, track and non-track sections increases with speed. Strip-tilled soil exhibited lower row unit acceleration by 18% compared to no-till soil. Finally, a proof-of-concept sensing and measurement (SAM) system was developed to calculate seed spacing, depth and geo-location of corn. This system could provide real-time feedback on seed spacing and depth allowing appropriate downforce control system management for more consistent seed placement during planting.

In summary, advances in planter technology paved the way for the addition of more row units across on the planter to increase planting productivity. With increasing width of planter toolbar, each row unit may need different downforce control to varying field and machine operating conditions. Appropriate downforce control management should be implemented to compensate for increased dynamics of planter row units across a highly variable field conditions to achieve the desired seed placement accuracy.

Table of Contents

List of Figures

List of Tables

Acknowledgements

I would like to express my deepest gratitude to my major professor, Dr. Ajay Sharda, for giving me the opportunity to pursue my doctoral degree. His time, guidance, support and mentorship allowed me to accomplish this monumental undertaking. Likewise, great appreciation is extended to the members of my supervisory committee - Dr. Ignacio Ciampitti, Dr. Daniel Flippo and Dr. Christopher Vahl, for their time and valuable suggestions in my research and other scholarly endeavors. Sincere appreciation also goes to Dr. C.B. Rajashekar for serving as chairperson of my examining committee.

I am also grateful to Jonathan Zeller for his help and assistance during field tests and laboratory activities. Likewise, to the machinery systems research group - Jonathan, Manoj, Prashanta, Ketan, Braden and Amar; to the Biological and Agricultural Engineering-Graduate Student Association (BAE-GSO) - Chetan, Ameneh, Mingqiang, Hasib, Ali, Devon, Jessica and Demilade; to the Philippine Student Association (PhilSA) - Tita Beth and family, Rachel, Amy, Rañia, Roselle, Xyza, Pong, Jared, and Tisha and family; to the International Coordinating Council (ICC) - Ruth, Eric, Theodora, Kehinde, Priyanka, Tahmineh, Lavania, Yash and Alexis; to Terry and Robbin Cole and family, and Bob and Mary and family of Helping International Students (HIS), thank you all for the friendship which made graduate school a lot more meaningful and enjoyable experience.

Profound thanks to Dr. Joseph Harner, Dr. Naiqian Zhang, Arlene Jacobson, Jamie Boeckman and other faculty and staff members in the Department of Biological and Agricultural Engineering for all their unwavering support.

Additionally, I want to acknowledge the scholarship and financial support of the Philippines' Department of Science and Technology - Engineering Research and Development for Technology (DOST-ERDT) and Central Luzon State University (CLSU).

Most importantly, I am deeply grateful to the love and support of my family. Above all, I want to thank God for with Him all things are possible.

Dedication

I dedicate this work to

my son King Luke Aizer and daughter Queen Lyza Athena,

spouse Glaiza Marie,

siblings Mark Anthony and Mariannie,

my parents Marietta and Antonio.

Chapter 1 - Introduction

1.1 Background

Agriculture and its allied industry is one of the largest sectors that fuels the economy of the United States with farming contributing to over $1.053 trillion to the gross domestic product in 2017 (USDA-ERS, 2019b). Of the 315 million acres for cropland, over 89.9 million acres were planted with corn making it the primary produced feed grain in the US (USDA-ERS, 2017a). Corn is processed into a wide variety of food and industrial products including starch, sweeteners, corn oil, beverage and industrial alcohol, and fuel ethanol (Figure 1.1).

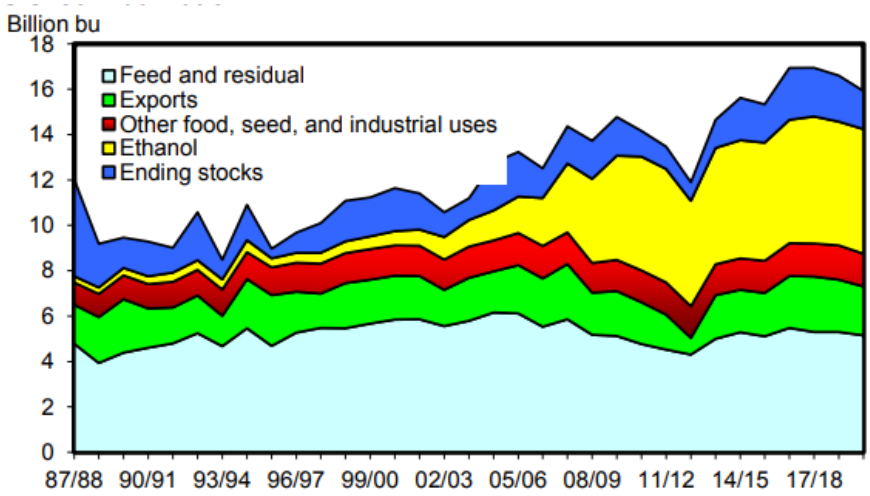

Figure 1.1. Industrial uses of domestically produced corn in the US (USDA-ERS, 2019a).

Corn supply for use in various applications have been declining since 2015 with usage showing a consistent increasing trend in decades (Figure 1.2) presenting the need to improve current level of production efficiently to sustain the demand for this highly valuable commodity.

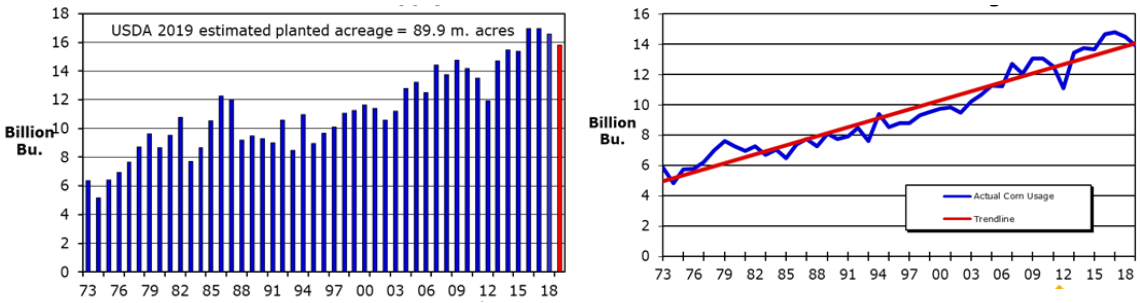

Figure 1.2. U.S. corn supply (a) and usage (b) (USDA-WASDE, 2019).

In 2019, farmers produced 13.7 billion bushels spending over $61 billion in production costs. Nearly 30% of the total operating cost accounts for seeds which is the second most expensive input next to fertilizer. Thus, seeds not properly utilized or singulated during planting could result in two scenarios; 1) growers tend to plant more than what is needed and 2) total plant population is compromised affecting yield at the end of the season; both of which can potentially reduce income of growers.

With increasing global demand for feed, fuel, and food, further research is needed to develop efficient crop production practices and optimize advanced agricultural machinery technologies providing growers the strategies to cut costs in order to sustain or further improve farming productivity and profitability without adding much to inputs.

1.2 Row-crop planter

The technological advancement of mechanical row crop planters have been remarkable since the humble beginning of the first John Deere planters in the late 18th century (Mowitz, 2018). Over the years, the size of planters have dramatically increased and numerous technologies have been developed to continuously improve planter operational performance in the field.

A row crop planter is an implement typically towed behind a tractor connected through the drawbar or the three-point hitch. Planter size is characterized by the number of row units mounted across the toolbar which usually varies from 4 to 54 row units (Figure 1.3) with row spacing ranging from 20, 22, 30 inches.

a **b**

Figure 1.3. Size of row crop planter from (a) 4 row units to (b) 54 row units (Photo courtesy of deere.com)

The primary goal of row crop planter is to place individual seeds along rows precisely at the desired spacing and depth. The row unit of a row crop planter consists of four major systems or mechanisms to accomplish the planting process.

1. Metering system

Metering the seed is one of the most crucial component of a planter. Seeds must be singulated consistently at equal spacing based on the desired seeding rate. Typical metering systems are finger pickup type or vacuum meter (Figure 1.4). Finger-pickup meters are capable of metering individual seeds of various shapes and sizes without changing the seed plate. Seed is trapped between the finger or cup and stationary plate as fingers rotates inside the metering assembly. Spring tension holds the seed securely until it reaches a discharge hole where is dropped into the seed delivery system. In vacuum meters, this system uses different seed plates depending on the crop but metering seed is more accurate than finger-pick up meters. A partial vacuum keeps the seeds secure in the holes

or slots of the metering disk. As the metering disk reaches the discharge hole, a seed extractor interrupts the vacuum allowing the seeds to fall into the seed delivery system.

a **b**

Figure 1.4. Two types of seed metering system. The vacuum (a) and finger pickup (b) (Photo courtesy of Kinze.com)

2. Seed delivery system

As the seed plate or metering disk rotates, it picks up one seed and discharges it into a hole passing through a seed delivery system where it guides the seed into the furrow. The purpose of this system is to deposit the seeds on the bottom of the trench translating the accuracy of the seed metering system to accurate seed placement (Murray et al., 2006). Two common types of delivery systems for a typical row crop planter are gravity type seed tube (Figure 1.5a) and seed conveyor belt system (Figure 1.5b). In a gravity type system, seeds fall straight into the seed tube to the ground. Seed bounce off the wall of the seed tube before dropping into the ground could potentially affect seed spacing especially if planting rough terrains at high ground speeds. The other type of seed delivery system is the seed conveyor belt system (Figure 1.5b). It was developed as an improvement to the gravity type system where it uses a brush or paddles attached to a conveyor to carry seeds after it exits the seed metering system. The conveyor carries the seed at equal intervals and discharge the seed to the trench once it reaches the opposite end of the conveyor.

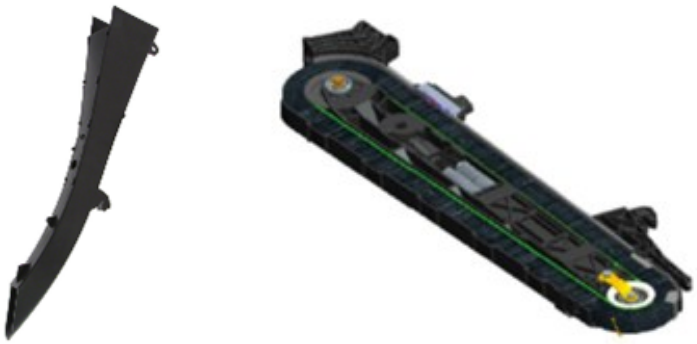

a **b**

Figure 1.5. Gravity type (a) and the seed conveyor belt type (b) seed tubes.

3. Furrow opener and depth control system

Seeds need to be placed at a depth where there is enough moisture to achieve proper emergence. The opening disks are responsible for creating a V-shaped furrow while the gauge wheel controls the seeding depth (Figure 1.6). Planters are equipped with mechanism to change the seeding depth which depends on actual field conditions at planting. Sometimes, a furrow cleaner is used to remove residues, weeds and other debris on the soil surface ahead of the opening disks.

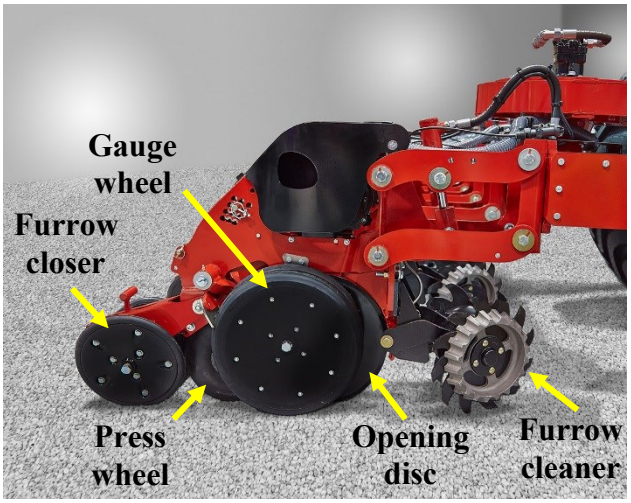

Figure 1.6. Basic components of a planter row unit

4. Furrow and seed covering system

Proper germination and emergence require good seed-to-soil contact. After seed is placed in the furrow, a seed covering device is used to provide the needed seed-to-soil contact by covering the planted seed with soil. The furrow closer or closing wheels (Figure 1.6) are designed to close the furrow and firm the soil removing air pockets around the seed providing ideal seed germination conditions. In addition, some planters use press wheels (Figure 1.6) to prevent seeds from bouncing around the furrow upon exiting the seed tube by gently pressing each seed into the bottom of the trench.

1.2.1 Downforce control system

Row crop planter must place all seeds nearly at the same depth and equal spacing along the rows. To achieve this, the opening discs uses the weight of the row unit to penetrate the soil creating a seed furrow at the right depth. The gauge wheels controls the furrow depth as it prevents the opening discs from getting any deeper. Excess weight acting on the gauge wheel as it rests on the ground surface is called the gauge wheel load (GWL). Due to varying soil resistance on the opening discs across the field, weight of the row unit could be inadequate which could result to the gauge wheels losing ground contact leading to shallow seeding depths. Manufacturers equipped row crop planters with mechanism to apply additional load on each row unit to achieve a furrow with the desired seeding depth and able to maintain this depth consistently across a field with varying soil compaction, soil type, and residue. This additional load together with the dead weight of the row unit is called row unit downforce.

Downforce can be applied using three systems: mechanical, pneumatic and hydraulic.

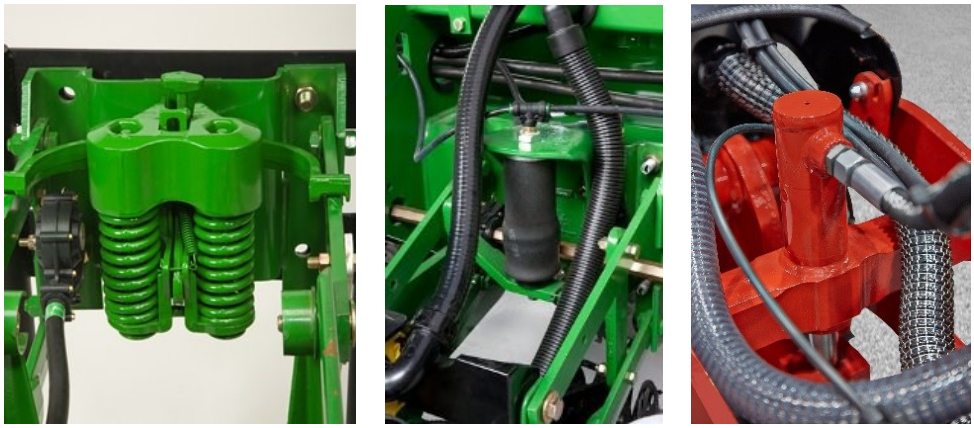

a b c

Figure 1.7. Planter downforce systems (a) Mechanical (b) pneumatic and (c) hydraulic (Photo courtesy of deere.com).

.

1. *Mechanical system*

This system (Figure 1.7a) uses springs to provide the additional load for proper functioning of the planter's key components. Load is adjusted by manually selecting a notch on the row unit using a lever where each notch corresponds to a certain amount of additional downforce with very few increments (0, 150, 250, 350 lbs). However, row unit downforce can greatly vary (F = kS, Hookes law) with this system as springs quickly react (compress or elongate) to varying terrain when planting resulting to significant change in load applied on row units.

2. *Pneumatic system*

This system (Figure 1.7b) uses rubber airbags using compressor to fill it with air when needed to keep downforce as uniform as possible as the planter travels across the field. This system is more convenient as downforce adjustment can be made by the operator inside the cab. Also, airbag system can provide more consistent downforce as you can select anywhere within the range of row unit additional downforce (0 to 400 lbs) compared to mechanical downforce systems. Gauge wheel sensors provides feedback on row unit downforce which can be used to adjust

downforce while planting. However, this system is not very responsive to quick changes it takes time to reach the desired pressure on the airbags.

3. *Hydraulic system*

Hydraulic system provides faster reaction time to changing row unit downforce requirement compared to pneumatic systems (Shearer & Pitla, 2014). This system (Figure 1.7c) uses hydraulic cylinders to apply additional downforce on the row units as necessary. Before planting, a target gauge wheel load is selected which is deemed to be enough for the planter to maintain the desired seeding depth during planting. The system will maintain this value to achieve the desired soil penetration and consistent planting depth without compacting the soil. A gauge wheel sensor provides feedback on the gauge wheel load which determines if downforce needs to be adjusted. This system is advantageous especially in fields with varying conditions (tillage, soil texture, terrain, residue, etc) requiring instantaneous response time to the constantly changing field conditions.

1.2.2 Automatic section control

Row crop planters can be equipped with automatic control section technology to improve planting efficiency by reducing production cost and improve productivity. Utilizing the global positioning system equipped on the planter together with coverage maps, automatic control section will allow row crop planters to prevent over planting by controlling individual row units or row units in section during planting operations. Typically, field boundaries are planted first then the rest of the field. During planting operators would manually turn on and off the row units across the full width of the planter as it approaches a planted or to be planted areas. At some point, one end of the planter will

begin to overlap with the end rows. Turning off the row units could result in skipped (not planted) areas while allowing the full width of the planter to meet end row before shutting off the row units could result in double planted areas (Figure 1.8a). Minimizing overlapping areas would be difficult especially when avoiding skipped areas during point-row planting. Likewise, planting on irregularly shaped fields, turning on headland and avoiding obstructions could also increase swath overlap (Velandia et al., 2013). Automatic section control technology works by automatically shutting off the sections or rows of the planter in areas of the field that had been previously planted (Fulton et al., 2011) and turns those individual planter sections or rows back on automatically when areas needed to be planted are approached (Figure 1.8b). This system could significantly reduce overlap saving costs on seeds (Fulton et al., 2011) and improves yield due to decrease in double planted or skipped areas (Velandia et al., 2013).

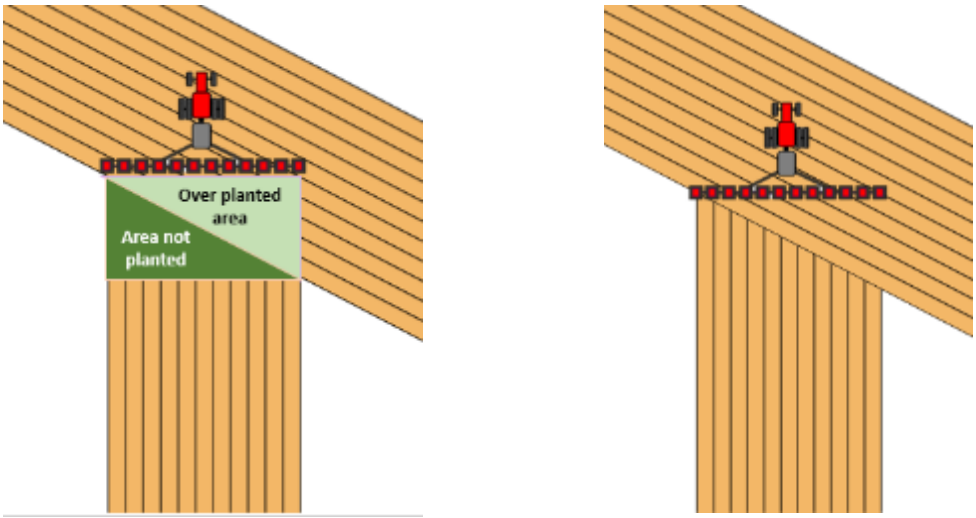

a **b**

Figure 1.8. Manual swath control (a) resulting to areas not planted or over/double planted areas. Automatic section control (b) of individual rows automatically shutting off row units as it reaches planted area minimizing not planted (skipped) and over planted areas.

Figure 1.9. The effect of automatic section control in reducing overlap

1.3 Problem Statement

Planting is one of the significant stage in crop production that highly influence potential yield. Accurate and consistent seed placement requires advanced precision technologies that is capable of sustaining these desired planting parameters under a highly dynamic field operating condition. In 2018, the global precision agriculture industry was worth $5.4 billion and projected to reach $11.3 billion in 2024 (IMARC, 2019). Precision agriculture technologies refers to guidance systems of farm various farm equipment using global positioning system (GPS), geo-referenced soil and yield maps and variable rate input systems (USDA-ERS, 2016) which aims to maximize food production, reduce production cost and minimize the effects of over application of inputs. The utilization of precision planters provides operators real-time feedback and allow them to make adjustment on-the-go which corresponds to the scale of spatial variability present in the field during planting operations. Hence, operators are capable of managing strategies allowing them to place the seeds at the right place and at the right time. Planting at the right time involves observing the recommended planting dates to prevent potential yield loss due to delayed planting.

The effect of delayed planting on potential yield can be influenced by shortened growing season increasing the occurrence of insect and disease infestation and undesirable weather conditions during pollination (Nielsen, 2019). Planting window in Kansas ranges from late March in southeastern counties to mid-May in the northwest (Roozeboom et al., 2007). However, with weather uncertainty there will be occasions where excessive moisture mostly due to rains could potentially reduce the days suitable for planting. This situation may lead growers to perform planting operations outside the optimal planting window. Previous studies have shown that late planting could potentially reduce yield (Licht et al, 2019 & Nielsen, 2019). Timely completion of planting may also require management strategy of producers as the average farming size on U.S. farms has been increasing (USDA-NASS, 2014). Such strategy may include increasing the planting speed to get more acres covered per day within the available days of the ideal planting dates. However, faster planting speed could result in uneven seeding depth and seed placement especially when field always vary in terms of soil texture, moisture, crop residues and terrain. Several studies have shown that uniformity of plant spacing and emergence are influenced by speed eventually affecting potential yield of corn. Liu et al. (2004) reported a reduction in yield by 4.7 bu/acre whenever the time to 50% emergence was delayed beyond 3 days and 0.6 bu/acre yield loss for every centimeter of standard deviation from the target plant spacing. The poor depth control of the seeder at faster planting speed might have caused the delay in emergence and variability in spacing (Liu et al., 2004). Studies conducted in Kansas reported a yield reduction of 2.4 bu/acre for every unit increase in planting speed ranging from 4.5 mph to 7.0 mph which can be attributed to non-uniformity in spacing. The study suggested a decrease in seed placement accuracy with increasing speed and suggests that

variability in spacing might be related to seed bounce in the trench due to planter unit vibration (Staggenborg et al., 2004). Likewise, non-uniform seeding depth have shown to result in poor crop emergence which resulted in reduced grain yield (Cox & Cherney, 2015).

Modern precision or row crop planters are capable of maintaining target seeding depth and spacing across varying field conditions by controlling downforce (Figure 1.10). The magnitude of additional load varies on every field and determined during actual planting operations and field conditions.

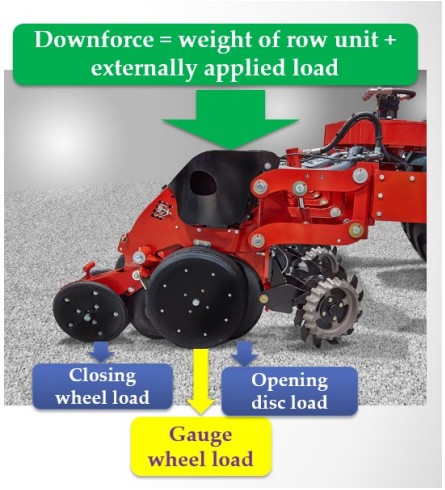

Figure 1.10. Load distribution of the row unit downforce during planting.

Excessive application of downforce could compact the soil potentially affecting germination and crop development while not enough downforce could result to lose of ground contact of the gauge wheels leading to uncertain seeding depth. In a typical field, spatial variability like soil texture, moisture, crop residues and terrain could influence the levels of downforce to maintain the desired seeding depth. Therefore, two key planter performance parameters that can highly influence corn stand establishment and yield are GWL and planting speed. The GWL and planting speed determines quality of crop stand

such as desired seed density, uniform emergence and planting depth. No single parameter is responsible for differences among fields in terms of final stand establishment rather often a combination of factors during the planting operation (Lauer & Rankin, 2004). The objective of this research is to optimize the downforce control system on row crop planters for accurate seed placement across wide range of field spatial variability during planting operations.

1.4. Research objectives

This research includes the following specific objectives:

1. Understand downforce variability across a typical field during planting.
2. Quantify the effect of downforce setting and planting speed on seed placement uniformity.
3. Evaluate the response of row units on wing, track and non-track sections implementing an automatic downforce control system.
4. Develop a system to automatically measure real-time seed placement and localization of corn.

Chapter 2 - Real-time gauge wheel load variability of a row-crop planter during field operation[1]

2.1 Abstract

Planter downforce control allows row units to maintain a target gauge wheel load (GWL) across a range of soil resistance within a field. Downforce control is typically set for a target seed depth and can be implemented either as fixed or by automatic or active control to attain the desired GWL. Recent advances allow for the control of individual row units into sections for improved GWL application. However, little knowledge exists on the spatial variability of GWL, row-to-row GWL variability, and on the recommended GWL control requirements on planters operating in actual field conditions. Therefore, the objectives of this study were to 1) quantify real-time GWL variability across individual row units within a 12-row crop planter programmed to implement a constant downforce control during field operations; 2) evaluate gauge wheel load range (GWLR) across individual row unit and within 2-, 3- or 4-row control sections to determine the optimal downforce control section size; and 3) assess the impact of soil texture and soil compaction due to tire tracks on GWL variability. To address these, a 12-row crop planter equipped with hydraulic downforce control was utilized to plant three fields. The planter was set to plant corn at 5.2 cm and 5.7 cm depths with fixed target GWL set at 35 ± 23 kg (12-57 kg) and GWLR set at 0 to 90 kg. A data acquisition system collected real-time GPS, planting speed, GWL, hydraulic pressure, and planter toolbar height data at 10 Hz. Real-time GWL data of individual row units were analyzed to determine the GWL distribution within or outside the set target GWL. Moreover, GWLR was measured in individual row units and across varying control section sizes. Soil electrical conductivity (EC) was measured using

a Veris Mobile Sensor Platform. Soil EC was used in defining zones of low, medium and high textured soil. Results show that GWL was within the target range of 12 to 57 kg at 33% of the total planting time across the three fields and GWLR within 0 to 45 kg at 9% of the total planting time. Results also indicate that a 2-, 3- and 4- row control section could provide GWLR within 0 to 45 kg at 76%, 46% and 28% of the total planting time, respectively. These findings suggest the need for automatic downforce system with lesser number of row units per control section to maintain target GWL within an acceptable range for all row units. Regression analyses indicate that soil texture is a significant variable that can influence real-time GWL. Furthermore, compacted soil due to tractor tires contributed towards significantly lower GWL. Our data suggest the need for an active downforce control to achieve improved GWL uniformity under varying field-operating conditions.

[1] Results have been published as a peer-review paper. Badua, S.A., Sharda, A., Flippo, D., & Ciampitti, I.A. (2018). Real-time gauge wheel load variability of a row-crop planter during field operation. *Trans. of the ASABE*, 61(5), 1517-1527. doi: 10.13031/trans.12511

2.2 Introduction

Seeding depth consistency and crop performance early in the growing season such as crop emergence rate and plant density are key parameters determining seeding performance of planters (Doan et al., 2005) and corn final yields (Assefa et al., 2016). Uneven seedling emergence can be attributed to non-uniform planting depth and varying field conditions such as distribution of crop residue in no-tillage systems, seedbed conditions and seed vigor (Andrade & Abbate, 2005). Studies have shown the importance of planting at optimum depth where planting beyond the threshold depth could result in non-uniform plant emergence (Özmerzi et al., 2002). Da Silva et al. (2004) showed that planting depth was one of the main factors underlying the emergence and vegetative development of corn. Achieving the desired final stand is essential for optimum yields (Grassbaugh & Bennett, 1998). Deep planting could result in decreased emergence and poor crop development (E. Nafziger, 2009), resulting in a 6 to 22% decrease in yield (Carter et al., 2019). Similarly, shallow planting may cause poor root growth or no germination at all.

Planting systems use downforce to provide the necessary row unit load for proper functioning of the planter's key components. Downforce is the total amount of load carried by the row unit which consists of 1) the weight of the row unit and, 2) externally applied load or forces. During planting, downforce is distributed among the four key components of the planter: opening discs, gauge wheels, closing wheels and row cleaners or coulters. Closing wheels and row cleaners absorb a relatively small portion of downforce, and this amount stays relatively constant. Majority of the downforce is shared between the opening discs which requires a certain amount of load to create a furrow at the desired depth for

seeding and the gauge wheels to maintain the seeding depth. During planting operations, the opening disc load requirement will vary significantly due to variability in actual field conditions such as variation in soil texture, moisture, surface residue, topography, terrain, ground speed, soil compaction from farm machinery movement, and the design of the furrow opening discs. With a fixed downforce applied for instance, planting on light textured soil requires less load on opening discs to create a furrow at the desired depth and more load will be carried by the gauge wheel. The load on the gauge wheel is called the gauge wheel load (GWL) and keeps the gauge wheel in contact with the ground ensuring desired depth is maintained during planting. On the other hand, creating a furrow on heavier textured soil requires more load on the soil opening discs thus reducing the amount of GWL. At some point, the opening discs may require additional load more than the available GWL and this situation may cause the gauge wheel to lose ground contact which could result in a shallow planting. The solution is to increase the amount of additional load applied on the row unit or sometimes referred to as the "margin" for the opening disc to reach the desired depth and to keep the gauge wheel firmly on the ground. However, applying too much load could cause deeper seeding depth as well as side wall compaction (Hanna et al., 2010) which can lead to poor root development (Raper & Kirby, 2006). Therefore, it is important to select the appropriate level of GWL that will allow the opening discs to have additional load available that it can utilize in any proportion without compromising seed depth and not causing side wall compaction.

The ability of soil to conduct electric current is measured by its electrical conductivity (EC) and typically reported in milliSiemens per meter (mS/m). An electrical current may be conducted through soil via 1) soil solution of water and ions within a web

of pores, 2) cations attached to the surfaces of clay particles, and 3) soil particles connected to each other. Research has shown that in most fields, higher EC values are correlated to higher clay and organic matter contents than lower EC zones (Farahani et al., 2011) thus electro-conductivity has a strong correlation to soil particle size and texture (Wiatrak, et al., 2009, Grisso et al.,2009; and Lund et al., 1999) and also with salinity (Denning et al., 2011). Therefore, spatial soil EC data could be utilized to differentiate soil texture within the field. A soil with higher soil EC would require a greater force applied by the opening discs to open the seed trench which would reduce the load (or force) on the gauge wheels and vice versa.

Finding an optimum down force can be difficult because planting conditions vary across the field (Sharda et al., 2017). Due to field and soil variability, row units may even require to be controlled separately of each other to achieve uniform planting depths (Buchholz et al., 1993). In general, controlling downforce on planters can be implemented either by individual row unit or by control-sections comprising of multiple row units using tension springs, airbags, or hydraulic cylinders. Generally, soil contact pressure of gauge wheels is increased by increasing down spring tension through parallel linkages which attach the planter row units to the toolbar frame (H Mark Hanna, n.d.). Newer planter technology utilizes hydraulic cylinder or pneumatic actuators to regulate the transfer of weight to row units (H Mark Hanna, n.d.) for proper soil contact of the gauge wheels. Proper planter downforce control mechanisms play an important role in preventing soil compaction and achieving uniform seeding depth. Past research had shown that draft requirements for opening discs was higher for heavier- compared to lighter-soils (Collins & Fowler, 1993). Varying field conditions require optimum down force management for

achieving uniform seeding depth. However, limited published recommendations for effective utilization of commercially available technologies and equipment in dealing with spatial GWL variability prevents producers to determine the appropriate system in managing GWL variability within a typical field during planting operations. Therefore, this study was designed with the objective to 1) quantify real-time GWL variability across individual row units within a 12-row crop planter programmed to implement a constant downforce control during field operations; 2) evaluate gauge wheel load range (GWLR) across individual row units and within 2-, 3- or 4-row control sections to determine the optimal downforce control section size; and 3) assess the impact of soil texture and soil compaction due to tire tracks on GWL variability.

2.3 Materials and Methods

Field tests were conducted using a 12-row Horsch Maestro 12 30 SW (Horsch Maschinen GmbH, Schwandorf, Germany) row-crop planter with variable-rate seeding and automatic section control technology. The planter was programmed to implement automatic section control for seed drop by shutting individual row motors (BG 45x15 SI, Dunkermotoren GmbH, Schwarzwald, Germany) on or off based on the coverage map. The planter was operated using a John Deere 8270R tractor. Planter control functionality was accomplished using a 2630 John Deere (GreenStar-3, Deere and Company, Moline, IL, U.S.A.) field computer connected to the planter electric control unit, hence forth referred to as ECU, (Horsch Maschinen GmbH, Schwandorf, Germany) through ISOBUS. The row units were spaced at 76.2 cm. The planter row units were segregated into four control sections (Figure 2.1).

Figure 2.1. Planter toolbar containing 12 row units numbered 1 through 12 from left to right along with hydraulic downforce control section. Each row unit was equipped with a gauge wheel load sensor and all sections were set at a constant hydraulic pressure for uniform downforce application.

Control sections 1 and 4 comprised three row units each on the left and right side of the planter bar. Control section 2 included four row units adjacent to following the tractor tire tracks (rows 4, 5, 8, 9). Control section 3 included the two rows (rows 6 and 7) in the middle center of the toolbar. The row units within control sections 1, 3, and 4 did not follow seed cart and tractor tire tracks, and henceforth are referred to as row units on non-tire track. The row units in section 2 followed tractor and seed cart tires, and are henceforth referred to as row units on tire track. A hydraulic pressure sensor (HDA 844L-A-0250-161, Hydac, Glendale Heights, IL, USA) was mounted to measure pressure for each control section. In order to maintain seed spacing during planter speed transitions, ECU utilized feedback from ground speed radar (Radar III, Dickey-John Corp., Auburn, IL, U.S.A.), which was sent to each row motor control module (Horsch Maschinen GmbH, Schwandorf,

Germany) to generate target motor rpm based on seed population using a planetary gearbox (PLG 42S, Dunkermotoren GmbH, Schwarzwald, Germany). The seed tube sensor on each row unit (Hy Rate Plus, Dickey-John Corp., Auburn, IL, U.S.A.) provided feedback on seed singulation, doubles and misses, to the field computer.

2.3.1 Planter set up and experimental design

Field tests were conducted with a planter equipped with hydraulic downforce control. The 4 section control system custom designed and integrated by the manufacturer was programmable to implement active or fixed downforce control. For this study, the downforce system was programmed to apply a fixed downforce by setting the system to maintain a constant hydraulic pressure. Laboratory tests were performed using a custom made downforce evaluation test stand (Strasser, 2017) to determine the amount of pressure needed to apply to achieve a certain level of GWL. The test stand suggested a pressure of 5.6 MPa to achieve a fixed GWL of 35 kg and this setting was verified at the field prior to planting. Typical planter setup recommendations from manufacturers and producer practices were studied to setup the planter for desired seed depth in the field and for assessing the target fixed downforce. The fixed downforce experiments were conducted in three locations, Field A (7 ha) located at Shannon, KS (39.470657, -96.523484), Field B (4 ha) located at Clay Center, KS (39.311761, -96.990277) and Field C (11 ha) located at Junction City, KS (39.051095, -96.847993). Fields were planted to corn at two different seeding depths based on the growers' preference. The planter depth setting was adjusted to plant at a seeding depth of 5.2 cm for Fields A and B and 5.7 cm for Field C. The planter's ECU was programmed to plant the growers' standard rate of 72,500, 74,000 and 79,000 seeds per hectare in Fields A, B and C, respectively. Planting was conducted with an

average speed of 11.3 kph and ranged from 7.2 kph to 12.0 kph. The experiments were conducted on fields adopting no-till management system for more than 10 years, varying soil type (clay-loam to sandy loam), and corn following soybeans crop rotation practice.

Previous research have utilized varying levels of gauge wheel load and downforce during field tests which ranges from 18 to 173 kg (Fulton et al., 2015 and Hanna et al., 2010). For this study, various producers and collaborators were consulted who expressed a common planter setup, and based on their qualitative feedback, the target GWL was set at 35 kg. The GWL was expected to stay within 12 to 57 kg during field operation. This ±23 kg range was selected based on previous study (Strasser, 2017) which revealed the HORSCH systems' capability to maintain the target GWL within this range 99% of the time for near uniform field conditions. Individual row unit GWL data were analyzed to quantify the percent time that GWL was 1) within the target range of 35±23 kg, 2) greater than target range, and 3) less than the target range. Additionally, all load sensor data points representing planter turning with toolbar lifted was analyzed to quantify no load response during the course of planting. The analysis would emphasize if all load sensors consistently maintained no-load response and the developed calibration curve truly represented the gauge wheel loads due to field and operating conditions. The gauge wheel load range (GWLR) represented GWL difference between the row-unit with highest and the row-unit with the lowest value at any given instance. GWLR would quantify the extent of GWL variability across the tool bar, and potentially exhibit the need for control sections for accurate control of target GWLs. A greater row-to-row GWLR variability would suggest need for row units control sections for high resolution control during dynamic field operations. The GWLR was quantified by calculating the difference for all 12 row units as

well as paired combinations of 2 adjacent rows, 3 adjacent rows and 4 adjacent rows. The 2 row combination, referred henceforth as 2-row section control option, was for row unit 1-2, 3-4, 5-6, 7-8, 9-10, and 11-12; 3 row combinations, referred hereafter as 3-row section control, was with row unit 1-2-3, 4-5-6, 7-8-9, and 10-11-12; and 4 row combinations, referred henceforth as 4-row section control option, was for row units 1-2-3-4, 5-6-7-8, and 9-10-11-12. The average GWLR within each section for the different section control scenarios for each of the three fields was compared to evaluate appropriate number of rows for section control with least GWLR. The section control with least GWLR would indicate downforce control required to achieve as uniform as possible GWL across all row units within the controlled section. The average GWL and GWLR from all rows were mapped using ArcMap 10.3 (ESRI, Redlands, CA, U.S.A.).

Spatial analysis was conducted in ArcGIS 10.3 (ESRI, Redlands, CA, U.S.A.) by using reclassification; conversion; and clip toolsets in Arc Map 10.3 to extract the data points that falls within each soil texture (soil EC) class for all the fields. Each data point that were extracted from each soil texture class were considered as replicate and were used to calculate the average GWL for each soil EC class. Finally, average GWL for row units on non-tire tracks (control section 1, 3 and 4) and tire tracks (control section 2) were computed for each field. Statistical analysis were performed in SAS University Edition 2016 (SAS Institute Inc., Cary, NC, USA). Multiple regression analysis between soil EC and GWL was performed using the proc reg procedure to determine if soil EC is a significant variable that can influence real time GWL. Analysis for significant differences between means of average GWL and soil EC; and average GWL and tire and non-tire tracks were performed using the proc mixed procedure and lsmeans statement.. Effects were

considered statistically significant at the 0.05 level of probability unless otherwise indicated.

2.3.2 Data acquisition system

The planter row units were factory installed with load sensors (Model 6784, Horsch Maschinen GmbH, Schwandorf, Germany) on each of the 12 row units to measure GWL (Figure 2.2).

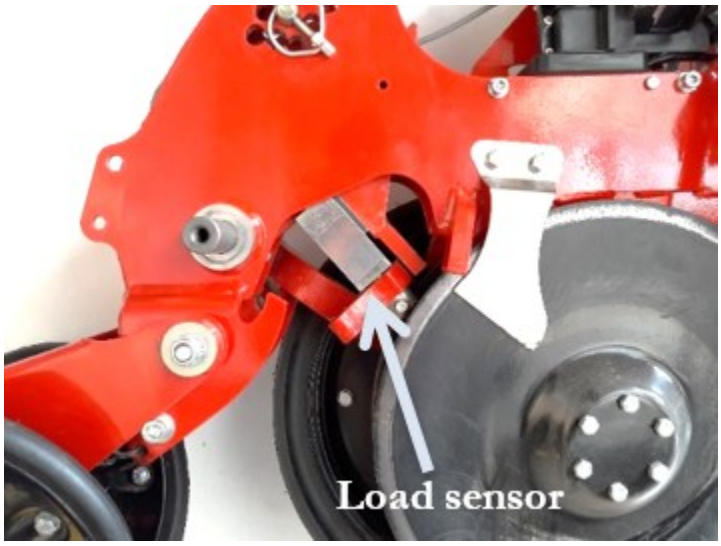

Figure 2.2. Load sensor mounted on the cam assembly placed across the gauge wheel arms.

The designed measurement range of load sensors was up to 9,806 N with a linear response on the scale of 4-20 mA. The load sensors were calibrated in the laboratory using known weights to record sensor signal versus force (kg). A regression line was fitted to sensor signal versus force sensor data to convert the real-time load sensor signal to force representing GWL (Figure 2.3). To measure the applied hydraulic oil pressure, one pressure transducer was installed on each of the four control sections. Since each control section used a hydraulic block and applied equal pressure on all row units within that control section, one pressure transducer was considered enough for each control section.

For control sections 1, 3 and 4, a pressure transducer with a 25 Mpa measurement range (HDA 844L-A-0250-161, Hydac, Glendale Heights, IL, USA) with a linear response on the scale of 4-20 mA was installed; while section 2 was fitted with a transducer with a measurement range of up to 52 MPa (Model KM41, Ashcroft Inc., Stratford, CT, USA) with a linear response on the scale 0.5-4.5 Vdc. Planting speed and position data were collected simultaneously using a sub-inch accuracy GPS unit (GR5, Topcon Positioning Systems, Inc., Livermore, CA, USA).

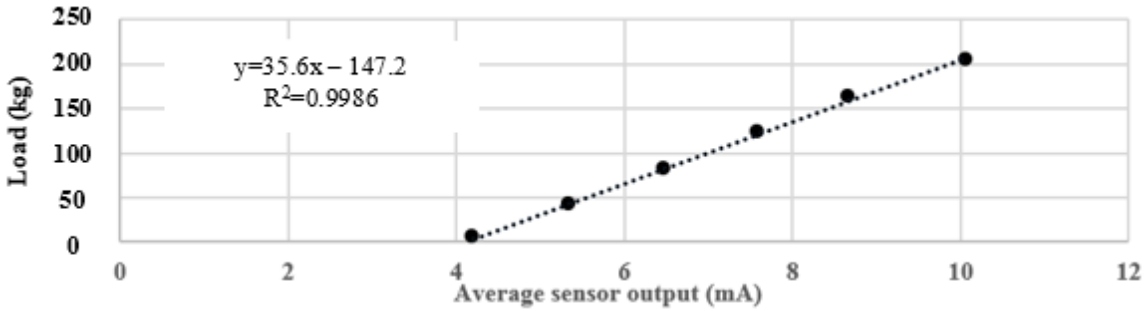

Figure 2.3. Regression line fitted between known loads versus gauge wheel load (GWL) sensor output.

The planter is equipped with hydraulic cylinders on the seed cart that are used to raise and lower the planter toolbar. A potentiometer (Model 424A11A090B, Elabou sensor Technology Inc., Waukegan, IL, USA), with a linear response on the scale of 4-20 mA, was mounted on seed cart axle to monitor relative position of planter toolbar (Figure 2.4) with respect to axle of the seed cart. Potentiometer was initially calibrated to ensure output will represent raised and planting position of toolbar. Planter toolbar height and sensor output from 4 mA to 20 mA at 1 mA intervals were recorded to quantify toolbar position during planting. Toolbar planting position indicated that the toolbar was at the desired position for selected planting depth. A custom data acquisition system was developed using national instruments (NI) cRio system and the acquisition program was developed using

LabVIEW to record signals from the 12 load sensors, 4 hydraulic pressure transducers, potentiometer, and GPS unit at 10 Hz. Raw data were used without manipulation for the statistical analyses. For the time series plots, the moving average of five consecutive data points was used.

a b

Figure 2.4. Potentiometer mounted on seed cart axle housing and lower link attached to the planter toolbar (a) to monitor the position of planter toolbar relative to the axel housing to quantify raised or planting position (b) of the toolbar.

2.3.3 Soil EC

On-the-go soil electrical conductivity (EC) was measured using a Veris Mobile Sensor Platform (MSP) (EC Surveyor 3150, VERIS Technologies, Salina, KS, U.S.A.). The Veris MSP was mounted on the three point hitch of a Kubota M9000 tractor. The Veris EC Mapper within MSP was programmed to measure EC at both shallow (0 to 0.3 m) and deep (0.0 to 0.9 m) zones. The Veris SoilViewer v2.70 logged real-time point data and GPS data at 1 Hz along 18.3 m transects. Veris MSP categorized real-time EC data in five

ranges: Low (8.0-19.7 mS/m), medium low (19.4-25.3 mS/m), medium (23.5-31.2 mS/m), medium high (29.8-48.1 mS/m), and high (37.1-87.2 mS/m). The area representing the lower two, middle and upper two EC ranges were selected as target regions for soil samples. After collecting soil EC measurements, soil samples were taken using a Classic Soil Probe soil sampler with a 1.9 cm diameter tip (Model L, Oakfield Apparatus, Fond du Lac, WI, USA). At each field site, 12 soil samples, 4 samples each from the different EC regions, were collected for laboratory analysis. Sampling depth was 30.5 cm. Collected soil samples were analyzed for electrical conductivity by the Department of Agronomy Soil Testing Lab at Kansas State University. Laboratory results of the soil tests were sent to Veris Technologies for post calibration of the collected in-field electrical conductivity measurements. Post calibrated soil EC data from Veris was used to create a smoothed EC maps using ArcGIS 10.3 using point ordinary kriging (Moral et al., 2010 and Li et al., 2008). To visualize the EC differences the generated maps were divided into three zones using natural breaks method in ArcMap. The defined soil EC zones corresponds to the regions where soil samples were taken and these zones were classified as low, medium and high soil EC. The average GWL for each soil EC zones was calculated and this was used to determine if average GWL distinctly vary for each soil EC regions within each field. Previous study showed that soil EC is correlated to soil texture, as such, for this study the terms soil with low, medium and high EC corresponds to low, medium and heavy textured soil. Soil moisture was measured using a Hydrosense II (Campbell Scientific, Inc., UT, USA) handheld digital soil-water sensor equipped with a 12 cm soil moisture probe. At each field site, 9 soil moisture readings, 3 readings each from the different EC regions at a

depth of 12 cm were recorded. The average soil moisture during EC mapping was 34.5% volumetric water content which ranges from 17.3% to 43.7%.

2.4 Results and Discussion

2.4.1 Planter fixed downforce setup validation

Hydraulic oil pressure measurement provided validation that a constant downforce was maintained for all row units throughout field operation. An example of the real-time hydraulic pressure during field operation is shown in Figure 2.5. The example data exhibited that the hydraulic system maintained a consistent down pressure of approximately 5.6 MPa throughout the test period. It can be observed that there were several instances the GWL was 0 N which implied that the row was losing ground contact during planting (Figure 2.5).

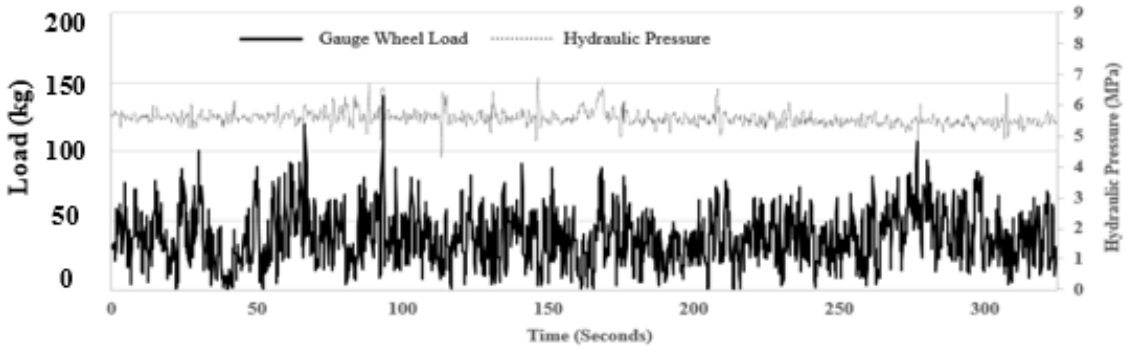

Figure 2.5. An example field data exhibiting hydraulic oil pressure for fixed downforce implementation on one row unit. Data were plotted using a moving average to smooth out random peaks by calculating the average of 5 consecutive data points.

Table 2.1 shows gauge wheel load sensors exhibited consistent no-load response as the toolbar was raised when turing at headlands at all times of planting operation. Low standard deviation suggests that every load sensor returns to the same, 0 load value each time the toolbar was not in the planting position. These results indicate that GWL sensors were calibrated accurately and provided stable output throughout the test period.

Table 2.1. Descriptive statistics of no-load readings of load cells for each row unit during planting.

Field		Load cell readings on each row unit, mA											
		1	2	3	4	5	6	7	8	9	10	11	12
A	avg.	4.43	-	4.17	4.05	4.46	4.73	4.56	4.32	4.07	4.33	4.02	4.31
	StDev	0.02	-	0.03	0.03	0.03	0.03	0.03	0.03	0.03	0.03	0.03	0.03
	min	4.26	-	3.95	3.70	4.15	4.46	4.29	4.04	3.82	4.00	3.70	4.03
	max	4.61	-	4.40	4.36	4.80	5.02	4.80	4.61	4.39	4.63	4.34	4.57
B	avg.	4.43	4.05	-	4.11	4.45	4.67	4.53	4.30	4.17	4.34	4.01	4.28
	StDev	0.02	0.06	-	0.11	0.03	0.03	0.02	0.02	0.03	0.03	0.03	0.02
	min	4.36	3.73	-	3.95	4.35	4.55	4.44	4.21	4.08	4.25	3.90	4.16
	max	4.55	4.36	-	4.39	4.59	4.81	4.61	4.43	4.26	4.45	4.11	4.39
C	avg.	4.44	4.06	4.18	4.07	4.44	4.67	4.53	4.29	4.48	4.33	4.02	4.25
	StDev	0.02	0.13	0.03	0.03	0.04	0.04	0.03	0.03	0.04	0.04	0.04	0.03
	min	4.26	2.39	3.90	3.68	4.04	4.30	4.16	3.90	4.10	3.98	3.66	3.92
	max	4.76	5.45	4.48	4.45	4.77	5.02	4.83	4.61	4.80	4.66	4.42	4.61

2.4.2 GWL distribution

Results highlighted that the desired GWL of 12 to 57 kg (25 to 125 lbs) was achieved for 27%, 34% and 38% of total planting time for Fields A, B and C, respectively (Figure 2.6). Figure 2.6 shows that the real-time GWL of individual row units varied significantly throughout the planting operation for all the fields. On average, 35% of the time the GWL was below zero for Field A, 28% of the time for Field B while only 12% of the time for Field C. The areas planted with GWL below zero indicated inadequate gauge wheel contact with the soil surface, and uncertain seeding depth. The frequency where the GWL was above 100 kg (225 lbs) was lowest at Field B which occurred only 6% of the time. Such distribution of real-time GWL over a wide range of < 0 to > 100 kg (225 lb) during the whole planting time agrees with Hanna et al., (2010) which reported that measured GWL of each row unit changes significantly (20 to 600 kg) over short distances as it travels along the seed furrow.

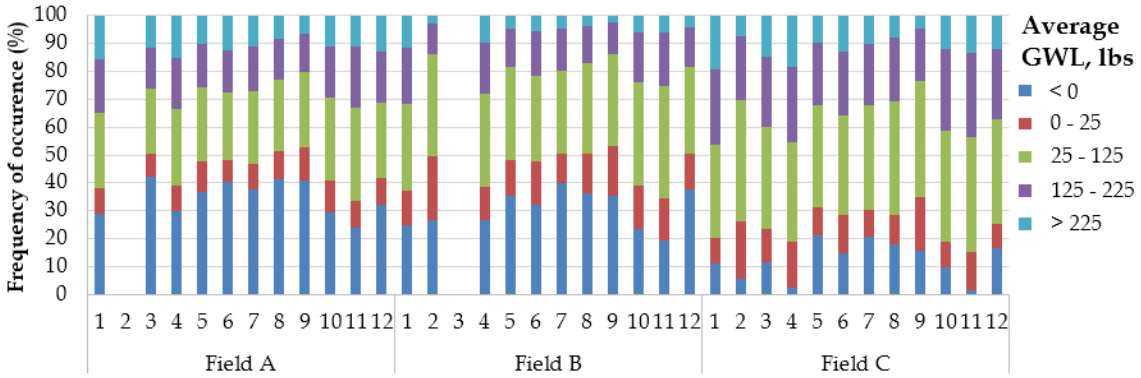

Figure 2.6. Percent time average gauge wheel load (GWL) for individual row units was within and above or below the target range of 12 to 57 kg (25-125 lbs) for Field A, Field B and Field C. Data for row unit 1 for Field A and row unit 3 for Field B are removed due to measurement errors.

The results indicate that the GWL resulted in significant area (Figures 2.7a, 2.8a and 2.9a) (14.7 hectares or 67%) planted with under-target and over-target of GWL. Deviations in GWL could be attributed primarily due to variations in opening disc load requirement as influenced by terrain, crop residue, planting speed, and compaction across varying soil EC to achieve seeding depth. The GWL was below desired range for 7% and over target for 24% of the time. The percent area planted where GWL was 0 kg was primarily due to the selection of the low target GWL based on grower's perception for planting operation. The downforce per row unit implemented was 138 kg (weight of row unit and target GWL) which may not be enough to keep the gauge wheels in contact with the ground during planting operation. Grisso et al., (2014) suggested that up to 220 kg of down pressure might be needed for adequate soil penetration of row units and insufficient weight may result in gauge wheel off the ground. Thus, the spatial GWL deviation that occurred across the field suggest the need to select a higher target GWL depending on field operating conditions. In addition, an automatic adjustment of downforce might be needed for selected row units as section control or for individual row unit for more uniform GWL application during planting.

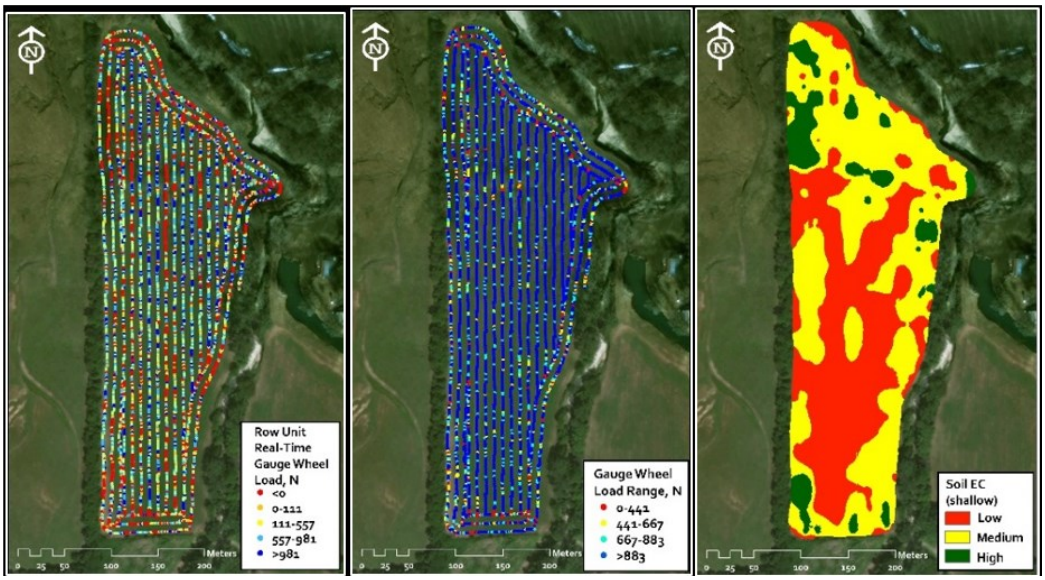

a b c

Figure 2.7. Gauge wheel load (GWL) of row unit 1 (a); gauge wheel load range (GWLR) (b) and; the soil EC map (c) for Field A.

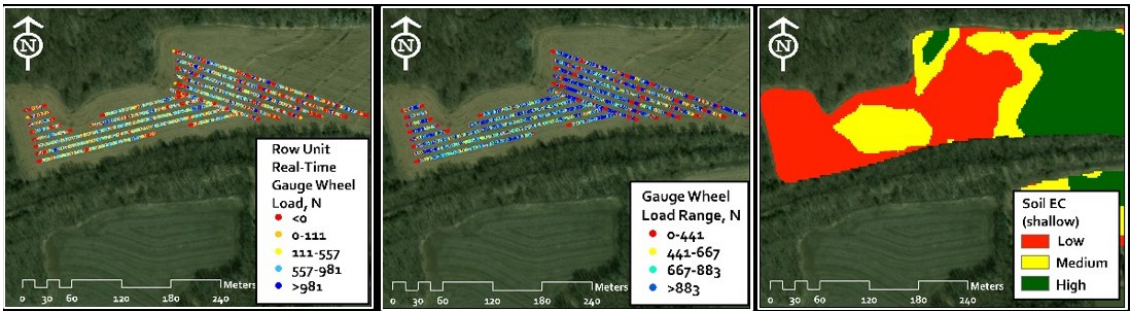

a b c

Figure 2.8. Gauge wheel load (GWL) of row unit 1 (a); gauge wheel load range (GWLR) (b) and; soil EC Map (c) for Field B.

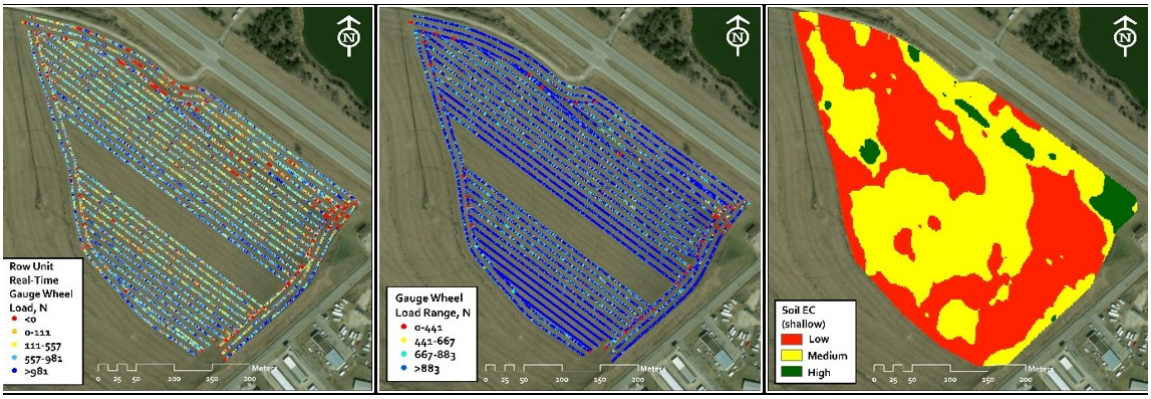

a b c

Figure 2.9. Gauge wheel load (GWL) of row unit 1 (a); gauge wheel load range (GWLR) (b) and; the soil EC map (c) for Field C. The data not included for (a) and (b) was not part of this study.

2.4.3 GWLR distribution

Test results showed that approximately 70% of the time the GWLR across the 12 row units was > 90 kg (200 lb) for Fields A and C while approximately 41% of the time for Field B (Figure 2.10). Field C had the lowest frequency of approximately 2% of the time the GWL difference between two row units across the toolbar was within the desired range of 0 to 45 kg (0 to 100 lb). Figure 8 show this extreme variation of GWLR was caused by the row units experiencing varying levels of real time loading during planting where one row unit is applying 0 GWL and another is applying more than 90 kg (200 lb). The row-to-row GWL variability across the tool bar indicated that for majority of the time, individual row unit would require a different level of downforce implementation to maintain target GWL. Therefore, one single setting for the entire toolbar would not be sufficient to achieve target GWL across all of the row units even with one control system managing downforce on all row units.

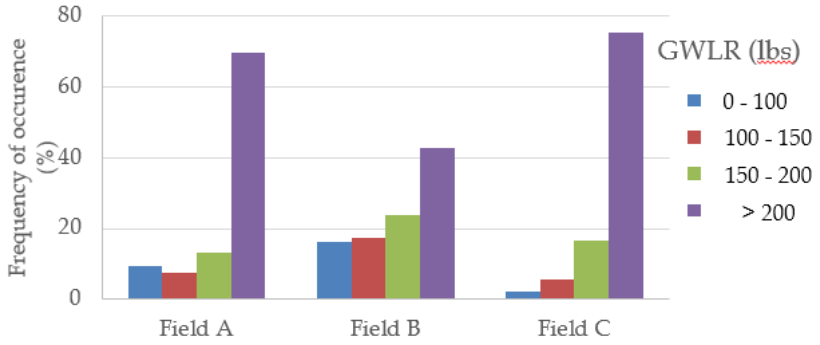

Figure 2.10. Percent time gauge wheel load range (GWLR) was within and beyond the desired 0-444 N for Field A, Field B and Field C.

2.4.4 GWLR – Different section control scenarios

Results with 2-row, 3-row and 4-row section control scenarios indicates that lower GWLR for greater percentage of time could be achieved with lesser number of row units

per section control (Figure 2.11). Approximately 81%, 85% and 60% of the total planting time GWLR was within the desired range of 0 to 45 kg (0 to 100 lb) for Fields A, B, and C, respectively, for a 2-row section control. On the other hand, the GWLR for a 4-row section control was within the desired range only 23%, 46%, and 15% of the total planting time for Fields A, B, and C, respectively. As the number of row units increase within a section control, the variability also increases with GWLR values of >90 kg (200 lb) was observed to be 23%, 4% and 19% of total planting time for Fields A, B and C, respectively, with a 4-row section control. Such result indicates that GWL requirements of row units varies significantly due to changing field conditions and selecting a lesser number of row units per section control could result in a more uniform application of GWL during planting.

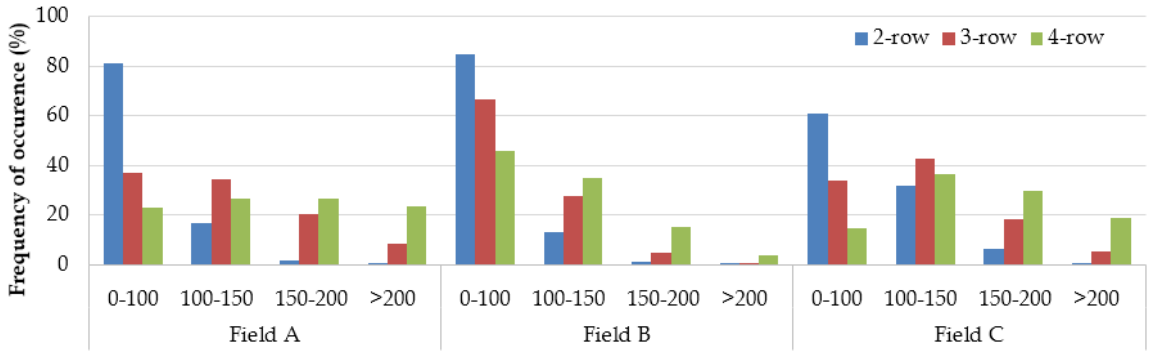

Figure 2.11. Row-to-row GWLR variability with different row section control combinations for all the fields.

2.4.5 Effect of soil type on average GWL

The soil EC maps shows that soil texture varied across the field. It should be noted that during a typical planting window many rainfall events may be experienced which could cause average moisture during planting to vary. Less than desired or spatially variable soil moisture during planting can further impact GWL variability due to its impact on varying soil resistance per row unit opening discs. Planting was done in one day for

Field A and Field B and C were planted on the next day. Soil conditions were at field capacity for all the fields and no rainfall events occurred 2-3 days prior to planting.

As expected, Fields A, B and C showed decreasing average GWL with increasing soil EC across the fields (Figure 2.12). Since soil EC is correlated with soil texture, higher textured soil which consists of finer soil particles and higher water holding capacity creates a denser soil. Interaction of soil texture and moisture present would vary the force needed by opening disc for soil penetration. In all fields, simple regression analysis indicated that soil EC or soil texture was a significant ($p<.001$) variable that can influence real-time GWL. Varying GWL during planting is associated with changing soil EC such that lighter soil or low soil EC resulted in a significantly higher GWL (Tables 2.2, 2.3 and 2.4). All fields resulted in significant differences on the average GWL on low, medium and high EC except for Field C between the low and medium EC soils. This result suggests that soil resistance to the row unit opening discs increased with higher soil EC which requires higher vertical force requirement for the planter's opening discs, reducing the amount of load carried by the planter gauge wheels thus decreasing GWL. This is in agreement with the findings of Collins & Fowler (1993) which suggests that draft requirements for clay soil is higher than sandy soil. Likewise, Kumar et al. (2012) and Lomeling (2013) reported an increase in soil cone index with sand fraction (sandy soil). Although statistical analyses suggested significant difference on force requirement of opening discs among soil textures, other factors such as planting speed as reported by Nkakini (2015) and Grisso (1996) and surface residues as reported by Morrison Jr. & Allen (1987) could potentially cause variability in opening discs load requirement on various soil types which may influence GWL during planting.

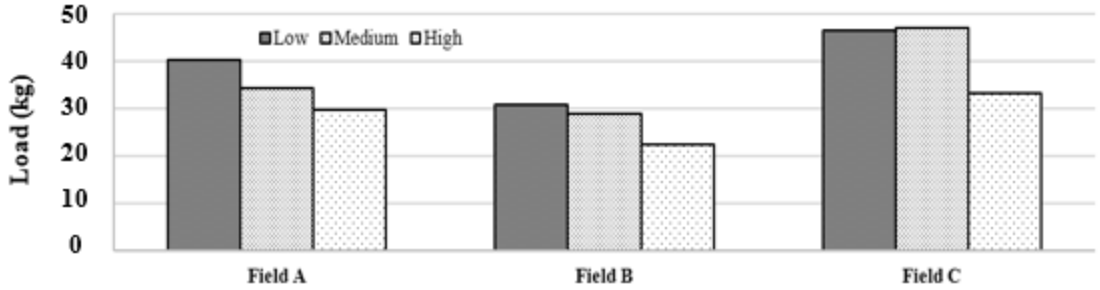

Figure 2.12. Average gauge wheel load (GWL) for Field A, Field B and Field C on low, medium and high soil EC classification.

Table 2.2. Descriptive statistics and comparison among means (CAM) of the GWL for field A on the different soil EC classification

Soil EC	Avg. GWL (kg)	StDev (kg)	CV (%)	Min. GWL (kg)	Max. GWL (kg)	Std. Error (kg)	No. of samples
Low	41.1[a]	23.2	5.8	-2.0	165.0	0.2	11496
Med	35.0[b]	25.0	7.3	-1.8	178.5	0.2	16383
High	30.2[c]	24.3	8.2	-1.8	159.5	0.4	3146

Means sharing the same superscript are not significantly different from each other at P<0.05

Table 2.3. Descriptive statistics and comparison among means (CAM) of the GWL for field B on the different soil EC classification.

Soil EC	Avg. GWL (kg)	StDev (kg)	CV (%)	Min. GWL (kg)	Max. GWL (kg)	Std. Error (kg)	No. of samples
Low	31.3a	23.1	7.5	-1.9	167.0	0.4	3965
Med	29.5b	29.5	8.2	-1.8	170.4	0.7	1868
High	22.7c	22.7	11.6	-1.7	133.8	0.7	1095

Means sharing the same superscript are not significantly different from each other at P<0.05

Table 2.4. Descriptive statistics and comparison among means (CAM) of the GWL for field C on the different soil EC classification

Soil EC	Avg. GWL (kg)	StDev (kg)	CV (%)	Min. GWL (kg)	Max. GWL (kg)	Std. Error (kg)	No. of samples
Low	47.5a	19.7	4.2	-2.3	207.9	0.2	16064
Med	47.9a	21.5	4.6	-2.6	233.8	0.2	14598
High	33.8b	22.4	6.8	-2.1	145.0	0.5	1974

Means sharing the same superscript are not significantly different from each other at P<0.05

Overall the three soil EC zones exhibited varying average GWL ranging from 30.2 kg to 41.1 kg for Field A, 22.7 kg to 31.3 kg for Field B and 33.8 kg to 47.9 kg for Field

C. The standard deviations (StDev) of the average GWL across the three fields were almost identical but the coefficient of variation (CV) shows that variability in the GWL increases from lighter to heavier soil. These results indicated that the fixed downforce system would not be able to provide the continuously varying downforce required to maintain target GWL as soil resistance changed with soil EC across the field. In addition, negative minimum GWL suggests instances where the opening discs might be requiring additional load more than what is available on the gauge wheel for soil penetration. The GWLR distribution also suggests that row unit section control would be required as row-to-row downforce requirement varied in the field. The GWL and GWLR across the 12-row units also indicates that when implementing downforce control the planter should have a control setup to implement loading and unloading of row units based on planting in varying soil resistance.

2.4.6 Tire compaction and GWL

Soil resistance can also vary with soil compaction due to tractor tires and movement of other agricultural equipment during the production season. Soil compaction due to the tractor tire resulted in a significant reduction in the GWL (Tables 2.5, 2.6 and 2.7). Results shows that strips planted along the non-tire tracks resulted in the average GWL reduction of 13%, 12% and 14% for Fields A, B and C, respectively (Figure 2.13).

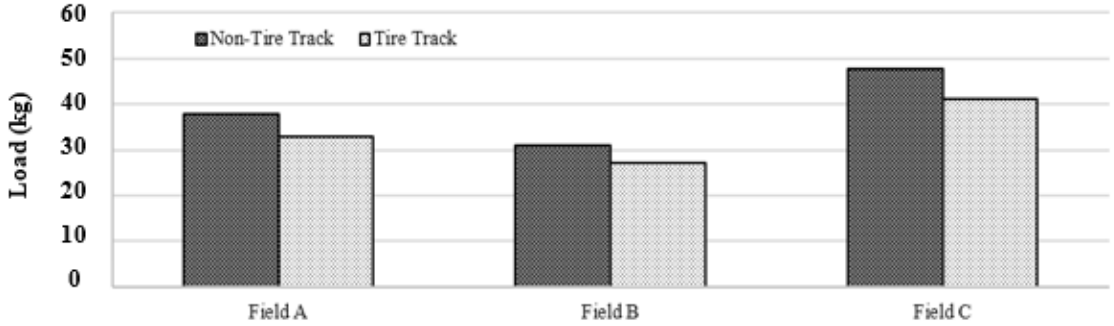

Figure 2.13. The average GWL for the three fields at two different strip location.

These result suggests that compacted soils caused by the tractor tires increases the resistance for opening discs to penetrate the soil in creating the furrow at the required seeding depth. Such findings are in accord with Doan et al. (2005) reporting a higher soil cone index along tire tracks that indicate soil compaction by the tractor tires during planting. The resulting increase in resistance would require the opening discs to take in additional load carried by the gauge wheels thus a reduction in the GWL. It also emphasizes the need for future research to 1) understand the implementation of downforce control system needs for compacted (tire tracks) versus non-compacted (non-tire tracks) field areas and, 2) if tire and non-tire track row units need a different target downforce ranges to maintain uniform GWL and seeding depth.

Table 2.5. Descriptive statistics and comparison among means (CAM) of the GWL for the three fields at two strip locations.

Row Strip	Avg. GWL (kg)	StDev (kg)	CV (%)	Min. GWL (kg)	Max. GWL (kg)	Std. Error (kg)	No. of samples
Tire Track	33.6a	28.5	8.6	-2.6	203.1	0.2	31025
Non-Tire Track	38.6b	25.8	6.8	-2.5	180.6	0.1	31025

Means sharing the same superscript are not significantly different from each other at P<0.05

Table 2.6. Descriptive statistics and comparison among means (CAM) of the GWL for the three fields at two strip locations.

Row Strip	Avg. GWL (kg)	StDev (kg)	CV (%)	Min. GWL (kg)	Max. GWL (kg)	Std. Error (kg)	No. of samples
Tire Track	27.7a	27.8	10.2	-2.2	187.2	0.3	6928
Non-Tire Track	31.6b	25.0	8.0	-2.0	176.8	0.3	6928

Means sharing the same superscript are not significantly different from each other at P<0.05

Table 2.7. Descriptive statistics and comparison among means (CAM) of the GWL for the three fields at two strip locations.

Row Strip	Avg. GWL (kg)	StDev (kg)	CV (%)	Min. GWL (kg)	Max. GWL (kg)	Std. Error (kg)	No. of samples
Tire Track	48.8	21.6	4.5	-5.4	212.3	0.1	32636
Non-Tire Track	41.9	26.3	6.4	-20.0	279.3	0.1	32636

Means sharing the same superscript are not significantly different from each other at P<0.05

2.5 Conclusions

This study provided the following key findings:

On an average, target GWL of 12 to 57 kg was achieved 27%, 34% and 38% of the time for Fields A, B and C, respectively. Real-time GWL below the target range was 38% and above the target 29% of the time across the three fields. Different row section control scenarios reveal that a 2-row resolution section control is preferred over 4-row section control to obtain more uniform row-to-row GWL control to account for varying soil conditions encountered during planting. It was observed that on average only 9% of the time the GWLR was within the range 0 to 45 kg across the 12-row units while 28% of the time for a 4-row section control and 76% of the time for 2-row section control.

Regression analysis shows that soil EC or soil texture was a significant parameter that can affect real-time GWL. Multiple comparisons revealed that low soil EC resulted in a significantly higher GWL compared to high soil EC across the three fields. However, ground speed and crop residue and other factors may have also influenced the GWL variability. Tire and non-tire tracks also resulted in a significantly different average GWL. The average GWL for row units on non-tire tracks was 38.6 kg, 31.6 kg and 48.8 kg for Fields A, B and C, respectively, which was 13%, 12% and 14% significantly lower compared to average GWL on row units on tire tracks.

These results suggest that the selected target GWL for fixed downforce control system was too low such that it was not able to implement the target GWL most of the time during planting. Such case might result in shallow seeding depth. Result also suggests the need for an automatic downforce control system that is capable of controlling smaller control sections and independent section control for row units along track and non-track which could result in a more consistent GWL application across all row units during planting.

Future studies need to be conducted with a row crop planter implementing automatic downforce control system to quantify the GWL uniformity of individual row units or control sections under varying operating field conditions.

Chapter 3 - Plant spacing and seeding depth of corn as influenced by downforce and ground speed of a row-crop planter[2]

3.1 Abstract

Uniform seed placement, herein understood as an outcome of plant spacing and seeding depth uniformity, requires proper selection of downforce control across varying field conditions especially when planting at faster ground speeds. Thus, the aim of this study was (1) to assess the effect of ground speed and downforce setting on plant spacing and seeding depth and (2) to evaluate the relationship of planting speed and row unit vibration on gauge wheel load. A 12-row planter was used to plant corn at no-till and strip-till fields. Treatment factors were downforce setting with two levels: 63 kg and 100 kg and ground speed with four levels: 7.2, 9.7, 12.1 and 16.1 kph. The planter was programmed to plant corn at 5.1 cm seeding depth at a seeding rate of 84,000 seeds per hectare equivalent to a theoretical plant spacing of 17.8 cm. No significant downforce effect was observed at both fields on plant spacing, although higher downforce setting resulted to higher plant spacing accuracy. Higher variability in spacing were observed with increasing ground speed. Target seeding depth at no-till field was achieved with high downforce and slower ground speed while deeper seeding depth at strip-till field was observed with high downforce setting. Finally, both downforce settings revealed increasing row unit acceleration as ground speed increases.

[2] This chapter was submitted for publication as a peer-reviewed research paper to the Journal of Precision Agriculture.

3.2 Introduction

The goal of precision planters is to place the seeds in the soil in a manner to provide the ideal environment for even emergence. Proper seed placement is important to allow adequate moisture for the seed to germinate and prevent exposure to undesirable environmental conditions (Grassbaugh & Bennett, 1998). Controlling seed placement can be difficult when planters are operated at faster speed. Increasing the planting speed could cause the seeds to bounce around the seed tube, consequently resulting in uneven spacing and depth. Studies have shown the importance of planting at optimum depth where planting beyond the threshold depth (too shallow or too deep) could result in poor crop performance (Özmerzi et al., 2002). Da Silva et al. (2004) showed that seeding depth was one of the main factor underlying emergence and vegetative development of corn (Zea mays L.). The same authors documented that time to emergence significantly increased when seeding depth increases from 3 cm to 7 cm. Similarly, Molatudi & Mariga (2009) investigated the effect corn seeding depth on emergence in a greenhouse setting, with differences on emergence at increasing seeding depth. Ozmerzi et al. (2002) conducted a study using a precision seeder revealing no significant difference on sowing uniformity at varying seeding depths. However, maximum rate of emergence was achieved at nominal seeding depth of 6 cm. Likewise, planting at higher speed cause vibrations in the row units (Staggenborg et al., 2004) which could reduce the gauge wheels rolling resistance due to inadequate application of downforce. Finding optimum down force at varying soil conditions and at increasing speeds can be challenging in terms of providing just enough load to prevent loss of ground contact of row units but not too much as to cause sidewall compaction. Downforce is the amount of load applied on the planter row unit to achieve

the desired seeding depth. This load consists of the weight of the row unit and additional load applied through mechanical springs, airbags or hydraulics to compensate for varying load requirements due to changing soil conditions (Badua et al., 2018). Previous researches have demonstrated negative effects of applying excessive load on the depth and emergence of corn. Applying too much load during planting could over compact the soil (H Mark Hanna, n.d.), while not enough load could result in a shallower seeding depth (Karayel & Šarauskis, 2011) but both situations could result in poor root development (Raper et al., 2006) and uneven plant emergence (Gratton et al., 2003; Hanna et al., 2010; Karayel & Šarauskis, 2011). Janelle et al. (1993) conducted a study on seed placement using different levels of double disc openers and downforces. Results suggested that insufficient seeding depth was achieved at the smallest downforce, thus negatively affecting the crop emergence. Similarly, Weirich Neto & Lopes (2012) conducted a static test on a planter portraying a significant effect on time to emergence and seeding depth produced by the applied static load on press wheels. Thus, the two key planter performance parameters that can influence corn stand establishment are load on gauge wheels and planting speed determining key planting parameters such as desired seed density, uniform emergence and planting depth. No single parameter is responsible for differences in final stand establishment among fields but rather often a combination of factors during the planting operation (Lauer & Rankin, 2004a). Several researches have examined the effect of ground speed on final stand establishment (Liu et al., 2004; Nielsen, 2013; Ozmerzi et al., 2002; Staggenborg et al., 2004). However, no data have been published to determine the effect of different downforce settings at varying ground speeds. Previous study (Badua et al., 2018) showed the variability on the gauge wheel loading on a planter equipped with a fixed

downforce control setting during field operation, recommending future research efforts to quantify the influence of different planting speeds and downforce settings on seed placement uniformity under varying field conditions. Therefore, the objectives of this study were: i) to assess the effect of planting speed and downforce setting on plant spacing and seeding depth, and ii) to evaluate the relationship of planting speed and row unit vibration on gauge wheel load and its impact on seed placement consistency.

3.3 Materials and methods

3.3.1 Equipment set up and instrumentation

A Horsch Maestro 30 SW planter (Horsch Maschinen GmbH, Schwandorf, Germany) with variable rate and section control technology operated by a John Deere 8250R tractor was used in planting. The 12 row units of the planter are spaced at 762 mm apart. Planter control was accomplished using a 2630 John Deere (GreenStar-3, Deere and Company, Moline, IL, U.S.A.) field computer connected to the planter electric control unit (ECU) (Horsch Maschinen GmbH, Schwandorf, Germany) through ISOBUS. The planter was programmed to implement automatic section control by automatically turning off electric motors (BG 45x15 SI, Dunkermotoren GmbH, Schwarzwald, Germany) of individual row units based on previously planted areas as recorded by the GPS on the planter. The ECU utilized the speed recorded by the GPS to generate the desired motor rpm to achieve the desired population. A seed sensor (Hy Rate Plus, Dickey-John Corp., Auburn, IL, U.S.A.) was placed along the seed tube on each row unit to provide feedback on seed singulation, doubles and misses shown in field computer. Each row unit was factory-installed with a load cell or sensors (6784, Horsch Maschinen GmbH, Schwandorf, Germany) designed to measure from 0 to 1000 kilogram-force (kgf) with a linear analog

output of 4 to 20 mA. The load cells were calibrated to establish the correlation between the sensors analog output in mA to the sensors measurement range in kgf. Calibration was done by using the sensor to measure known weights and the resulting regression curve was used in calculating the gauge wheel load (GWL) by converting the real-time load sensor signal mA into kgf. The row units were grouped into control sections (Figure 3.1) where a pressure transducer was installed on each section to measure the real-time hydraulic oil pressure applied during planting operation. Oil pressure readings will indicate the hydraulic system applying constant pressure on row units thus maintaining a constant downforce during planting. Control section 1 included the first three row units (rows 1, 2, 3), control section 2 consisted of row units in the middle of the toolbar (rows 6 and 7), control section 3 contained the last three row units (rows 10, 11 and 12) and section 4 comprised the row units along the tire tracks (rows 4, 5, 8 and 9). Control sections 1, 2 and 4 were fitted with transducers having a measuring range between 0 to 25 mPa with an output signal of 4 to 20 mA (HDA 844L-A-0250-161, Hydac, Glendale Heights, IL, USA). Control section 2 was equipped with a transducer with measurement ranges from 0 to 52 mPa with an output signal of 0.5 to 4.5 Vdc (Model KM41, Ashcroft Inc., Stratford, CT, USA). Four row units (rows 1, 5 7, and 12) were equipped with accelerometers (Model 3741E1210G, PCB piezotronics, Depew, NY, USA) to record vibration of row units during planting. A potentiometer (Model 424A11A090B, Elabou sensor Technology Inc., Waukegan, IL, USA) was mounted on one row unit to measure the vertical movement of the toolbar which indicates its operating position. It has a measurement range of 0 to 90 degrees with an output signal ranging from 4 to 20 mA. A sub-inch accuracy GPS unit (GR5, Topcon Positioning Systems, Inc., Livermore, CA, USA) was used to collect the location and speed

simultaneously during planting. Load cells, pressure transducers, accelerometers, potentiometer and GPS unit were connected to a NI cRIO chassis via C Series modules (National Instruments, Ausin, TX, USA) and signals were collected at 10 Hz sampling frequency using a custom-made LabVIEW program through a control laptop computer (Latitude 14 3470, Dell, Round Rock, TX, USA).

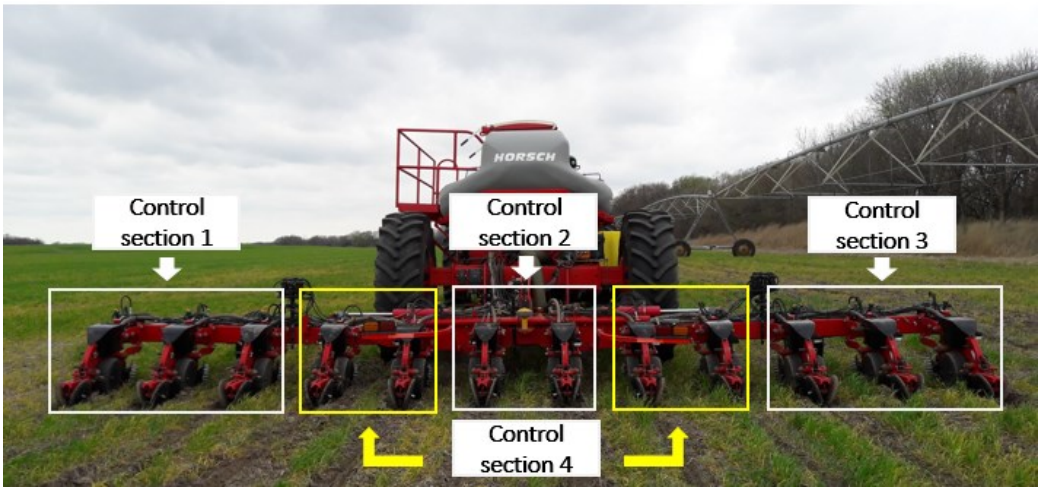

Figure 3.1. The planter toolbar segregated into 4 different control sections.

3.3.2 Field layout

Location of experimental test plots are shown in Figure 3.2. Two load levels of active downforce were selected which will implement low and high downforce. Consultation from producers and collaborators suggested to set the target gauge wheel load (GWL) at 63 kg (140 lb) to implement a low downforce, referred herein as “active low setting” and set the GWL at 100 kg (220 lb) for high downforce implementation, referred herein as “active high setting”. Experimental test runs were applied in 6 plots (150 meters long) implementing a split-plot design structure. The experiment consisted of two treatment factors: downforce setting with two levels: 63 kg and 100 kg (D1 and D2) and ground speed with four levels 7.2 kph (4.5 mph), 9.6 kph (6.0 mph), 12.0 kph (7.5 mph) and 16.1 kph (10.0 mph) (S1, S2, S3 and S4). Each plot (whole plot) were divided into 4

equally sized smaller plots (subplot) where downforce setting was randomly assigned to the whole plot and ground speed were randomly assigned to each subplot. Each subplot consists of 12 rows and 0.6 m (17.5-ft) within one-row was randomly selected to collect measurements on plant spacing and seeding depth. This row length is equivalent to 1/1000th acre for a row width of 76-cm (30 inches) which is recommended to achieve an adequate sample that would represent the rest of the field (Benson, 1990). Active low setting was implemented by applying a hydraulic pressure of 1,700 psi while pressure of 2,100 psi was applied to implement the active high setting. A seeding rate of 84,000 seeds ha-1 (34,000 seeds acre-1) was applied which corresponds to a target spacing of 17.8 cm (7 in). Target seeding depth was set at 5.1 cm (2 in) by manually placing the depth adjustment pin on the appropriate slot on the row unit. Analysis of variance (ANOVA) were performed using the GLIMMIX procedure in SAS University Edition (2017 version, SAS Institute Inc, Cary, NC, USA). Comparison among means were done using Fishers protected (Least significant difference) LSD test. Unless otherwise indicated, effects were considered statistically significant at the 0.05 level of probability.

Field A *Field B*

Figure 3.2. Aerial view of the fields showing the location of experimental plots.

3.3.3 Field description

The experiment was conducted in a 26.1 hectare field (64.6 acre) located near Belvue, KS (39.299714°,-96.207936°) referred herein as Field A and in a 43.1 hectare field (106.6 acres) located near Blaine, Kansas (39.358076°, -96.159382°) referred herein as Field B. Field A adopted a no-till management system with cover crops (Figure 3.3a) while Field B is a strip-tilled field (Figure 3.3b). Both field were measured for soil electrical conductivity (EC) using a Veris mobile sensor platform (MSP) (EC Surveyor 3150, Veris Technologies, Salina, KS, USA). During EC data collection, the Veris EC Mapper within the MSP represented the field into areas of low, medium and high EC. Each EC zone were marked as target regions for soil sampling on which soil samples will be taken after EC data collection is done. At each field, 9 soil samples (three samples from three different zones) were collected at a depth of 30.5 cm using a Classic Soil Probe soil sampler with a 1.9 cm diameter tip (model L, Oakfield Apparatus, Fond du Lac, WI, USA). Collected soil samples were submitted for soil textural analysis at the Department of Agronomy Soil Testing Laboratory at Kansas State University. Soil textural characteristics of the two fields are presented in Table 3.1.

a **b**

Figure 3.3. (a) Field A showing the cover crops and (b) Field B showing the strip-tilled field.

Table 3.1. Soil textural properties of field A and B.

Composition	Field A	Field B
Percent sand	28.0	18.7
Percent silt	50.3	57.0
Percent clay	21.7	24.3
EC (mS/cm)	0.9	0.8

3.3.4 Field data collection

3.3.4.1 Plant spacing

Plant spacing was measured after emergence was considered complete. A 7.6-meter (25-feet) standard measuring tape (Leverlock, Stanley Black and Decker, New Britain, CT, USA) was laid out along the 0.6 meter strip and accumulated spacing readings were recorded. Theoretical plant spacing was calculated based on the plant population applied during planting and spacing of planter row units. Using the prescribed plant population and spacing of the planter row units, the equivalent theoretical plant spacing was 17.8 cm (7 in). Since standard deviation alone does not indicate uniformity in stand (Nafziger, 1996), multiples and doubles along with singulation and precision were determined to quantify the consistency of plant spacing relative to the theoretical spacing (S_t). Thus, measures of plant spacing uniformity used in this study was in accordance with the indices set by the International Organization for Standardization (1984) also used in the study by Kachman & Smith (1995). These are multiples index, miss index, quality of feed index and precision. Multiples index (D) specifies the number of spacings on each EU less than or equal to 0.5 times the S_t. This was calculated using the formula:

$$D = n_D/N \quad (1)$$

where n_D is the number of measured spacings less than or equal to 8.25 cm for the FDF and 8.9 cm for the ADF. N is the total number of spacings measured on each EU. Miss

index (M) indicates the number of spacings on each EU that are greater than 1.5 times the S_t. This index was calculated using the formula:

$$M = n_M/N \quad (2)$$

where n_M is the quantity of measured distance between successive plants that are greater than 24.75 cm and 26.7 cm for FDF and ADF, respectively. Quality of feed index (A) or singles calculates the proportion of measured spacings on each EU that are within 0.5 and 1.5 times the S_t. The following formula was used to calculate this index:

$$A = n_A/N \quad (3)$$

where n_A is the number of spaces measured that are within 8.25 cm to 24.75 cm for the FDF and 8.9 cm to 26.7 cm for the ADF. Precision index (C) quantifies the variability of plant spacing after skips and doubles are removed or spacings that are are considered singles and was calculated using the following formula by Kachman & Smith (1995). Lower value indicates lower spacing variability.

$$C = s_A/ S_t \quad (4)$$

where s_A is the standard deviation of n_A.

3.3.4.2 Seeding depth

Determining the seeding depth was performed by manually digging the seed of the emerged plants and measuring the distance of the seed from the ground surface. Measurement was done by scraping away loose soil to get down to the bare field level and a flat stick was placed on the furrow along the direction of travel of the planter. A standard 0.47-meter (1 –foot) ruler (STAEDTLER, Nurenberg, Germany) was used to measure the depth by placing it perpendicular to the flat stick with the zero-end placed beside the seed (Figure 3.4). Readings were recorded to the nearest 1.0-centimeter resolution.

Figure 3.4. Measurement of seeding depth by digging the seed of an emerged plant and placing a straight sturdy object across the row and place a standard ruler perpendicular to it where the 0-end is on the seed.

3.4 Results and discussion

3.4.1 Plant spacing

Mean plant spacing, quality of feed index, miss index, multiple index and precision in Fields A and B are shown in Table 3.2.

Table 3.2. Mean plant spacing, quality of feed index, miss index, multiple index and precision as influenced by downforce setting in no-till and till field conditions.

Field	Downforce Setting	Spacing (cm)	PSV (in)	Quality of feed index (%)	Miss index (%)	Multiple index (%)	Precision index (%)
A	D1	18.2a	6.2	85.0a	8.4a	4.1a	27.7a
	D2	18.4a	7.1	87.5a	10.2a	4.8a	24.5a
B	D1	17.9a	6.1	87.1a	7.4a	5.5a	22.1a
	D2	18.1a	6.5	87.8a	7.6a	4.7a	20.5a

PSV-plant spacing variability

Result suggests that plant spacing was not influenced by downforce setting across both fields in this study. Observed results with the selected GWL of 63 kg and 100 kg were

similar to Hanna et al. (2010) which reported that down-pressure (18 kg to more than 90 kg) did not significantly affect mean plant spacing. Although not significantly different, downforce setting D2 yielded the highest plant spacing variability (PSV) in both fields. Moreover, PSV of 7.1 cm in Field A was outside of the optimum value for row crop planters. A PSV value of 6.7 cm is an acceptable precision in mechanical planting (Liu, et al, 2004) considering the planter performance and germination rate of seeds. Although Lauer & Rankin (2004) reported a reduction of yield for PSV greater than 12 cm. However, Nielsen (2013) suggest that lower PSV could translate into more grain yield potential. Results suggests that both levels of downforce may not be enough to minimize row unit movement due to the presence of cover crop and crop residue in the field which resulted in a higher skips (miss index) and (doubles) multiple index which negatively affected the quality of feed index (singulation) and precision index. The quality of feed index defines how close the measured spacing to the nominal spacing (S. D. Kachman & J. A. Smith, 1995) and higher values indicate better planting performance (Fallahi & Raoufat, 2008). On the other hand, lower precision index is a measure of variability on spacing after removing skips and doubles. Lower values indicates better performance of planter (Fallahi & Raoufat, 2008). Such result are consistent with Fallahi & Raoufat (2008) which suggested that high surface residue would affect the performance of seed metering system. Such result indicates the need to apply higher levels of downforce to compress residue into the soil reducing the instances of row units from bouncing too much. Applying both downforce setting on Field B resulted in a lesser spacing variability. Although more uniform spacing is expected on a field with few crop residue and tilled, the presence of soil

clods may have caused row unit bounce which could have affected the consistency of seed placement.

Table 3.3 shows that average plant spacing was can be affected by faster planting speed when planting on no-till field. On both fields, plant spacing is highest at 16.1 kph with variability shows an increasing trend as planting speed increases. Such result are in accordance with the findings of previous studies (Nielsen, 2013; Nafziger, 2009; Staggenborg et al., 2004) which reported increased in PSV at increasing planting speed. These results suggest that seed placement is compromised as the speed of planting increases. The result is non-uniform seed spacing that could be due to inefficiency of metering unit at faster planting speed and row unit vibration which causes the seeds to bounce along the seed tube or during seed placement along the furrow (H Mark Hanna et al., 2010; Staggenborg et al., 2004).

Table 3.3. Mean plant spacing, quality of feed index, miss index, multiple index and precision as influenced by ground speed across three field locations.

Field	Ground Speed	Plant spacing (cm)	PSV (cm)	Quality of feed index (%)	Miss index (%)	Multiple index (%)	Precision index (%)
A	7.2	18.0a	5.8	93.5a	5.3a	1.2a	22.7a
	9.6	18.1a	5.9	88.9a	9.2a	4.3a	25.0b
	12.0	17.5a	6.7	87.6a	7.9a	4.5a	27.3b
	16.1	19.5b	8.9	77.5a	14.8a	7.7a	29.5b
B	7.2	17.6a	4.8	92.0a	4.6a	3.4a	18.3a
	9.6	18.0a	6.0	87.7a	7.0a	5.3a	19.9a
	12.0	18.0a	6.3	88.2a	9.0a	2.9a	21.6b
	16.1	18.3a	7.4	81.9a	9.4a	8.7a	25.4b

Planting up to 12 kph ground speed resulted in a very consistent plant spacing on both fields resulting in a PSV within the optimum and high singulation and low frequency of misses and doubles. However, at 16.1 kph, the load may not be sufficient to minimize vibration of row units increasing the average plant spacing together with the PSV. These

results suggest that within the field conditions of the study, the selected level of downforce for each setting was sufficient to achieve uniform plant spacing when planting up to 12 kph. However, planting at no-till and more than 12 kph ground speed suggests higher load requirement to achieve the desired seed placement uniformity.

3.4.2 Seeding depth

The interaction between ground speed and downforce setting significantly affected the seeding depth across the two field locations (Figure 3.5 and 3.6). Result implies that deeper seeding can be expected with higher downforce setting (D2) at faster ground speed.

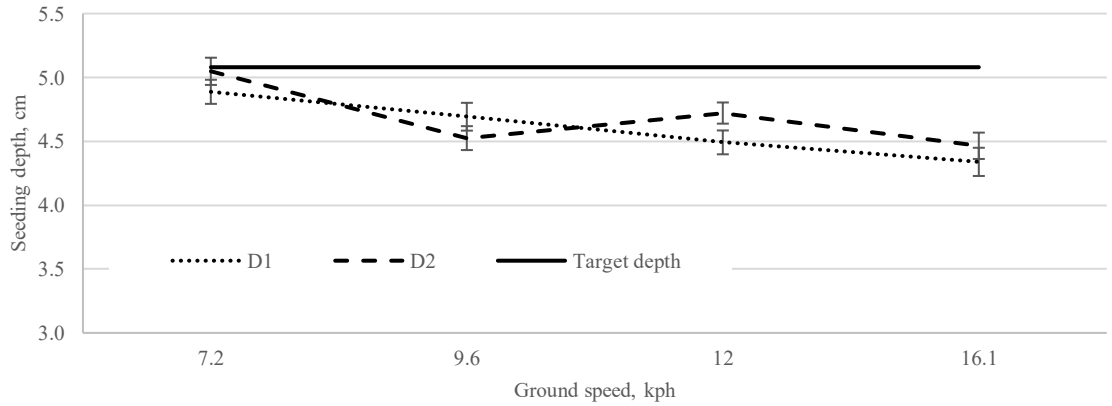

Figure 3.5. Seeding depth response to ground speed and downforce setting in no-till with cover crop field. Error bars indicate the 95% confidence interval for the means.

In the no-till field, no significant difference on seeding depth was observed between downforce settings D1 and D2 at 7.2 and 9.6 kph. Seeding depth tends to get shallower at downforce setting D1 when ground speed increased from 12 to 16.1 kph. For both downforce setting, seeding depth was below the target at 9.6 kph ground speed suggesting implemented GWL was sufficient to maintain seeding depth for the field under this study (Figure 3.5). Such result indicates that GWL may not be able to keep the row units in contact with the ground due to the opening discs requiring additional load for soil

penetration to achieve the desired seeding depth particularly at faster ground speed in a no-till field. Moreover, the presence of surface crop residue may have caused the row units to create non-uniform seeding depth (Buchholz et al., 1993) due to the compressed crop residue which allowed the gauge wheel to "float" resulting in a shallower seeding depth (Morrison & Gerik, 1985). The presence of crop residue and cover crop may have contributed to the shallower seeding depth especially on low downforce setting which may require additional load to compress these materials to allow opening disc achieve the desired depth. Morrison & Gerik (1985) planted corn and sorghum on a no-till field with sorghum and wheat stubbles using a planter row unit implementing a down pressure of 490 to 934 N. Results indicate shallow seeding depth caused by additional thickness created by the compressed crop residues suggesting higher down pressure to minimize variations in seeding depth.

For a strip-tilled field, downforce setting D2 achieve a seeding depth above the target except at 16.1 kph ground speed (Figure 3.6). Such results suggest that the selected downforce setting may be too much for the tilled field under this study resulting in a deeper seeding depth which could also result to sidewall compaction. Similar findings were reported by Fulton et al. (2015) and Hanna et al. (2010) suggesting an increased in actual seeding to the desired seeding depth with an increase in downforce setting. On the other hand, seeding depth for downforce setting D1 was at target at 7.2 kph but gets shallower as ground speed increases. Such result indicates that the selected low downforce setting may be enough for tilled field at slower ground speed but additional load may be required with increase in speed to provide opening disc enough load for proper soil penetration.

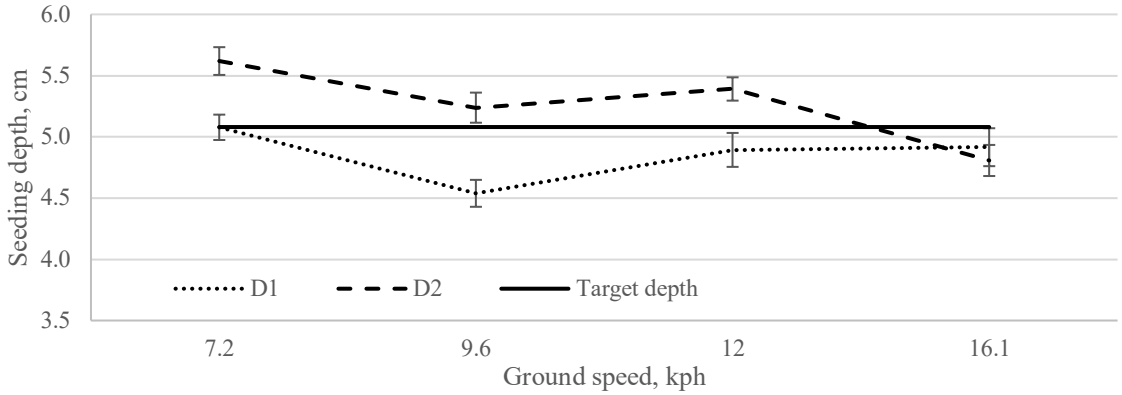

Figure 3.6. Seeding depth response to ground speed and downforce setting in tilled field. Error bars indicate the 95% confidence interval for the means.

For both fields, seeding depth tend to get shallow at faster ground speed which indicate decrease in rolling resistance which prevents the opening disc from penetrating the soil at the desired depth. Such observations were similar with the results reported by Brandelero et al. (2015) and Modernal da Silveria et al. (2011) suggesting excessive soil disturbance at increased operating speed might have caused some soil to be thrown outside of the furrow line thus resulting in a shallower seed placement. Similarly, Modernal da Silveria et al. (2011) reported that shallow depth at faster speed could be due to the inability of the depth control to maintain the target furrow depth as draft requirement decreases with increasing operational speed. Morover, Furlani et al. (2007) also reported that increasing speed would result in reduction draft requirement. This situation may have caused the opening discs to create a shallower trench at faster planting speed.

3.4.3 Row unit vibration and gauge wheel load

Row unit vibration was monitored using an accelerometer which provides the magnitude of row unit movements as shown in g-force (Figure 3.7). Both downforce setting show a nearly consistent GWL application across all planting speeds (Figure 3.7 and 3.8).

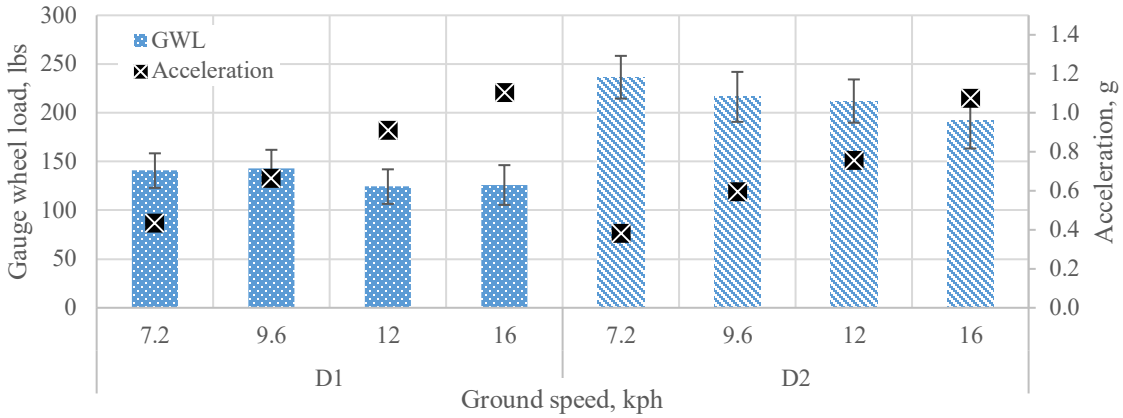

Figure 3.7. Row unit bounce across increasing ground speed for low and high downforce setting in a till field. Error bars represent the 95% confidence interval for the means.

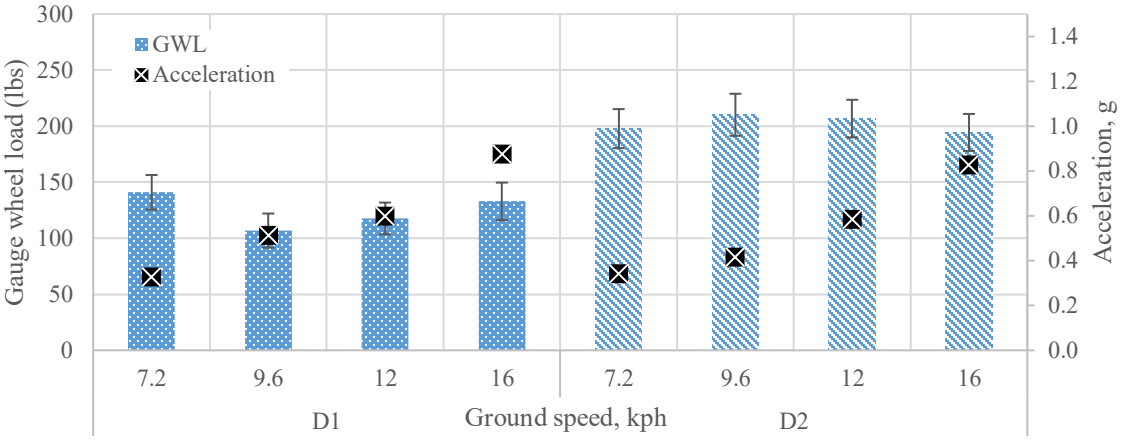

Figure 3.8. Row unit bounce across increasing ground speed for low and high downforce setting in a no till field. Error bars represent the 95% confidence interval for the means.

While GWL stayed relatively the same for D1 and D2 downforce setting on both fields, row unit bounce for increases with speed across. Such result support the work of Staggenborg et al. (2004) who reported that faster planting speed are likely to increase the vibration of the seed metering unit caused by row unit bounce which resulted to increasing variability (coefficient of variation) of the average GWL measurements. Metering unit vibration could influence seed placement uniformity (Staggenborg et al., 2004) and varying load suggest over or under application of GWL which could affect seeding depth. These

results suggests higher downforce settings selection at faster planting speed to implement the optimum amount of GWL which could result in a uniform seed spacing and seeding depth.

3.5 Conclusions

This research provided the following key findings:

First, no difference in plant spacing between downforce settings D1 and D2 corresponding to target GWL of 63 kg and 100 kg. Faster ground speed resulted to wider plant spacing in no-till field. In both fields, seed spacing accuracy as measured by precision index decreases at 9.6 kph or faster ground suggesting that seed placement is compromised as the ground speed increases. Such result could be due to faster planting speed impacting the effectiveness of the metering unit or row unit vibration causes the seeds to bounce along the seed tube.

Second, ground speed and downforce setting influenced seeding depth. Higher downforce setting (D2) selection at slower ground speed achieved the desired seeding depth but consistently getting shallow as ground speed increases in no-till field. With low downforce selection (D1), seeding depth was consistently shallow across all ground speeds. Such result indicate that no till field requires higher downforce selection especially with faster planting speed which will allow opening discs to have enough load to overcome soil resistance in penetrating the soil and cutting across crop residue and cover crops to achieve the desired seeding depth. Likewise, selection of higher downforce will prevent the possible loss of ground contact of row units that may have resulted in shallower seeding depth. On the other hand, deeper seeding depth was attained when implementing high downforce setting with ground speed up to 12 kph on strip-till field suggesting too much

load application that may resulted in side wall compaction. Low downforce achieved the target seeding depth at slower ground speed.

Finally, both settings across two field conditions revealed increasing row unit bounce as planting speed increases. Such conditions are likely to increase the vibration on the seed metering unit which could compromise the ability of the unit to singulate seeds effectively. In summary, results indicate one downforce setting may not be appropriate in between fields considering conditions may vary in terms of soil properties, residue and cover crop management which could result in sufficient load requirement for one field and inadequate load application for the other field. Thus, proper selection of downforce setting for a particular field condition is necessary to achieve uniform seed placement especially at faster ground speed. The effects of the observed variability is seeding depth and plant spacing on yield will be an interesting aspect for future investigations.

Chapter 4 - Row-unit response to active downforce system during planting operations[3]

4.1 Abstract

Implementation of required planter setting determines uniformity of seed placement across highly variable field conditions at planting. Row crop planters equipped with downforce technology allows planting at the desired seeding depth by maintaining optimum level of gauge wheel load to prevent shallow planting depth or soil compaction. This study aimed to evaluate the response of row units on wing, track and non-track sections implementing an automatic downforce system during actual planting operations. Planting was conducted in no-till and strip-tilled fields using a 12-row planter equipped with hydraulic downforce system. Row unit acceleration was assessed in spatial scale at constant 12 kph ground speed and on test strips at 7.2, 9.6, 12 and 16.1 kph ground speeds. Results showed that row unit acceleration on wing, track and non-track sections increase with speed. Highest row unit acceleration was observed on wing sections in both no-till and strip-tilled fields. Strip-tilled soil exhibited lower row unit acceleration by 18% compared to no-till soil. On spatial scale, the active downforce system was able to maintain the gauge wheel load within the target range across row unit sections for only 39% of the total planting time on both fields. Strip tests showed that average real-time gauge wheel load decreases with faster ground speed on both no-till and strip-tilled fields. Gauge wheel load stayed within the target range on every row unit section for both fields with ground speeds increasing from 9.6 to 12 kph. Downforce requirement increases with ground speed greater than 12 kph in no-till field across wing, track and non-track row unit sections and in track section for strip-tilled field. Excessive row unit acceleration potentially affected

seed placement accuracy due to abrupt and erratic movements that interrupted the flow of seeds from the metering system to the ground. The impact of varying row unit vibration with speed on individual row unit sections on seed placement and grain yield would be an interesting aspect to address in future studies.

[3] This chapter will be submitted for publication as a peer-reviewed research paper to the Biosystems Engineering Journal.

4.2 Introduction

Plant growth and development are highly influenced on how seeds are placed in the soil at planting. Consistent seed spacing and depth allows the seeds to have the right moisture and seed-to-soil contact for ideal emergence. To achieve this conditions, proper selection and implementation of planter downforce settings during planting are crucial. Downforce is the amount of load carried by the row unit majority of which are taken up by the opening discs to cut through the soil to the desired depth. The gauge wheels carries the excess load preventing the opening discs from penetrating any deeper thus maintaining the seeding depth. The opening disc can use the excess load on gauge wheels anytime when additional load is needed for soil penetration. However, planting on heavier textured soil (clay) may require greater amount of downforce (Baker et al., 2007) and load on the gauge wheels may be insufficient preventing the opening disc to penetrate the soil to the desired depth causing the gauge wheels to float above ground resulting to shallow seeding depth. On the other hand, soil compaction may happen when the excess load on the gauge wheel is too much (H Mark Hanna et al., 2010). As such, it is important to always maintain an optimum level of load on the gauge wheel to prevent shallow planting or soil compaction. More often, downforce requirement varies across the field due to the inherent spatial field variability. Soil moisture, texture and crop residue are several field conditions that affects openings discs ability for proper soil penetration. Likewise, insufficient load on the row unit could cause low row unit ride quality which could result in uncertain seeding depth and non-uniform seed spacing (Badua et al.,2018b). Ride quality can be defined as the amount of vertical movement row unit experience during planting. Thus, proper downforce selection is critical to achieve desired seed placement consistency.

Currently, downforce are implemented via three systems: Mechanical, pneumatic and hydraulic systems. In a mechanical downforce system, total row unit downforce stays relatively the same during planting. Planters equipped with this system consists of mechanical springs and levers which can be adjusted to determine the appropriate load to be applied to achieve the desired seeding depth. Once set, this fixed load will be implemented during planting across the field. With varying field soil moisture and texture requiring different levels of downforce, the planter may be applying varying downforce during planting which could result in planting at the target depth, shallow depth or compacting the soil. Such situation may occur as operators are not provided any feedback on the effect of field variability on the applied downforce. As such, an active downforce systems using airbags (pneumatic) and hydraulics has been developed to replace mechanical springs. These systems enable operators to adjust the load applied based on the actual field conditions at planting providing a more consistent downforce compared to mechanical spring system resulting in a uniform seeding depth and good seed-to-soil contact across the field. An active downforce control system consists of load cells mounted on each row units providing real-time gauge wheel load signals. The control system automatically adjust the downforce by comparing the load measured by the load cells to a programmed target gauge wheel load. The target load is selected by the operator which is just enough to maintain desired seeding depth without worrying about soil compaction and planting shallow. During planting, the hydraulic or pneumatic system is activated by the control system to either increase or decrease the downforce in order to maintain the target gauge wheel load. The pneumatic downforce system consists of load sensors that can be used to monitor downforce during planting and airbags to adjust downforce by inflating

and deflating based on the load sensor readings. However, response time of this system is slow which sometimes takes up to 20 seconds for the airbags to inflate or deflate to implement the desired downforce adjustment (Bedord, 2015). On these situations, the system could miss areas in the field which may have required more downforce for proper seeding depth. The newest downforce system utilizes hydraulic cylinders and actuators for almost instantaneous adjustments and implementation of the required downforce. When the load cells indicate the need for additional downforce, the actuator responds immediately by increasing the hydraulic pressure providing additional force applied to the row unit.

Evaluation of a planter's automatic downforce system is important for understanding the planter's ability to maintain the applied settings for more uniform seed placement across the field. Currently, assessing a row crop planters' active downforce system ability to implement the desired settings using different scenarios to simulate variable field conditions can be performed using a downforce test stand developed at Kansas State University (Strasser, 2017). The test stand consists of a horizontal platform that can move up and down to simulate changes in field terrain. It is also capable of applying a load to the opening discs to simulate varying soil texture. However, the test stand can only be used for one scenario at a time. Further test is required to fully understand system response on actual field conditions. Results could provide growers better perspective on how individual row units respond to the downforce system implementation during actual field operations. Therefore, this study aimed to evaluate the row unit response to automatic downforce implementation during actual planting operations. Specifically to determine the response of row unit acceleration and real-time gauge wheel load on each

row unit sections on spatial scale at a constant ground speed and on test strips with varying ground speeds.

4.3 Materials and methods

4.3.1 Study site

The study was conducted in 2018 at two production cornfields in Kansas. Field A (Figure 4.1a) was a 72.8 acre field located near Clay Center (39.304310, -97.000470) and Field B (Figure 4.1b) is a 62.8 acre field located near Wamego (39.299486, -96.207226). Field A is adopting a no-till with cover crop field management system and moderate amount of crop residue while Field B adopts a strip-till management system. Both fields practices corn following soybeans crop rotation. Using the USDA Web soil survey, soil type ranges from silty loam to silty clay and moderately well drained soil property.

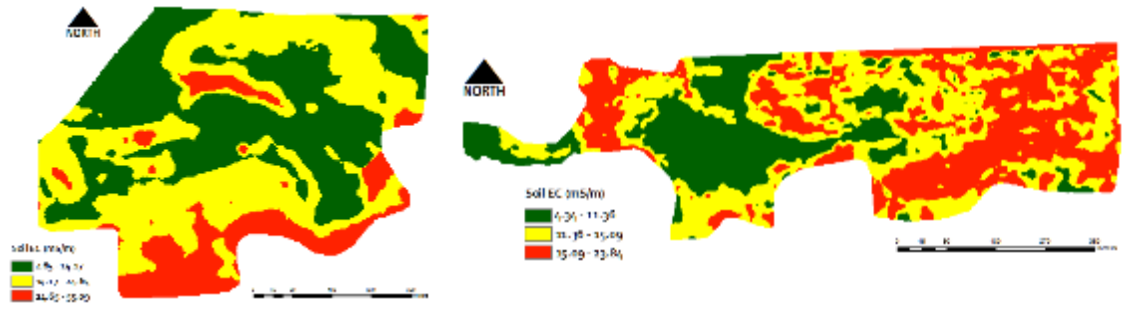

a **b**

Figure 4.1. EC maps of study sites showing the distribution of soil texture across the field.

4.3.2 Planter configuration and data acquisition system

Planting was performed using a 12-row planter (Figure 4.2a) operated using a John Deere 8270R tractor. Planter control functionality was accomplished using a 2630 John Deere (GreenStar-3, Deere and Company, Moline, IL, U.S.A.) field computer connected to

the planter electric control unit, hence forth referred to as ECU, (Horsch Maschinen GmbH, Schwandorf, Germany) through ISOBUS.

a b

Figure 4.2. The (a) row-crop planter used in the study and the (b) segregation of row units in control sections.

The planter was programmed to implement automatic section control with planter row units segregated into four control sections (Figure 4.2b). Control section 1 is the right end of the toolbar comprised of rows 1, 2 and 3 while control section 4 is the right end of the toolbar which include rows 10, 11 and 12. Control sections 1 and 4 is referred herein as wing section (WG). Control section 2 follows the tractor tire tracks refereed herein as track section (TR) consisted of row 4,5, 8 and 9. Finally, control section 3 follows the center of the toolbar referred here in as non-track section (NT) which include rows 6 and 7. Downforce was implemented by manually placing the target GWL in the control monitor and the ECU will determine the amount of hydraulic oil pressure to apply on each control section in order to achieve the desired level of downforce. The system is programmed to maintain the target GWL for each section by adjusting the applied hydraulic pressure when GWL is above or below the target. A current output pressure sensor with 4-20 mA range (HAD 844L-A-0250-161, Hydac, Glendale Heights, IL, USA) was installed in control sections 1, 3 and 4 while control section 2 was fitted with a voltage output pressure transducer (Model KM41, Ashcroft Inc., Stratford, CT, USA) with a linear response range of 0.5-4.5 Vdc. Ground speed and planter position data were simultaneously collected

using a sub-inch accuracy GPS unit (GR5, Topcon Positioning Systems, Inc., Livermore, CA, USA). An accelerometer (Model 3741E1210G, PCB piezotronics, Depew, NY, USA) was installed on row units 1, 5, 7 and 12 (Figure 4.3) to measure row unit acceleration. Row unit planting position was monitored using a potentiometer (Model 424A11A090B, Elabou sensor Technology Inc., Waukegan, IL, USA) mounted on one of the row units.

Figure 4.3. The row units where accelerometers were mounted to measure row unit acceleration

A compact rio (cRIO) real-time controller (9204, National Instruments, Austin, Texas) and modules (National Instruments, Austin, Texas) were utilized in developing the data acquisition system. A custom data acquisition program was developed using LabVIEW to record signals from the load sensors, hydraulic pressure transducers, potentiometers, accelerometers, and GPS. All data were collected at 10 Hz sampling frequency.

4.3.3 Dana analysis

Planting was performed in accordance with typical planting practices of the growers. Tests strips were planted with ground speed varying from 7.2 kph to 16.1 kph. Length of test strip for each field is about 30 m equivalent to a total Average speed during planting on straight rows was 12 kph with slow speed from 7.2 kph to 9.6 kph happening when traversing contours, waterways, terraces and headland turns. Target gauge wheel load

during planting was set at 100 +/- 23 kg. Observation frequency of real-time gauge wheel load and row unit acceleration for each control section was plotted in Microsoft Excel.

4.4 Results and discussion

4.4.1 Planting speed

Ground speed during planting in spatial on both fields are shown in Figure 4.4. Maps show the speed of planting on test strips ranged from 7.2 kph to 16.1 kph. Rest of the field were planted at the typical planting speed of 12 kph with slow speed from 7.2 kph to 9.6 kph happening when traversing contours, waterways, terraces and headland turns. Although planting speed was slower on boundary for Field A which was less than 7.2 kph.

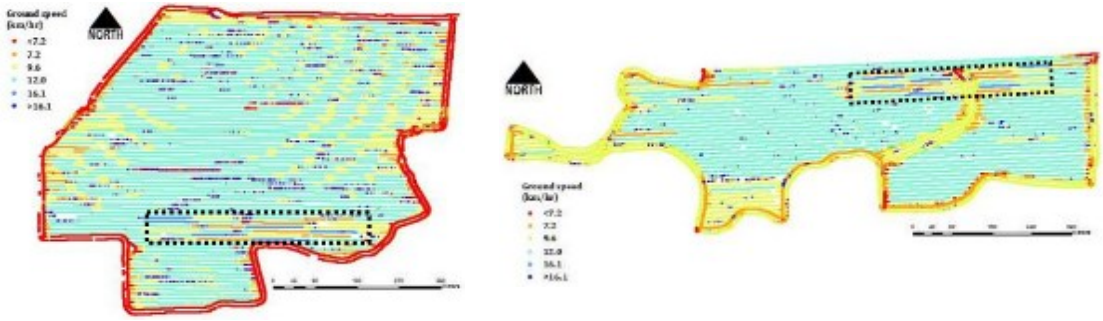

Field A Field B

Figure 4.4. Spatial maps showing speed on strips (inside the boxed area) and for the rest of the field on both fields.

4.4.2 Spatial scale average row unit acceleration

Spatial distribution of average row unit acceleration across the toolbar of the planter for both fields is shown in Figure 4.5. It can be observed that majority of the time average row unit acceleration stayed within 4 to 8 m/s^2 on Field A with few areas showing acceleration of more than 8 m/s^2. Similarly, row unit acceleration on Field B stayed on 4 to 8 m/s^2 range with some areas showing lower acceleration of less than 4 m/s^2. Lower row

unit acceleration on Field B is somehow expected due smoother ride of row units caused by loosed soil structure of strip-tilled field.

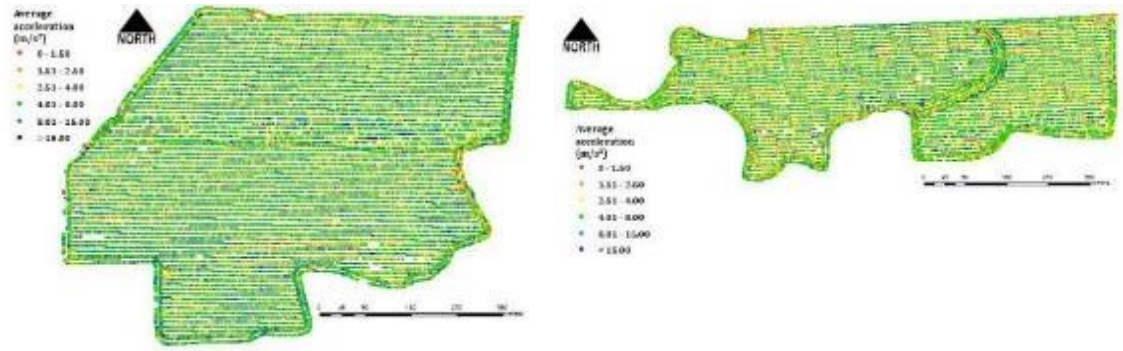

Field A Field B

Figure 4.5. Spatial map of average row unit acceleration on both fields.

4.4.3 Spatial scale row unit acceleration on sections

Figure 4.6 shows the frequency of row unit acceleration across individual row unit sections of the planter for both fields during planting.

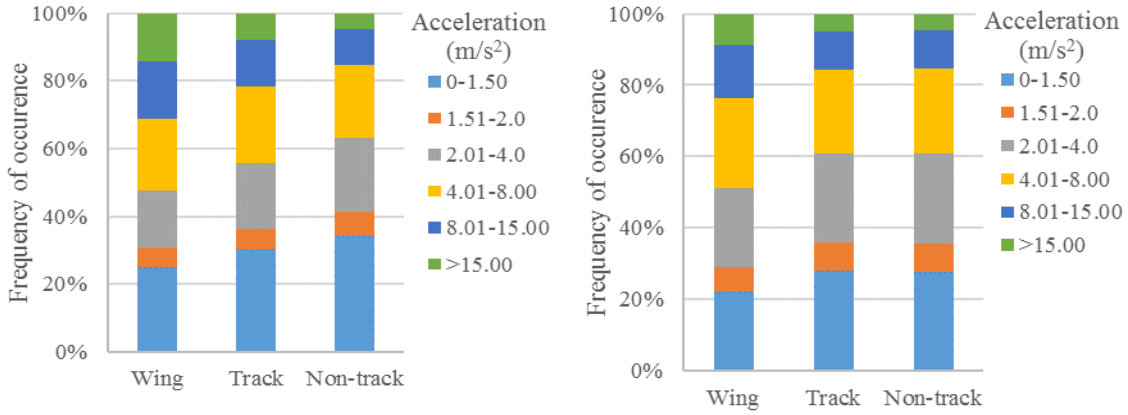

Field A Field B

Figure 4.6. Row unit acceleration distribution for each row unit sections on spatial scale on both fields.

More than 55% of the time row unit acceleration across the row unit sections on Field A was within 2.1 to 4 m/s^2 or below. Wing section experienced higher row unit vibrations as evidenced by the lowest frequency of acceleration within this range with 48%

of the time while non-track sections showed the highest with over 63% of the time. Similar trend can be observed for Field B although results suggests lower row vibrations on row units was as showed by higher frequency of occurrence for row unit acceleration within 2.1 to 4 m/s^2 or below. More than 58% of the time row unit acceleration was within this range with 42% of the time it was within the range of 4.01 to 8 m/s^2 or higher. Again, wing section showed higher row unit vibration with 49% of the time row unit acceleration was within 4.01 to 8 m/s^2 range as compared to non-track section with only 39% of the time.

Summary statistics of row unit acceleration across the three row sections on spatial scale are shown in Table 4.1. On Field A, wing section showed the highest row unit acceleration of 8.56 m/s^2 and variability of 12.07 m/s^2 while track and non-track sections showed the lowest at 6.15 and 5.05 m/s^2, respectively, with almost identical standard deviation. Similarly, row unit acceleration was higher on wing section for Field B although the average and variability were reduced. Row unit acceleration variability in track section was lower compared to non-track section. This could illustrate that in a strip-tilled field, soil compaction of tractor tires along the track sections could smoothen the soil surface potentially lowering the row unit acceleration.

Table 4.1. Summary of row unit acceleration (m/s2) on row sections in spatial scale for both fields.

Row unit sections	Field A		Field B	
	Mean (m/s^2)	Stdev (m/s^2)	Mean (m/s^2)	Stdev (m/s^2)
Wing	8.56	12.07	6.48	8.93
Track	6.15	8.30	4.85	7.08
Non-track	5.05	8.20	5.03	8.18

4.4.4 Row unit acceleration on test strips

Figure 4.7 shows the relationship between row unit acceleration and ground speed across the row unit sections. For both fields, acceleration on each row unit section

increases linearly with speed. Similar findings were reported by Zhai et al. (2019). Higher slope on wing section indicates higher row unit acceleration is expected on wing section as ground speed increases from 7.2 kph to 16.1 kph.

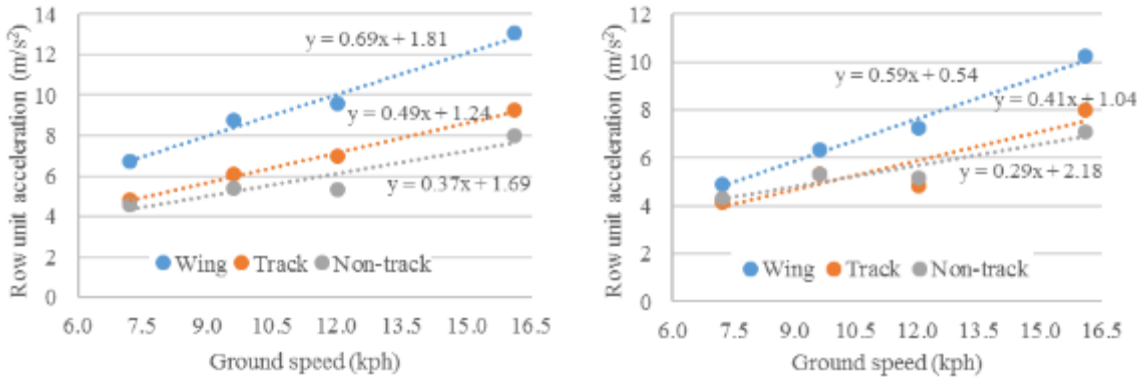

Field A Field B

Figure 4.7. The row unit acceleration as a function of ground speed across row unit sections on both fields.

Such results illustrate how vibration on the wing sections could potentially reduce row unit ride quality due to vertical movement of row unit in response to ground surface irregularities especially when traveling along ground undulations and faster planting speed. Too much row unit vibration especially at higher ground speed could potentially impact seed placement uniformity at planting which could affect plant emergence and total live population. Unlike wing sections, non-track section, which is located on the center of the toolbar, experienced minimal vibration therefore more stable row units resulting in lower row unit acceleration. Moreover, firmer soil on no-till field could also impact row unit ride quality on the tire track control sections. For strip-tilled field, soil compaction of tires on tilled soil smoothens soil surface which could reduce the row unit vibration. This could be one potential reason for comparable row unit acceleration between track and non-track section on strip-tilled field. On average, row unit acceleration was 18% higher in no-till

soil. Such result was in accordance with Baker et al. (2007) highlighting furrow openers experiencing more bounce on no-till soil especially at faster speeds. Abrupt and erratic movements of the row unit when hitting hard spots across the field could interrupt the flow of seeds from the metering system to the ground.

4.4.5 Spatial scale real-time gauge wheel load

The spatial distribution of average real-time gauge wheel load across the planter toolbar for both fields during planting is shown in Figure 4.8. About 55% of the time average real-time gauge wheel load was within the target range of 77 to 122 kg on Field A while only around 40% of the time on Field B.

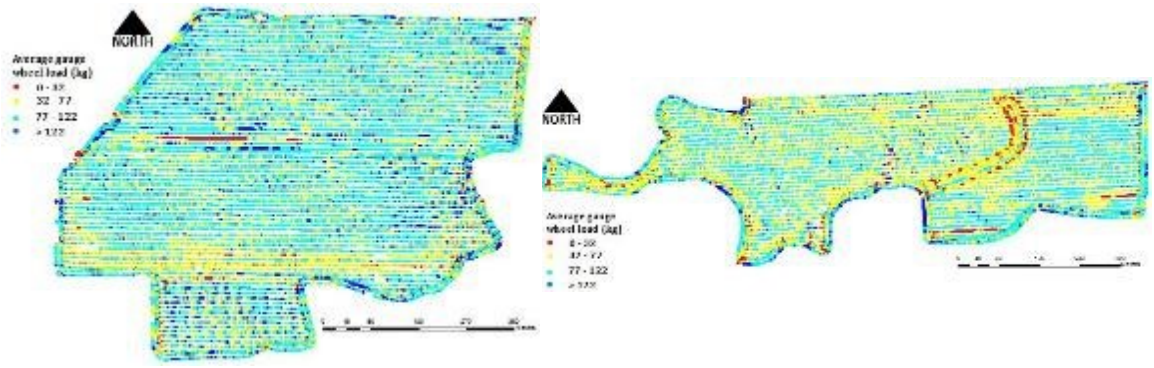

Field A Field B

Figure 4.8. Spatial map of real-time gauge wheel load on both fields.

Figure 4.9 shows the distribution of real-time gauge wheel load across the row unit sections of the planter on both fields.

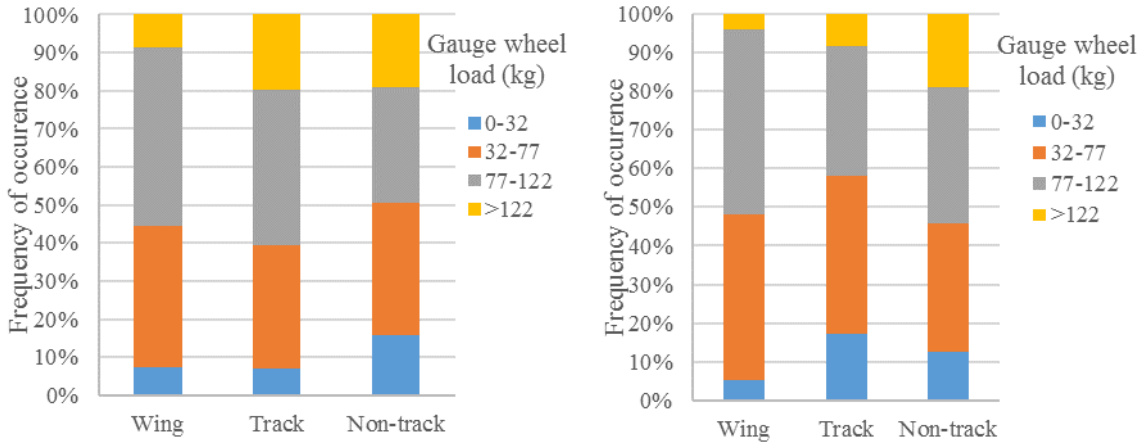

Figure 4.9. Row unit gauge wheel load distribution for each row unit sections on spatial scale on both fields.

Results show that frequency of time average gauge wheel load across row unit sections was within the target range was 39% for both fields. Wing section showed the highest frequency of time with over 47% and 48% and non-track section the lowest with 30% and 36% for Fields A and B, respectively. Although wing section showed the highest row unit acceleration, flexing of the toolbar could have helped absorbed rapid row unit vibrations which allowed the gauge wheel load to stay within a tighter range. Non-track sections may have showed fewer instances of row unit vibration compared to wing section but row units on this section could experience more sudden row unit vibrations as it is located on a more rigid section the toolbar. This result suggests increase in row unit acceleration does not correspond to decrease in gauge wheel load which shows the ability of the downforce system to maintain a uniform gauge wheel load across the toolbar even with varying vibration on row units at nearly constant 7.2 kph ground speed.

Real-time gauge wheel load not concentrated on one gauge wheel load range indicate that the system was not able to respond to changing load requirement during planting. This can be due to the dynamic field conditions causing a significant change of

gauge wheel load measurements for a very short travel distance Badua et al. (2018) and Hanna et al. (2010). Although load for soil penetration on no-till soil is generally higher compared to tilled soil (Baker et al., 2007), results show that the active downforce system was able to provide comparable gauge wheel load across a varying ground resistance on each row unit sections with nearly identical gauge wheel load distribution frequency on both fields.

Table 4.2 shows spatial real-time gauge wheel load across row sections for both fields. Average gauge wheel load ranged from 80.88 kg to 88.46 kg with non-track section showing the highest variability and wing section the lowest. On the other hand, average gauge wheel load on Field B ranged from 70.50 kg to 84.05 kg. Similar on Field A, wing section resulted to lowest variability in gauge wheel load while non-track the highest. Results indicate that planter gauge wheel load on wing sections stayed fairly uniform during planting. On the other hand, non-track section showed higher variability with the highest standard deviation.

Table 4.2. Summary statistics of spatial scale real-time gauge wheel load (kg) on row sections for both fields.

Row unit sections	Field A		Field B	
	Mean (kg)	Stdev (kg)	Mean (kg)	Stdev (kg)
Wing	80.88	29.62	76.99	26.07
Track	88.46	36.97	70.50	36.47
Non-track	80.62	47.64	84.05	44.52

During planting, similar target gauge wheel load was set on both fields. However, no-till field may have required higher load for opening disc penetration which resulted to higher applied hydraulic pressure compared to strip-tilled field. About 40% of the time hydraulic pressure was within 13.81 to 17.20 mPa and about 48% of the time it was within 17.21 to 20.70 mPa range (Figure 4.10). On the other hand, about 80% of the time hydraulic

pressure was within 13.81 to 17.20 mPa on Field B. On both fields, non-track sections showed the highest applied hydraulic pressure which suggests more load is required on rows along the center of the toolbar to achieve the desired gauge wheel load.

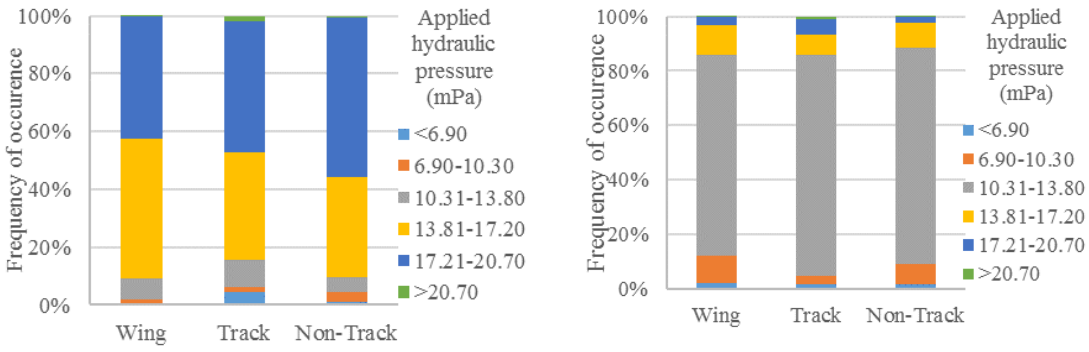

Field A Field B

Figure 4.10. Applied hydraulic pressure across row unit sections on both fields.

4.4.6 Real-time gauge wheel load on test strips

Figure 4.11 presents the effect of ground speed on real-time gauge wheel load across the row unit sections. It appears that average real-time gauge wheel load decreases with increasing ground speed across all row unit sections on both fields. Field A indicates higher reduction in gauge wheel load compared to Field B. Wing and non-track sections shows higher downforce requirement in Field A while wing and track sections in Field B. Since Field B is strip-tilled, the effect of losing gauge wheel load at increasing speed is more visible on Field A as no-till field requires higher load for soil penetration.

Results indicates the potential correlation between row unit acceleration and gauge wheel load which highlights the importance of selecting the ideal downforce for a specific speed of planting to minimize row unit vibration. Previous study have shown that row unit bounce impact uniformity of seed placement (Zhai et al., 2019; Badua et al., 2018 & Staggenborg et al., 2004). The increased row unit vibration with speed on individual row

unit sections could also influence on seed placement uniformity which represents the need for future research.

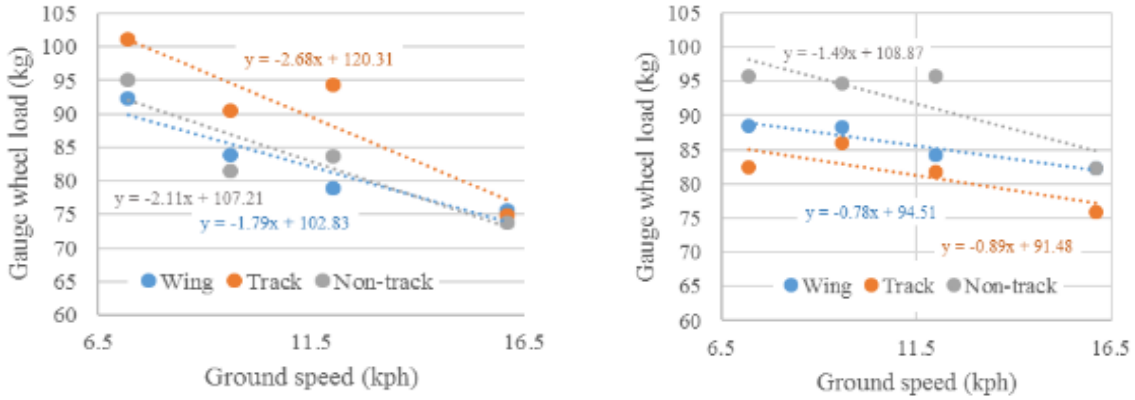

Field A Field B

Figure 4.11. Real-time gauge wheel load as influenced by ground speed across row unit sections on both fields.

4.5 Conclusion

Results of the study revealed the following conclusions:

1. Row unit acceleration on wing, track and non-track sections increases with speed.
2. Highest row unit acceleration was observed on wing control sections on a no-till and strip-tilled field.
3. Strip-tilled soil exhibited lower row unit acceleration by 18% compared to no-till soil.
4. On spatial scale, the active downforce system was able to maintain the gauge wheel load within the target range across row unit sections for only 39% of the time on both fields.
5. With varying ground speed on strip tests, the active downforce system showed its ability to maintain the desired gauge wheel load within the target range on each row unit section on no-till field for ground speeds ranging from 9.6 to 12 kph. Gauge wheel

load on strip-tilled field stayed within target range on wing and no-track sections across all ground speeds. Downforce requirement increases at 16.1 kph ground speed for no-till field across all row unit section and on track section for strip-tilled field.

Chapter 5 - Sensing system for real-time measurement of seed spacing, depth and geo-location of corn: A proof-of-concept study[4]

5.1 Abstract

Proper seed placement during planting is critical to achieve uniform emergence which optimizes the crop for maximum yield potential. While uniform plant spacing and seeding depth are often used by corn growers to determine the performance of precision planters, these parameters can be influenced by factors other than machinery such as seed germination, insects, diseases and soil properties (e.g., temperature, moisture). Currently, the ideal way to determine planter performance is to manually measure plant spacing and seeding depth. However, this process is both cost- and labor-intensive and prone to human errors. Therefore, this study aimed to develop and test a proof of concept sensing and measurement (SAM) system to measure seed spacing and seeding depth and providing the geo-location of each planted seed. The system consisted of a high-speed camera, light section sensor, potentiometer and survey grade real time kinematic (RTK) global positioning system (GPS) unit. Results demonstrate the potential of the proof of concept SAM system for measuring seed spacing, seeding depth and geo-location of corn seeds. Results showed that seed spacing can be calculated using the generated stitched images achieving a root-mean squared error (RMSE) of 0.63 cm and a coefficient of determination (R2) of 0.87 when compared to actual seed spacing measurements. Likewise, 98% of the recorded seeding depth was within the acceptable tolerance ±10% error. Finally, GPS

coordinates were recorded for individual images which can be used to locate individual seeds and provide detailed information on missing plants (no seeds).

[4] Results have been published as a peer-review paper. Badua, S.A., Sharda, A., & Flippo, D. (2019). Sensing System for Real-time Measurement of Seed Spacing, Depth and Geo-location of Corn: A Proof-of-Concept Study. *Trans. of the ASABE*, 62(6). https://doi.org/10.13031/trans.13593

5.2 Introduction

Corn is one of the primary agricultural commodities in the United States, accounting for more than 13% of the total area planted with crops (USDA-ERS, 2017b). Total production was 15.1 billion bushels in 2017 which is equivalent to an average operating cost of more than $41 billion spent by corn growers (USDA-ERS, 2017b). However, cash income from corn sales in 2017 is expected to be 0.7% or over $0.3 billion lower than in 2016 and has been continuously declining since 2013. In addition, it is projected that acres planted for corn will be reduced by over 9% in the next 10 years (USDA, 2017), consequently decreasing projected corn production (USDA, 2019). With the current high production costs, continuous decline of corn receipts (USDA-ERS, 2017b) and projected reduction in production area and yield, more growers are relying on precision agriculture technologies to cut costs or improve savings, maximize land area and improve yield to sustain farming productivity.

Planting is one of the most critical stages in crop production because it is at this stage where there is an opportunity to place seeds in conditions for uniform emergence setting the foundation for attaining maximum yield. Proper seed placement will provide an ideal environment for germination and growth. As such, uniform seed spacing and seeding depth are two of the most essential parameters to be achieved during planting. Uniformity of spacing and depth could result in a final seeding rate with the desired plant density and uniform emergence. Studies have shown the influence of multiple plants, non-uniform plant spacing, delayed emergence and uneven seeding depth on grain yield. Chim et al., (2014) conducted a controlled experiment to evaluate effects of varying plant spacing and plants per hill on corn yield. Results suggested greater grain yield at narrower uniform

plant spacing with one plant per hill. However, wider uniform plant spacing resulted in a greater yield when the number of plants per hill is increased. Likewise, non-uniform plant spacing caused by multiple or missing plants measured by the spacing standard deviation presented varying effects on corn yield. Nielsen (2001) suggested a significant difference on yield across the different plant spacing variability (PSV) treatments. An average of 106.7 kg ha-1 yield loss is reported for every 2.5 cm increase in standard deviation (SD) of plant spacing. Similar results were reported by Krall et al. (1977) where yield continuously decreased with increasing spacing variability at two different study areas. Previous studies showed that reducing the spacing standard deviation by 2.5 cm could result in an average yield increase of 213.4 kg ha-1 (Doerge & Hall, 2002) and 395.4 kg ha-1 when spacing standard deviation was reduced by 5.1 cm (Nielsen, 2001). Thus, improving planter performance by reducing seed spacing variability is important for improving corn productivity. Furthermore, variability in seeding depth can affect emergence. Knappenberger & Koller (2012) reported that emergence of corn was significantly correlated with seeding depth, with deeper placement resulting in greater emergence due to favorable soil and moisture conditions for seedling emergence. Grain yield was affected when seeds emerged unevenly. Thomison et al (2012) conducted a two-year study on effects of seeding depth on yield of corn, demonstrating a 13% to 40% yield difference between shallow and deep planting depths, respectively. Observed yield effects for the shallow planting depths were due to reduced final plant density, potentially caused by slow and uneven emergence.

While uniform plant spacing and seeding depth are often used by corn growers to determine the performance of precision planters, these parameters can be influenced by

other factors which are not machine related such as germination percentage, diseases and various soil properties. The ideal way to determine planter performance is to measure seed to seed spacing (Nakarmi & Tang, 2012) and ability to maintain a consistent actual depth during planting (Poncet et al., 2018). Post emergence, seed spacing can be measured through emerged plants whereas seeding depth measurement by manually digging emerged plants and measuring the distance of the seed to the ground level. Each year, agronomists, service professionals, producers and engineers manually measure seed spacing and depth on a high number of plants to validate the accuracy of the planting systems. Thus, automating the process will be critical to improve the effectiveness, efficiency and on-demand real-time measurements as manual process is labor-intensive, time-consuming, and highly susceptible to errors.

Computer vision and image-based technologies have been widely utilized in agriculture to automate various crop production activities and measurement applications. One of the most utilized techniques in image processing is image mosaicking. This technique is used to combine overlapping images using common points and creating a single image with a wider field of view. Creating a mosaicked image can be done using a direct or feature based algorithms (Ghosh & Kaabouch, 2016; Fathima et al., 2013 & Jain & Shandliya, 2013). Direct methods work by finding a consistent set of correspondence and calculating correlations between features in the image using all pixels and is usually performed using a correlation matrix (Renuka, 2016). This method is useful when mosaicking images with large regions of overlaps including small translations and rotations (Jain & Shandliya, 2013; Prados et al., 2014; Renuka, 2016) but it requires complex calculation (Fathima et al., 2013). Feature based methods find distinct low level features

such as edge, corner or pixel between two images (Ghosh & Kaabouch, 2016b) and matching them together to form a global correspondence (Fathima et al., 2013). This process reduces the computational complexity (Renuka, 2016) and usually handling images with small regions of overlap (Jain & Shandliya, 2013; Renuka, 2016) and detection of common features is possible even at changing geometric viewpoints (Ghosh & Kaabouch, 2016b). Sanchiz et al (1996) proposed a vision system to automate the application of chemical treatments on cabbage. A camera was mounted on an agricultural vehicle to track plants and apply treatments accurately. A Kalman filter was used to estimate the plants exact location in the field and a feature-based algorithm called Hough transform was performed to cluster regions for plant identification using consecutive image frames that consisted of complete view of the object of interest. Similarly, Shrestha et al (2004) used a feature based method of image mosaicking in developing a sensing system using a video camera to measure corn plant density (stand) at early growth stage. The image sequencing algorithm was developed to match common attributes of two images before separating plants from other non-plant regions using an image segmentation method based on color intensities of surface influenced by changing lighting conditions. On the other hand, Tang & Tian (2008) implemented a direct method in the development of a machine vision-based system to reconstruct an image for automatic measurement of corn plant spacing. Real time video frames, captured using a video camcorder, were mosaicked using a correlation based matching algorithm by combining two overlapping consecutive video frames and successfully created reconstructed segments of the test rows. Furthermore, numerous studies have investigated other applications of machine vision technologies in agriculture such as plant health and growth assessment (Kacira & Ling, 2001) plant

diseases (Garcia & Barbedo, 2013) and weed detection (Nejati et al., 2008; Tang et al., 2000). However, no studies have been published which can automatically measure the actual seeding depth and seed spacing using an imaging system during planting operation. Automating the process could provide significant information on the movement and location of the seeds in the furrow, automatically obtaining seed spacing and depth; planter performance, and implementing appropriate planter control and feedback to optimize planter functionality. Therefore, the objective of this study was to develop a sensing and measurement (SAM) system to measure real-time seeding depth, seed spacing and seed localization during planting. Specifically, the secondary objectives of this study were to determine the performance of the system to 1) stitch captured real-time images of individual seeds planted, (2) measure seed spacing using the stitched image, (3) record actual seeding depth during planting, and (4) provide GPS coordinates of individual images for geo-locating seeds.

5.3 Materials and Methods

5.3.1 Image acquisition and seed-geo location

Images were acquired using a high-speed camera (acA640-750uc, Basler AG, Ahrensburg, Germany) fitted with a C-mount lens with a fixed focal length of 4 mm and aperture range from F1.8 - F22 (C125-0418-5M, Basler AG, Ahrensburg, Germany). The camera lens provided a field of view (FOV) corresponding to an image size of 15.7 cm by 11.7 cm at a distance of 20.3 cm between the lens and the ground. The high-speed camera was selected over a regular camera because it is inexpensive and capable to be synchronized with the data acquisition system using the NI Measurement and Automation Explorer (MAX) installed in LabVIEW (National Instrument, Austin, TX, USA).

Moreover, its frame rate provides flexibility to scale measurements for further studies. The camera was connected to a control laptop computer (Latitude 14 3470, Dell, Round Rock, TX, USA) with a 2.5 GHz Intel Core i7-6500U CPU (Intel, Santa Clara, CA, USA) and an 8 GB installed memory (RAM) through the USB 3.0 interface. Exposure time was set at 488 microseconds (μs) to prevent capturing blurred objects or features on the images. Since the amount of light is proportional to the exposure time, an LED strip tape (4NFLS-x2160-24V, SBL, St. Louis, MO, USA) was used to provide additional lighting to illuminate features or objects of interest on the ground. To ensure the camera will capture more than 50% overlap on the images for effective image stitching, the high-speed camera was configured to transmit and record at 10 fps at a bit rate of 92 MB/s over a USB 3.0 interface using the Pylon Viewer (Basler AG, Ahrensburg, Germany). Image resolution is about 0.3 Megapixel with pixel dimension of 656 x 496 pixels. Likewise, the Horsch Terminal ME controller (Horsch LLC, Mapleton, North Dakota) was programmed to plant corn at 103,200 seeds/hectare seeding rate which corresponds to a seed spacing of 12.7 cm. A narrow seed spacing was selected for this study to enable to capture at least one non-identical seed per image compensating for overlap and seed bounce.

An RTK GPS unit consisting of a rover receiver and base station (GR5, Topcon Positioning Systems, Inc., Livermore, CA, USA) with an RTK accuracy of H: 5.0 mm + 0.5 ppm, V: 10 mm +0.8 ppm was used to provide the geo-location for each captured image. Since the distance of the base station from the rover was always close to 50 m, the degradation in accuracy was considered to be negligible. The row unit was mounted on a gantry placed on a customized cultivation assessment test apparatus (CAT App) (Figure 5.1) which consists of row unit toolbar that can be raised/lowered and moved back/forth

along the 12.2-m long rails by a 31 HP gasoline engine (Vanguard, Briggs and Stratton, Wauwatosa, WI). A four-wheel drive tractor (LA1251, Kubota, Grapevine, TX) was used to pull and move the CAT App within the field during testing.

Figure 5.1. The cultivation test apparatus where testing of the SAM system was performed.

A separate program controlled the speed of the engine which was programmed to run the gantry at a constant ground speed of 6.4 kph for all the tests. During testing, the closing wheels of the row unit were raised to prevent it from closing the furrows. Raising the closing wheels exposed the planted seeds allowing the manual measurement of seed spacing. Measured spacing was then compared to the calculated seed spacing using the SAM system. Accuracy was determined using the root mean square error (RMSE) using equation 1 where n is the sample size, y_i is the measured seed spacing and y^_i is the calculated seed spacing.

$$\text{RMSE} = \sqrt{\frac{\sum_{i=1}^{n}(\hat{y}_i - y_i)^2}{2}} \quad (1)$$

5.3.2 Image stitching

A feature based matching algorithm (Vedaldi & Fulkerson, 2008) was used to combine captured images to create a panoramic image for seed spacing measurement. The scale invariant feature transform (SIFT) algorithm is an effective tool to extract common feature points and perform matching between two images with significant overlap and invariant to noise, occlusion and illumination changes. The matching algorithm developed in MATLAB (R2017a, Natick, MA, USA) was used to find corresponding points between the reference image and the image to be matched. There are five steps on how the algorithm is implemented as outlined by Ghosh & Kaabouch (2016) and Lowe (2004). These are scale-space construction, scale space extrema detection, keypoint localization, orientation assignment and keypoint descriptors. The first step involves the construction of scale space by generating several octaves or blurred images from the input image by applying a Gaussian filter or Gaussian blur operator to reduce noise and image details. Mathematically, this can be expressed by equation 2 as defined by Lowe (2004).

$$L(x, y, \sigma) = G(x, y, \sigma) * I(x, y) \quad (2)$$

where $L(x, y, \sigma)$ is the blurred image, $*$ is the convolution operator, $G(x, y, \sigma)$ is the Gaussian blur operator and $I(x, y)$ is the input image. Next step was detecting key feature points in the scale space using a difference-of-Gaussian (DoG) operation by calculating the difference of two adjoining blurred images, L, using equation 3 as defined by Lowe (2004).

$$D(x, y, \sigma) = G(x, y, k\sigma) - L(x, y) \quad (3)$$

where k is a constant multiplicative factor. Keypoint candidates in a stack of DoG images are detected by comparing a pixel to its neighboring pixels at the current and adjacent scales

(Figure 5.2). This process generated low contrast keypoints or extrema located on an edge which are then eliminated to improve matching efficiency of the algorithm.

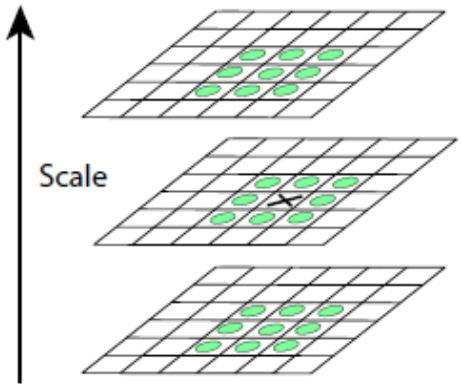

Figure 5.2. Keypoint detection in a stack of DoG images (Lowe, 2004).

Assigning an orientation for the keypoint is done to provide rotation invariance. This process was done by assigning the dominant orientation to the keypoint based on gradient directions and magnitude around it. The orientation, θ (x , y), for each image, L(x,y), is calculated using equation 4 defined by Lowe (2004).

$$\theta(x, y) = \arctan\left((L(x, y+1) - L(x, y-1)) / (L(x+1, y) - L(x-1, y))\right) \quad (4)$$

This procedure resulted in an orientation histogram where dominant local gradient orientations were identified and used to create a keypoint with that orientation. The last step is computing a descriptor or a fingerprint of the keypoint to differentiate it from other keypoints generated.

Recognizing distinct features or objects in an image is performed by first matching each feature or keypoint independently to the database of keypoints extracted from a reference image. However, many of these initial matches will be incorrect due to some outliers or indistinguishable features that arise from background noise in the image. Thus, a random sample consensus (RANSAC) algorithm was used to remove false matches or

outliers and created a transformation or homography matrices which was used to stitch two overlapping images producing a stitched image.

5.3.3 Spatial calibration

After generating the stitched image, a process called simple spatial calibration was performed to determine the relation of image pixels to real-world units. By using an imagery with two seeds of known spacing or distance, this distance in pixels was calculated by a spatial calibration algorithm developed in MATLAB using the Euclidean distance formula as shown in equation 5.

$$d = \sqrt{(x_2 - x_1)^2 + (y_2 - y_1)^2} \quad (5)$$

where d is the number of pixels between the two objects in the image, (x_1, y_1) is the coordinate of the first object and (x_2, y_2) is the coordinate of the second object. The derived conversion factor from the spatial calibration was then added in the seed spacing algorithm that was used in the calculation of the seed spacing. The spatial calibration process is outlined in Figure 4.

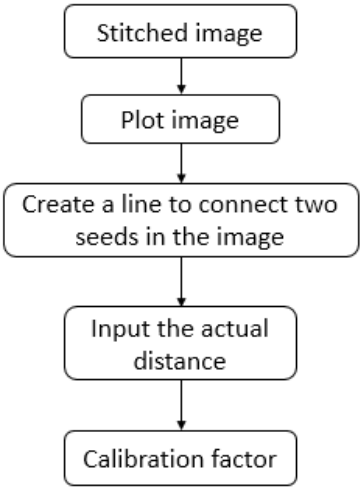

Figure 5.3. The framework of the spatial calibration algorithm.

5.3.4 Seed spacing calculation

Once spatial calibration is done, two succeeding images were stitched and the seed spacing was measured using the seed spacing algorithm. The algorithm calculates the spacing in pixels then multiplied to the calibration factor. This process was done independently for each stitched image.

5.3.5 Seeding depth measurement

A light section sensor (OXH7-Z0150.HI0720.VI short, Baumer Electric AG, Frauenfeld, Switzerland) was used to record the seeding depth. The sensor (Figure 4) is capable of measuring height difference between the lowest and highest point on the ground using a laser. As long as the sensor is fixed in one position, it can accurately measure height difference of 50 mm which is its maximum measuring depth. Thus, the SAM system can only measure depths of up to 50 mm. However, once the light section sensor moves either upward or downward from its position, the depth readings varies. To address this problem, a potentiometer (model 424A11A090B, Elobau sensor technology, Inc., Waukegan, Il, USA) with a linear response of 4 to 20 mA and 12 mA as the center position was used to determine the correction on depth readings based on changes in row unit vertical movement. A laboratory set up (Figure 5.4) was constructed to develop a linear relationship between the light section sensor and the potentiometer at changing potentiometer positions, corresponding to row unit movement, using 12 mA as the reference position. Recorded data were plotted in Microsoft Excel to generate linear functions (Figure 5.5) where seeding depth measured by the light section sensor was the response variable and the measuring position measured by the potentiometer as the predictor variable. Two linear functions were generated where one linear function (Figure 5.5a) represented downward

movement of row unit and the second linear function (Figure 5.5b) indicated upward movement of row unit. The slope of the generated linear functions represented the amount of change in seeding depth for every unit change in the vertical position of the row unit. These equations were used to adjust the measured seeding depth of the SAM system due to row unit vertical movement. To illustrate, during testing the data acquisition system records the row unit movement using the potentiometer. The recorded value was then subtracted to the reference position which is 12 mA. The difference was then used to calculate the correction needed to adjust the seeding depth due to the row unit movement using the linear equations. The correction was added or subtracted, depending whether row unit moved upward or downward, to the measured seeding depth of the SAM system to obtain the correct seeding depth. After the tests, seeding depths of planted seeds were manually measured which was then compared to the seeding depth obtained from the SAM system. A seeding depth error of ± 10% between the measured and recorded seeding depth was considered acceptable for the SAM system to provide a considerable seeding depth measurement confidence. The % error was calculated using eq. 6.

$$\%error = \left(\frac{D_M - D_R}{D_R}\right) x100 \quad (6)$$

where *% error* is the is the seeding depth error, D_M is the measured seeding depth using SAM system and D_R is the recorded (actual) seeding depth.

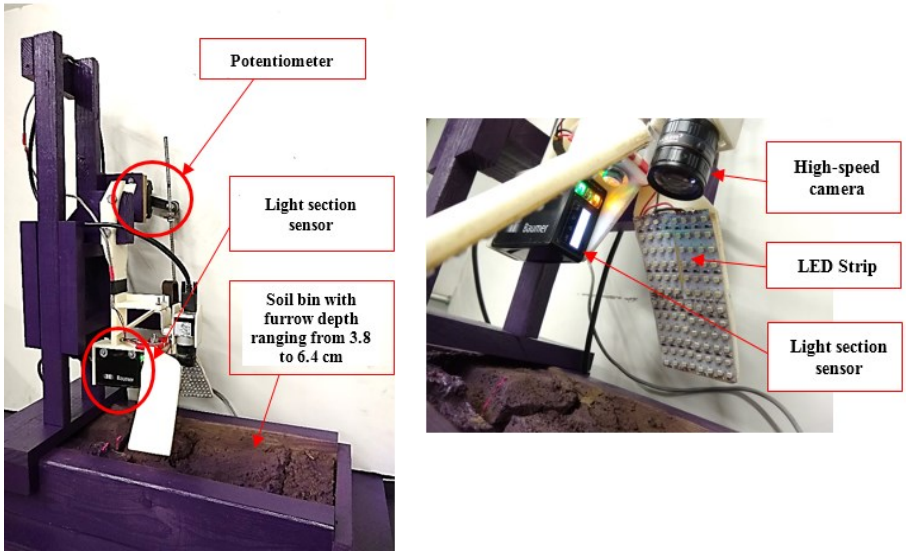

a **b**

Figure 5.4. The laboratory set up (a) for calibrating the light section sensor and (b) components of the system.

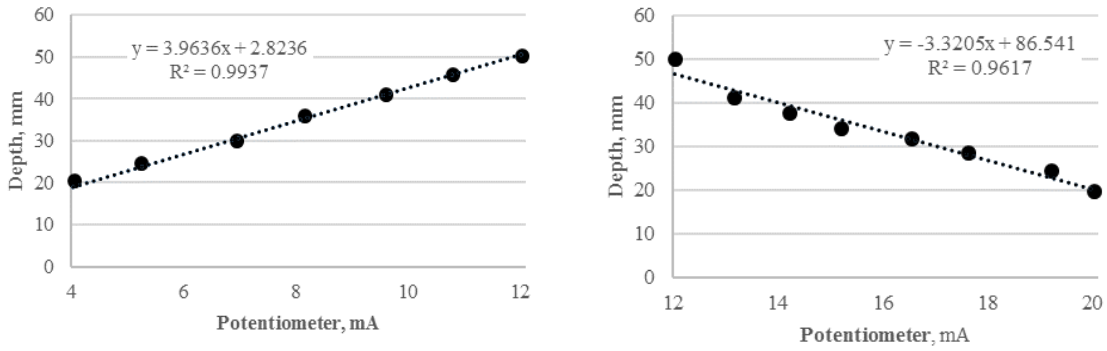

a **b**

Figure 5.5. The two linear functions fitted between recorded depths of the light section sensor versus the potentiometer readings during laboratory tests. Linear function (a) is when potentiometer reading was 12-4 mA suggesting downward movement of row unit and linear function (b) is when potentiometer reading was 12-20 mA indicating upward movement of row unit.

5.3.6 Sensing and measurement system setup

The developed SAM system used to measure seed spacing, depth and geo-location of corn is composed of a high-speed camera, light section sensor, LED light strip, potentiometer, GPS, data acquisition system and a control computer (Figure 5.6).

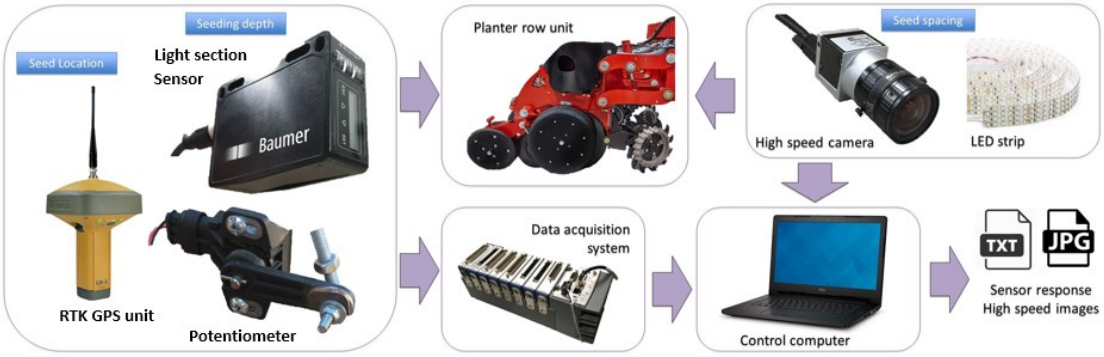

Figure 5.6. The components of the developed measurement system to record seed spacing, depth and geo-location of corn.

The camera, light section sensor and the LED light strip were mounted on a 3D printed frame placed between the gauge wheels and the closing wheels (Figure 5.7).

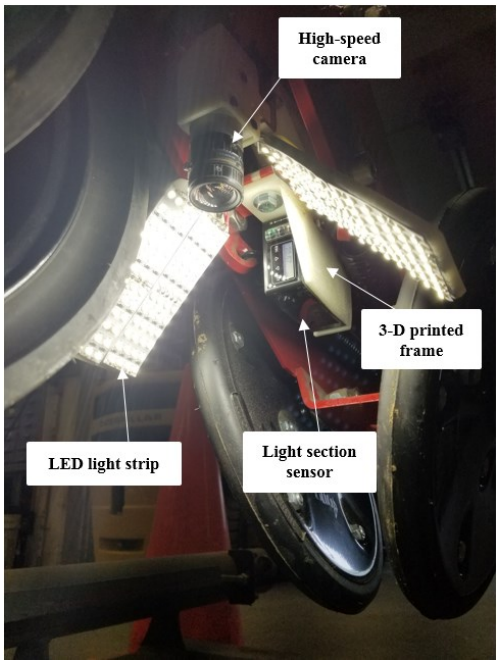

Figure 5.7. The location of the SAM system in the row unit.

All components were interfaced such that the high-speed camera was oriented to face the furrow and aligned vertically with the RTK GPS rover receiver mounted on top of the row unit. The light section sensor is placed beside the camera which allows it to record

the depth of planted seeds. The potentiometer was rigidly mounted on the toolbar using a 25.4 mm x 3.2 mm steel flat bar as a support while the rotating arm is connected to the parallel linkage using a 6.4 diameter steel rod. (Figure 5.8).

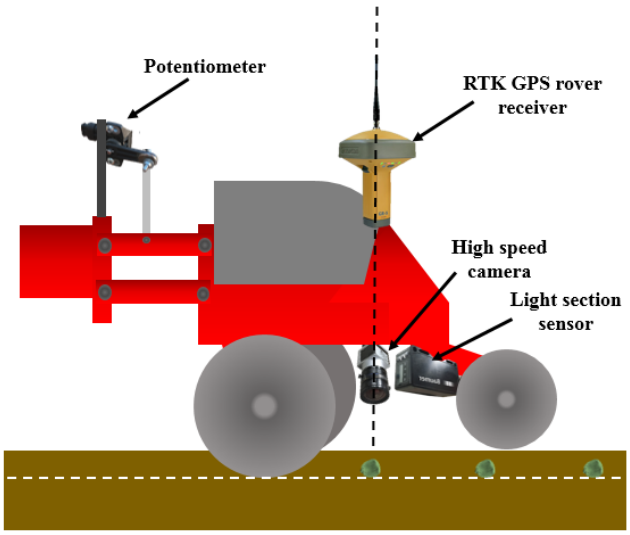

Figure 5.8. Diagram showing how the components of the SAM system are placed on the row unit.

The system consists of two separate LabVIEW programs simultaneously collecting data at 10 Hz. The first program was used to record seeding depth and geo-location that outputs data in a .txt file and the second program was used to capture images of seeds planted which outputs data in a .jpg file. As the system is initiated, the high-speed camera captured images of individual seed, the light section sensor recorded seeding depth, the potentiometer measured row unit vertical movement and the GPS unit acquired geo-locations simultaneously and saved them onto an external hard drive (Transcend, Orange, CA). Thus, each image which ideally should have one seed consisted of a data on seeding depth, row unit movement and geo-location.

5.4 Results and discussion

5.4.1 Seed spacing

The test location was a no-till field at the North Agronomy Farm at Kansas State University with average soil moisture content during tests of 19.1% volumetric water content, ranging from 18.0% to 20.8%. Because the objective of this study is to determine the functionality of the SAM system, the selected field was relatively flat and removed most residues thus creating an ideal test condition to evaluate performance of the system. After each test runs, actual seed spacing was manually measured by laying a measuring tape along the furrow. The measured seed spacing was used to calculate the error using the SAM system. An example of two consecutive images with overlap used in spatial calibration is shown in Figure 5.9.

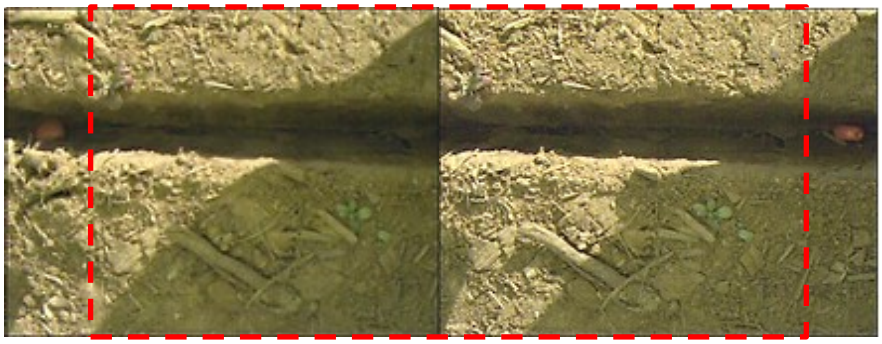

a **b**

Figure 5.9. An example of the overlap (red window) between the (a) reference image, (b) the target image.

The image stitching algorithm used the overlap area between two images as the matching window to extract common features to determine the correspondence between the two images before combining them into one single stitched image (Figure 5.10). After generating the stitched image, the spatial calibration was performed resulting in a pixel-to-

actual distance calibration factor converting a pixel into basic unit of measurement. This procedure resulted in a calibration factor of 0.022 cm per pixel (Figure 5.11).

Figure 5.10. The generated stitched image

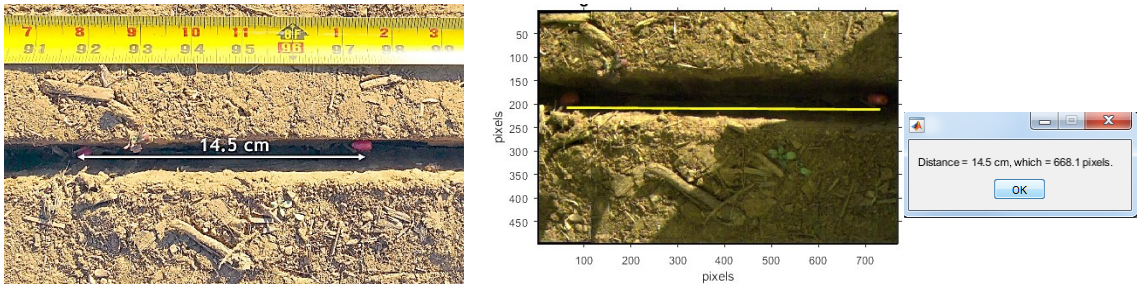

a **b** **c**

Figure 5.11. (a) The known spacing and (b) the image used is spatial calibration and (c) the calibration value.

Another set of two successive images was stitched (Figure 5.12) to calculate the seed spacing (Figure 5.13).

a **b** **c**

Figure 5.12. A set of images (a and b) stitched together creating an image (c) for seed spacing measurement.

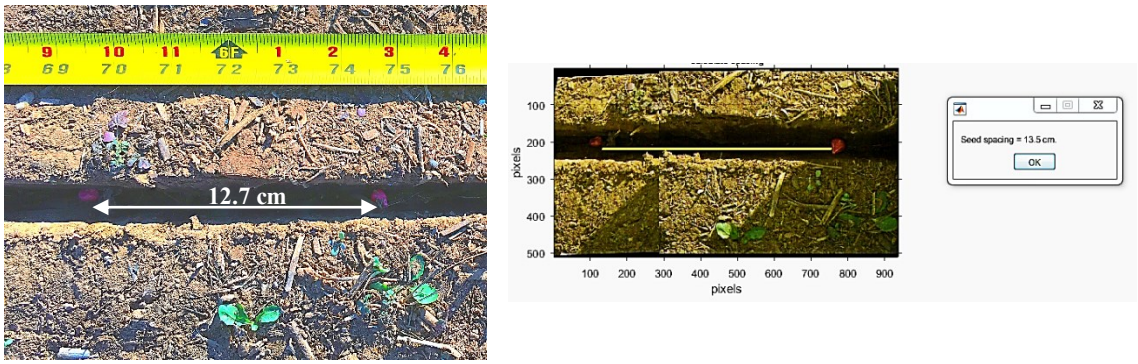

a **b**

Figure 5.13. The (a) actual seed spacing and (b) measured seed spacing using the stitched image.

Results of the field tests showing the seed spacing measured using the SAM system and manual measurements are presented in Table 5.1. The RMSE was used to measure the SAM system accuracy and the estimated or calculated spacing were regressed to actual spacing measurements to determine the models' coefficient of determination (R^2). Overall, the system was able to achieve an RMSE of 0.63 cm and an R^2 of 0.87. Measurement errors shown by the residuals can be caused by several factors which consists of distortion of acquired images caused by the camera lens and potential human errors during manual measurement of actual seed spacing.

Table 5.1. Seed spacing test results (RMSE=0.63 and R^2=0.87).

Actual seed spacing, cm	Distance, pixel	Conversion factor, cm/pixel	Calculated seed spacing, cm	Residual, cm
12.7	425	0.028	13.5	-0.8
11.9	410	0.028	11.5	0.4
14.5	490	0.028	13.7	0.8
10.7	370	0.028	10.4	0.3
12.7	425	0.028	11.9	0.8
11.7	410	0.028	11.5	0.2
10.9	420	0.028	11.8	-0.9
11.4	420	0.028	11.8	-0.4
14.7	480	0.028	13.4	1.3
13.2	460	0.028	12.9	0.3

Actual seed spacing, cm	Distance, pixel	Conversion factor, cm/pixel	Calculated seed spacing, cm	Residual, cm
10.4	350	0.028	9.8	0.6
12.4	450	0.028	12.6	-0.2
8.9	325	0.028	9.1	-0.2

5.4.2 Seeding depth

The recorded and measured seeding depths are shown in Figure 5.14. Recorded seeding depth are from the SAM system while measured seeding depths are actual seeding depths collected during the experiment. Measured seeding depth varied from 40 mm to 47 mm while recorded seeding depth varied from 42 mm to 47 mm. Discrepancy between the recorded and measured seeding depth can be due to the accuracy of the quadratic line model to predict the correction for the seeding depth measured by the SAM system. The average seeding depth % error between the recorded and measured seeding depths was -0.1% with standard deviation of 5.6%. Overall, 98% of the recorded seeding depth was within the acceptable tolerance ±10% error suggesting that the SAM system can accurately measure real-time seeding depths. The SAM system's capability to monitor real-time seeding depth could potentially be used to either provide feedback to operators or the control system to adjust gauge wheel load levels to achieve target seeding depth at all times. An active feedback of seeding depth could also improve control system response and minimize over- and under application of load during planting which could potentially reduce areas with shallow seeding depth or instances of sidewall compaction.

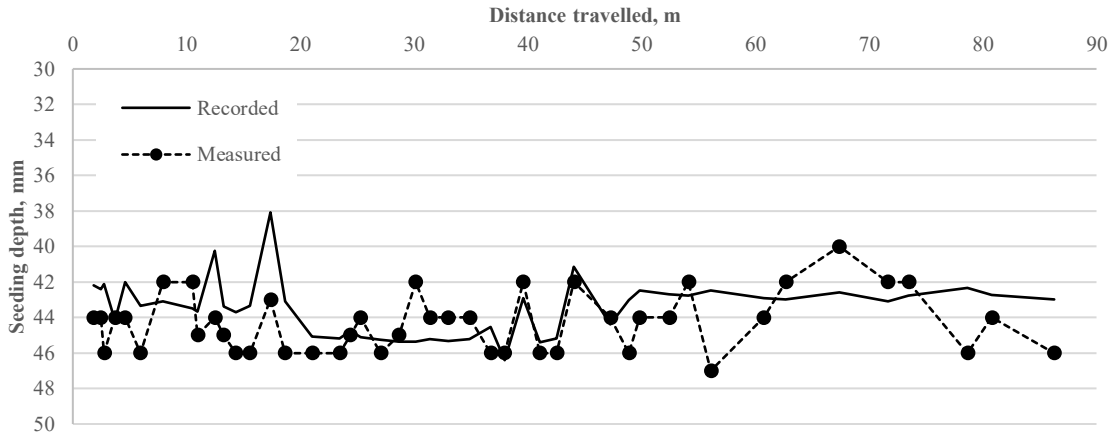

Figure 5.14. The measured seeding depth during planting. Black dots represent planted seeds.

5.4.3 Image GPS coordinates

An example image and its GPS coordinates is shown in Figure 5.15. In the current system the seed geo-location was within ±11.7 cm horizontal accuracy.

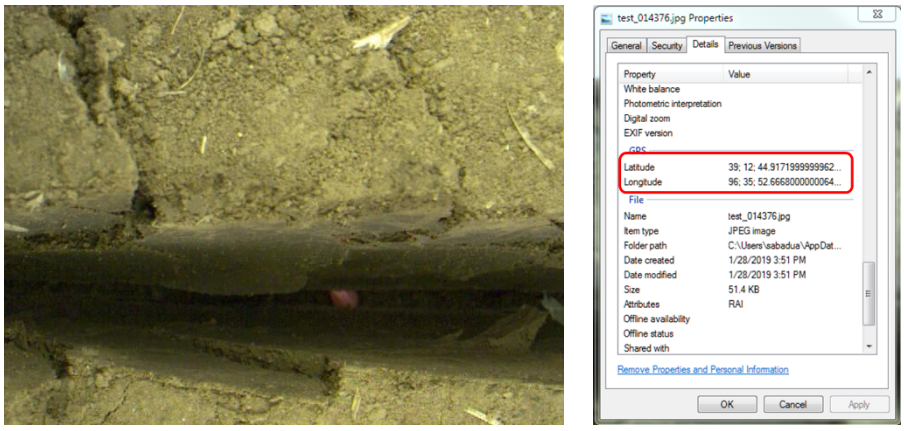

a **b**

Figure 5.15. (a) Sample image and its (b) GPS coordinate

The SAM system can report images with no seed, which can be used for an analysis of missing plants. Additionally, one seed may be shown in multiple images due to the programmed degree of overlap. Since the target distance between seeds is very narrow, certain instances can have two images having the same seed and GPS coordinates.

Therefore, visual inspection of individual images was performed to locate similar seeds to allow accurate assignment of GPS coordinate to each seed. To illustrate, refer to Figure 5.16 where seed 2 can be seen on images a, b and c. Images b and c have the same GPS coordinate which can be used to locate seed 2. On the other hand, for image a where two seeds are present, the GPS coordinate of that image can be used to locate seed 1 since seed 2 was already assigned with its own GPS coordinate.

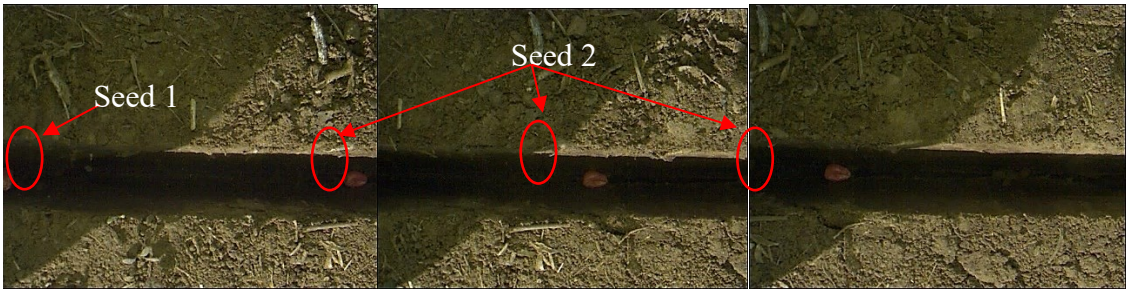

Figure 5.16. Set of images to be stitched and before seed spacing was measured

The ability to geo-locate seeds will provide information on the cause of wide gaps after emergence. GPS locations of areas with wide gaps can be collected and matched to the recorded GPS coordinates which can be used to confirm placement of the seed. The presence of a seed in between plants indicates proper seed metering of the planter and non-emergence can be attributed to seed germination issues or other factors. For example, in areas where plants did not emerge evenly, finding the GPS coordinates of gaps between emerged plants and matching them to the collected coordinates of images with the planted seeds allows the growers to determine if there was a seed planted and it did not emerge or if there was no seed planted. Such results can provide insights to planter metering performance or germination issues. Overall, geo-locations can provide a more accurate

estimate of the actual number of planted seeds per hectare and its spatial spread, providing critical information on the accuracy of planting system.

5.5 Conclusion

The results of this study demonstrate that the potential of the proof of concept system for measuring seed spacing, seeding depth and geo-location of corn seeds on row crop planters. These two seed placement parameters (seed spacing and depth) are the most critical to corn growers, researchers, machinery service professionals and manufacturers. Having the ability to understand real-time seeding depth and spacing allows operators to adjust planter settings on the go. At present, seeding depth is manually measured by digging individual plants locating the seed then measuring the distance to the ground. The current seeding depth measurement process requires a lot of manpower, hours of operation and is prone to measurement errors. Simply digging a couple of plants is not sufficient to represent whole field variation (thousands of plants). Likewise, plant spacing is currently being measured by laying measuring tape and recording the spacing. The developed system can radically change the method of measurement seed localization and provide stakeholders more accurate spatial quantification of planting systems. The developed SAM system was capable of capturing real-time images of seeds in the trench during planting. The seed spacing from stitched image presented a RMSE of 0.63 and a R^2 of 0.87. Likewise, 98% of the recorded seeding depth was within the acceptable tolerance ±10% error which suggested the system can potentially measure real-time seeding depths accurately. Furthermore, the system could assign GPS coordinates to individually map planted seeds. The data collected via the SAM system can provide direct feedback to the

control system for managing planting technology for achieving more uniform seed placement, plant stand, and potentially improving yield.

Future recommended investigations will be accomplished by mounting the SAM system on an actual planter and testing it across variable ground speeds, dusty conditions and dynamic planting conditions to validate the robustness of the sensing system. Likewise, further improvement on the data acquisition system to fully automate data measurements on-the-go is required.

Chapter 6 - Conclusion and future work

6.1 Conclusions

The following conclusions were drawn from this study:

1. Implementing a fixed downforce system with target gauge wheel load (GWL) set at 35 kg showed that GWL was maintained within the target range of 34 +/- 50 kg for 33% of the total planting time. It was also observed that 25% of the total planting time GWL was less than 0 which indicate the gauge wheels losing ground contact resulting to areas planted with uncertain seeding depth. Different row section control scenarios showed that lower number of row units within a section is preferred for more uniform row-to-row GWL control to account for the varying soil conditions during planting. Soil texture as measured by soil electrical conductivity and soil compaction due to tire tracks could influence GWL uniformity. Results suggest low target GWL for the fixed downforce setting and the need for an automatic downforce control system that is capable of controlling smaller sections providing a consistent GWL application across all row units that could potentially result in uniform seed placement during planting.
2. Implementing an automatic downforce system with downforce A (63 kg) and downforce B (100 kg) as the target GWL showed no differences on plant spacing but downforce B resulted in higher plant spacing accuracy. Downforce B at 7.2 kph ground speed achieved the desired seeding depth but seeding depth gets shallower as ground speed increases to 16.1 kph. With downforce A, seeding depth was consistently shallow on ground speeds ranging from 9.6 kph to 16.1 kph on both fields. Both downforce setting revealed increasing row unit acceleration as ground speed increases on both

fields. Such conditions are likely to increase the row unit vibration potentially affecting effectiveness of the seed-metering unit to singulate seeds accurately.

3. Row unit acceleration on wing, track and non-track sections increases with ground speed increasing from 7.2 kph to 16.1 kph. Wing control section showed the higher row unit acceleration compared to track and non-track sections with an average acceleration of 8.6 m/s^2 on a no-till and 6.5 m/s^2 on strip-tilled field. Strip-tilled field exhibited lower row unit acceleration by 18% compared to no-till field. The active downforce system showed its ability to maintain the desired GWL within the target range on each row unit section across ground speed ranging from 9.6 to 12 kph on strip-tilled field. Gauge wheel load on strip-tilled field stayed within target range on wing and no-track sections across all ground speeds. Downforce requirement increases with increasing ground speed across all row unit sections especially for no-till field.
4. A proof-of-concept sensing and measurement (SAM) system was developed to measure and calculate seed spacing, depth and geo-location of corn. The system uses a high speed camera to capture successive images of planted seeds and a RTK-GPS unit provided each image a GPS coordinate. Images were stitched and seed spacing was calculated. A light section sensor measures seeding depth by calculating difference between the distance from the bottom of the trench and the ground surface. Calculated and actual seed spacing revealed a root-mean squared error (RMSE) of 0.63 cm and a coefficient of determination (R^2) of 0.87 and 98% of the recorded seeding depth was within the acceptable tolerance ±10% error.

6.2 Recommendations for future work

Results of the study suggest ideal target GWL ranging from 80 kg to 100 kg for ground speed of 12 kph or lower when implementing an active downforce setting. At faster ground speed of over 12 kph, more than 100 kg GWL is desirable to maintain seed placement uniformity. Although careful GWL selection is needed to prevent soil compaction caused by too much load application. Future investigations may consider conducting more intensive field tests over multiple years selecting wider downforce settings at varying driving speeds observing stability of individual row units and understand crop response in terms of emergence, seeding depth, plant spacing uniformity and grain yield. Moreover, improving the data acquisition and image processing component of the developed sensing system is needed to fully automate data measurements on-the-go. Actual field tests are also recommended to assess robustness and to further increase the utilization of the SAM system. An advanced control system will provide more direct feedback to operators on real-time seeding depth allowing the selection and management of the desired downforce automatically on-the-go as field operating conditions and operator driving styles change. Therefore, integration of such system would take away the guess work and provide real-time accurate control.

6.3 Practical implications

Placing seeds at the desired depth and spacing consistently and within schedule is always a challenge for growers during planting season. Row crop planters have become bigger and sophisticated with all the breakthrough technologies developed to accomplish planting operations more precise and faster than ever before providing growers the opportunity to maximize yield over a wide range of operating conditions. With increasing

width of planter toolbar so does the variability on seed placement across all row units. Understanding how planting technologies respond to field heterogeneity will provide growers the decision tools to maximize planter performance based on the actual planting requirements of their field.

Downforce technology in row crop planters have progressed from mechanical springs to hydraulic cylinders aiming to accurately manage weight acting on individual row units. Ideal downforce prevents soil compaction and ability to place seeds at the right depth with the right soil moisture and temperature providing the ideal seed-to-soil contact leading to proper seed germination and plant development. Field conditions vary between fields and have shown to cause variability in real-time gauge wheel load (GWL) of individual row units which could potentially affect planting performance. Soil strength and moisture can be indicated by soil texture which can be defined as the ability of the soil to hold water. Coarse-textured or sandy soils have a lower capacity to hold moisture and requires lower resistance for soil penetration. On the other hand, fine-textured or clay soils has higher water holding capacity and higher penetration resistance. Planting on soil with varying soil texture requires different levels of downforce to overcome soil resistance in creating the seed furrow. Actual planting operations revealed that fixed downforce setting resulted in significant areas where the row unit applied too much or less than 0 GWL. Too much GWL could cause the seeds to be planted too deep or create furrow sidewall compaction restricting seed emergence and affecting plant development. Less than 0 GWL suggests uncertain seeding depth due to potential loss of contact between the gauge wheels and the ground surface. Understanding gauge wheel variability and its impact on planter

operation is critical for both selecting the type and resolution of downforce control systems for planters.

Most manufacturers started by manufacturing pneumatic downforce control system with section control. However, more recently most manufacturers have moved to adopting hydraulic downforce on a row-by-row control. Agronomic response as reported in this research showed the need for varying levels of downforce control system management across a range of machine and field operating conditions. Selecting the ideal downforce at planting is critical at it defines how plants will develop throughout the whole growing season. This was observed during the research that selection of incorrect downforce can impact the accurate seeding depth without operator knowing it from the cab display, although the monitor would indicate correct management of user selected target downforce.

Rapid advancement will continue to innovate planting system technology. Seeding placement, and machine dynamics during planting could impact yield variation. Limited data during this research indicated that there might be significant row-to-row yield variations. Therefore, some version of the seed placement sensing system developed could provide direct information on most critical seed placement parameters. Since operators could not ascertain seeding depth accuracy from the cab, a seeding depth sensing system could not provide direct feedback to the user but also to control system to fine tune machine control to correctly place seed. Further improvement of the developed sensing and measurement system will provide operators feedback on real-time spacing and depth allowing downforce adjustments according to actual soil conditions.

In summary, adoption of precision planting technologies requires understanding of in-field conditions and requirements providing growers the ability to make informed decisions leading to efficient land utilization, improved crop performance and sustainable production.

References

Abendroth, L. J., Woli, K. P., Myers, A. J. W., & Elmore, R. W. (2017). Yield-Based Corn Planting Date Recommendation Windows for Iowa. *Crop, Forage & Turfgrass Management*, *3*(1), cftm2017.02.0015. https://doi.org/10.2134/cftm2017.02.0015

Andrade, F. H., & Abbate, P. E. (2005). Response of maize and soybean to variability in stand uniformity. *Agronomy Journal*, *97*(4), 1263–1269. https://doi.org/10.2134/agronj2005.0006

Assefa, Y., Vara Prasad, P. V., Carter, P., Hinds, M., Bhalla, G., Schon, R., Jeschke, M., Paszkiewicz, S., & Ciampitti, I. A. (2016). Yield responses to planting density for US modern corn hybrids: A synthesis-analysis. *Crop Science*, *56*(5), 2802–2817. https://doi.org/10.2135/cropsci2016.04.0215

Badua, S. A., Sharda, A., Flippo, D., & Ciampitti, I. A. (2018). Real-time gauge wheel load variability of a row-crop planter during field operation. *Transactions of the ASABE*, *61*(5), 1517–1527.

Baker, C. J., Saxton, K. E., Ritchie, W. R., Chamen, W. C. T., Reicosky, D. C., Ribeiro, F., Justice, S. E., & Hobbs, P. R. (2007). *No-tillage Seeding in Conservation Agriculture*.

Bedord, B. L. (2015). *The evolution of down force tech*.

Benson, G. O. (1990). Corn Replant Decisions: A Review. *Journal of Production Agriculture*, *3*(2), 180–184. https://doi.org/10.2134/jpa1990.0180

Brandelero, E. M., Adami, P. F., Modolo, A. J., Baesso, M. M., & Fabian, A. J. (2015). Seeder Performance under Different Speeds and its Relation to Soybean Cultivars Yield. *Journal of Agronomy*, *14*(3), 139–145. https://doi.org/10.3923/ja.2015.139.145

Buchholz, D. D., Palm, E., Thomas, G., & Pfost, D. L. (1993). No - Till Planting Systems. *University of Missouri Extension*, *October 1993*, 1–7.

Carter, P. R., Nafziger, E. D., & Hick, D. R. (2019). Effects of Uneven Seedling Emergence in Corn. *Service, Cooperative Extension Lafayette, West*, 1–6.

Chim, B. K., Omara, P., Macnack, N., Mullock, J., Dhital, S., & Raun, W. (2014). Effect of Seed Distribution and Population on Maize (Zea mays L .) Grain Yield. *International Journal of Agronomy*.

Collins, B. A., & Fowler, D. B. (1993). *Effect of soil characteristics, seeding depth, operation speed, amd opener design on direct seeding draft forces*. 413–418.

Cox, W. J., & Cherney, J. H. (2015). Field-scale studies show site-specific corn population

and yield responses to seeding depths. *Agronomy Journal*, *107*(6), 2475–2481. https://doi.org/10.2134/agronj15.0308

Da Silva, R. P., Korah, J. E., Filho, A. C., Lopes, A., & Furlani, C. E. A. (2004). Effect of press wheels submitted to vertical loads in sowing depth on the development of corn 1. *Engenharia Agricola*, *24*(2), 396–404.

Denning, J., Eliason, R., Goos, R. J., Hoskins, B., Nathan, M. V, & Wolf, a. (2011). *Recommended Chemical Soil Test Procedures for the North Central Region*. *221*(221), 75.

Doan, V., Chen, Y., & Irvine, B. (2005). Effect of residue type on the performance of no-till seeder openers. *Canadian Biosystems Engineering / Le Genie Des Biosystems Au Canada*, *47*.

Doerge, T., & Hall, T. (2002). On-farm evaluation of within-row plant spacing uniformity. *Wisconsin Fertilizer, Aglime and Pest Management Conference.*

Fallahi, S., & Raoufat, M. H. (2008). Row-crop planter attachments in a conservation tillage system : A comparative study. *Soil and Tillage Research*, *98*, 27–34. https://doi.org/10.1016/j.still.2007.10.005

Farahani, H. J., Khosla, R., & Buchleiter, G. W. (2011). Field EC Mapping : A New Tool to Make Better Decisions. *Fact Sheet*, *0.568*.

Fathima, A. A., Karthik, R., & Vaidehi, V. (2013). Image stitching with combined moment invariants and sift features. *Procedia - Procedia Computer Science*, *19*, 420–427. https://doi.org/10.1016/j.procs.2013.06.057

Fulton, J., Mullenix, D., Brooke, A., Winstead, A., & Ortiz, B. (2011). *Automatic Section Control (ASC) Technology for Planters*. www.AlabamaPrecisionAgOnline.com

Fulton, J. P., Poncet, A., Mcdonald, T., Knappenberger, T., Shaw, J., & Bridges, R. (2015). Considerations for Site-specific Implementation of Active Downforce and Seeding Depth Technologies on Row-crop Planters Downforce by depth settings influence seeding depth. *73rd Conf. Land, Technik - AgEng*.

Furlani, C. A., Júnior, Á. P., Lopes, A., Silva, R. P., Grotta, D. C. C., & Cortez, J. W. (2007). Operational performance of seeder in different forward speed and winter cover crop management. *Eng. Agríc., Jaboticabal*, *27*(2), 456–462.

Garcia, J., & Barbedo, A. (2013). *Digital image processing techniques for detecting , quantifying and classifying plant diseases*. 1–12.

Ghosh, D., & Kaabouch, N. (2016a). A survey on image mosaicing techniques q. *JOURNAL OF VISUAL COMMUNICATION AND IMAGE REPRESENTATION*, *34*,

1–11. https://doi.org/10.1016/j.jvcir.2015.10.014

Ghosh, D., & Kaabouch, N. (2016b). A survey on image mosaicing techniques q. *JOURNAL OF VISUAL COMMUNICATION AND IMAGE REPRESENTATION*, *34*, 1–11. https://doi.org/10.1016/j.jvcir.2015.10.014

Grassbaugh, E. M., & Bennett, M. A. (1998). Factors affecting vegetable stand establishment. *Scientia Agricola*, *55*(spe), 116–120. https://doi.org/10.1590/s0103-90161998000500021

Gratton, J., Chen., Y., & Tessier, S. (2003). Design of a spring-loaded downforce system for a no-till seed opener. *Canadian Biosystems Engineering / Le Genie Des Biosystems Au Canada*, *45*.

Grisso, R. B., Engineer, E., Engineering, B. S., & Tech, V. (2014). *Planter / Drill Considerations for Conservation Tillage Systems*.

Grisso, R. B., Engineer, E., & Tech, V. (2009). Precision Farming Tools: Soil electrical conductivity. *442-508*.

Grisso, R. D., Yasin, M., & Kocher, M. F. (1996). Tillage Implement Forces Operating in Silty Clay Loam. *Transactions of the ASABE*, *39*(6), 1977–1982. https://doi.org/10.13031/2013.27699

Hanna, H. M., Steward, B. L., & Aldinger, L. (2010). Soil loading effects of planter depth-gauge wheels on early corn growth. *Applied Engineering in Agriculture*, *26*(4), 551–556. https://doi.org/10.13031/2013.24631

Hanna, H Mark. (n.d.). *Planter Setup and Adjustments for Accurate Seeding of Corn and Soybean*.

Hanna, H Mark, Steward, B. L., & Aldinger, L. (2010). Soil Loading Effects of Planter Depth-Gauge Wheels on Early Corn Growth. *Applied Engineering in Agriculture*, *26*(4), 551–556.

IMARC. (2019). *Precision Agriculture Market: Global Industry Trends, Share, Size, Growth , Opportunity and Forecast 2019-2024*. https://www.imarcgroup.com/precision-agriculture-market

International Organization for Standardization. (1984). *Sowing equipment-Test methods-Part 1: Singe seed drills (precision drills)*.

Jain, M. P. M., & Shandliya, ijaya K. (2013). A Review Paper on Various Approaches for Image Mosaicing. *International Journal of Computational Engineering Research*, *3*(4), 106–109.

Kacira, M., & Ling, P. (2001). Design and development of an automated and non-contact sensing system for continuous monitoring of plant health and growth. *Transactions of the ASABE*, *44*(4), 989–996. https://doi.org/10.13031/2013.6231

Karayel, D., & Šarauskis, E. (2011). *Effect of downforce on the performance of no-till disc furrow openers for clay-loam and loamy soils*. *43*(3), 16–24.

Knappenberger, T., & Koller, K. (2012). Spatial assessment of the correlation of seeding depth with emergence and yield of corn. *Precision Agriculture*, *13*, 163–180. https://doi.org/10.1007/s11119-011-9235-4

Krall, J. M., Esechie, H. A., Raney, R. J., Clark, S., TenEyck, G., Lundquist, M., Humburg, N. E., Axthelm, L. S., Dayton, A. D., & Vanderlip, R. L. (1977). Influence of Within-row Variability in Plant Spacing on Corn Grain Yield. *Agronomy Journal*, *69*(5), 797. https://doi.org/10.2134/agronj1977.00021962006900050016x

Kumar, A., Chen, Y., Sadek, A., & Rahman, S. (2012). Soil cone index in relation to soil texture, moisture content, and bulk density for no-tillage and conventional tillage. *Agricultural Engineering International: CIGR Journal*, *14*(1), 26–37.

Lauer, J. G., Carter, P. R., Wood, T. M., Diezel, G., Wiersma, D. W., Rand, R. E., & Mlynarek, M. J. (1999). Corn hybrid response to planting date in the northern corn belt. *Agronomy Journal*, *91*(5), 834–839. https://doi.org/10.2134/agronj1999.915834x

Lauer, J. G., & Rankin, M. (2004a). Corn response to within row plant spacing variation. *Agronomy Journal*, *96*(5), 1464–1468. https://doi.org/10.2134/agronj2004.1464

Lauer, J. G., & Rankin, M. (2004b). Corn Response to Within Row Plant Spacing Variation. *Agron. J.*, *96*, 1464–1468.

Li, Y., Shi, Z., Wu, C., Li, H., & Li, F. (2008). Determination of potential management zones from soil electrical conductivity , yield and crop data *. *Journal of Zhejiang University SCIENCE B*, *9*(1), 68–76. https://doi.org/10.1631/jzus.B071379

Licht, M., Baum, M., & Archontoulis, S. (2019). *Late Corn Planting Options*. Integrated Crop Management. https://crops.extension.iastate.edu/cropnews/2019/05/late-corn-planting-options

Liu, W., Tollenaar, M., Stewart, G., & Deen, W. (2004). Within-Row Plant Spacing Variability Does Not Affect Corn Yield. *Agronomy Journal*, *96*, 275.

Lomeling, D. (2013). *The Influence of Soil Texture on Spatial Variability of the Cone Index in a Sandy Loam Soil (Eutric Leptosol). Open Science Repository The Influence of Soil Texture on Spatial Variability of the Cone Index in a sandy loam soil (Eutric Leptosol)*. https://doi.org/10.7392/openaccess.23050428

Long, N. V., Assefa, Y., Schwalbert, R., & Ciampitti, I. A. (2017). Maize yield and planting date relationship: A synthesis-analysis for us high-yielding contest-winner and field research data. *Frontiers in Plant Science*, *8*(December), 1–9. https://doi.org/10.3389/fpls.2017.02106

Lowe, D. G. (2004). Distinctive Image Features from Scale-Invariant Keypoints. *International Journal of Computer Vision*, *60*(2), 91–110.

Lund, E. D., Christy, C. D., & Drummond, P. E. (1999). Practical applications of soil electrical conductivity mapping. *Proceedings of the 2nd European Conference on Precision Agriculture*, *July*, 1–9.

Modernal da Silveria, J. C., Fernandes, H. C., Modolo, A. J., De Lima Silva, S., & Trogello, E. (2011). Furrow depth , soil disturbance area and draft force of aseeder-fertilizer at different seeding speeds Furrow depth , soil disturbance area and draft force of a seeder-fertilizer at different seeding speeds Profundidade de sulco , área de solo mobilizada. *Revista Ceres*, *58*(3), 293–298. https://doi.org/10.1590/S0034-737X2011000300008

Molatudi, R. L., & Mariga, I. K. (2009). The effect of maize seed size and depth of planting on seedling emergence and seedling vigour. *Journal of Applied Sciences Research*, *5*(12), 2234–2237.

Moral, F. J., Terrón, J. M., & Silva, J. R. M. da. (2010). Delineation of management zones using mobile measurements of soil apparent electrical conductivity and multivariate geostatistical techniques. *Soil and Tillage Research*, *106*(2), 335–343. https://doi.org/10.1016/j.still.2009.12.002

Morrison, J. E., & Gerik, T. J. (1985). Planter Depth-Control : I . Predictions and Projected Effects on Crop Emergence. *Transactions of the ASAE*, *28*(5), 1415–1418.

Morrison Jr., J. E., & Allen, R. R. (1987). Planter and drill requirements for soils with residues. *Southern Region No-Tillage Conference*, 44–58.

Murray, J. R., Tullberg, J. N., & Basnet, B. B. (2006). *Planters and their Components Types, attributes, functional requirements, classification and description*.

Nafziger, E. (2009). Corn. In *Illinois Agronomy Handbook* (pp. 13–26).

Nafziger, E. D. (1996). Effects of missing and two-plant hills on corn grain yield. *Journal of Production Agriculture*, *9*(2), 238–240. https://doi.org/10.2134/jpa1996.0238

Nakarmi, A. D., & Tang, L. (2012). Automatic inter-plant spacing sensing at early growth stages using a 3D vision sensor. *Computers and Electronics in Agriculture*, *82*, 23–31. https://doi.org/10.1016/j.compag.2011.12.011

Nejati, H., Azifimar, Z., & Zamani, M. (2008). Using Fast Fourier Transform for Weed Detection in corn fields. *2008 IEEE International Conference on Systems,Man and Cybernetics*.

Nielsen, R. L. (1995). Planting speed effects on stand establishment and grain yield of corn. *Journal of Production Agriculture*, *8*(3), 391–393. https://doi.org/10.2134/jpa1995.0391

Nielsen, R. L. (2001). *Stand establishment variability in corn* (Vols. 91–01, pp. 1–10).

Nielsen, R. L. (2019). *The Planting Date Conundrum for Corn*. https://www.agry.purdue.edu/ext/corn/news/timeless/PltDateCornYld.html

Nkakini, S. O. (2015). Draught force requirements for a disc plough at various tractor forward speeds in loamy sand soil during plowing. *International Journal of Advanced Research in Engineering and Technology (IJARET)*, *6*(7), 52–68.

Özmerzi, A., Karayel, D., & Topakci, M. (2002). Effect of sowing depth on precision seeder uniformity. *Biosystems Engineering*, *82*(2), 227–230. https://doi.org/10.1006/bioe.2002.0057

Poncet, A. M., Fulton, J. P., McDonald, T. M., Knappenberger, T., Shaw, J. N., & Bridges, R. (2018). Effect of heterogeneous field conditions on corn seeding depth accuracy and uniformity. *Applied Engineering in Agriculture*, *34*(5), 819–830.

Prados, R., Garcia, R., & Laszlo, N. (2014). *Image Blending Techniques and their Application in Underwater Mosaicing*.

Raper, R. L., Kirby, J. Mac, Raper, R. L., & Kirby, J. Mac. (2006). *Soil Compaction: How to Do It, Undo It, or Avoid Doing It*. *913*, 1–14.

Renuka, D. (2016). Image mosaicing using phase correlation and feature based approach: A review. *International Journal of Engineering Research*, *4*(1).

Roozeboom, K., Delvin, D., Duncan, S., Janssen, K., Olson, B., & Thompson, C. (2007). Optimum planting practices. In *Corn Production Handbook*. Kansas State University Agricultural Experiment Station And Cooperative Extension Service.

S. D. Kachman, & J. A. Smith. (1995). Alternative Measures of Accuracy in Plant Spacing for Planters Using Single Seed Metering. *Transactions of the ASAE*, *38*(2), 379–387. https://doi.org/10.13031/2013.27843

Sanchiz, J. M., Pla, F., Marchant, J. A., & Brivot, R. (1996). Structure for motion techniques applied to crop field mapping.pdf. *Image and Vision Computing*, *14*, 353–363.

Sharda, A, Strasser, R., Ciampitti, I., & Griffin, T. W. (2018). *Influence of Planter Downforce Setting and Ground Speed on Seeding Depth and Plant Spacing Uniformity of Corn*. 1–13.

Sharda, Ajay, Fulton, J., Badua, S., & Griffin, T. (2017). Planter Downforce Technology for Uniform Seeding Depth. *Kansas State University Agricultural Experiment Station and Cooperative Extension Service Precision*, *MF3331*, 7.

Shearer, S. A., & Pitla, S. K. (2014). Precision Planting and Crop Thinning. In S. L. Young & F. J. Pierce (Eds.), *Automation: The Future of Weed Control in Cropping Systems* (pp. 99–124). Springer Netherlands. https://doi.org/10.1007/978-94-007-7512-1_6

Shrestha, D. S., Steward, B. L., & Birrell, S. J. (2004). Video Processing for Early Stage Maize Plant Detection. *Biosystems Engineering*, *89*(2), 119–129. https://doi.org/10.1016/j.biosystemseng.2004.06.007

Staggenborg, S. A., Taylor, R. K., & Maddux, L. D. (2004). *Effect of planter speed and seed firmers on corn stand establishment*. *20*(1996), 573–580.

Strasser, R. S. (2017). *Development of a test stand for the evaluation of row crop planter automatic downforce systems and the evaluation of a row crop planter electronic drive singulation seed meter.*

Tang, L., & Tian, L. F. (2008). *Real-time crop row image reconstruction for automatic emerged corn plant spacing measurement*. *51*(3), 1079–1087.

Tang, L., Tian, L., & Steward, B. L. (2000). Color image segmentation with genetic algorithm for in-field weed sensing. *Transactions of the ASAEE*, *43*(4), 1019–1027.

Thomison, P., Jeschke, M., & Butzen, S. (2012). *Planting Depth Effects on Corn Stand and Grain Yield* (pp. 4–7).

Urban, D. W., Roberts, M. J., Schlenker, W., & Lobell, D. B. (2015). The effects of extremely wet planting conditions on maize and soybean yields. *Climatic Change*, *130*(2), 247–260. https://doi.org/10.1007/s10584-015-1362-x

USDA-ERS. (2016). *Precision Agriculture Technologies and Factors Affecting Their Adoption*. https://www.ers.usda.gov/amber-waves/2016/december/precision-agriculture-technologies-and-factors-affecting-their-adoption/

USDA-ERS. (2017a). *Farm Sector Income Forecast*. https://www.ers.usda.gov/topics/farm-economy/farm-sector-income-finances/farm-sector-income-forecast/

USDA-ERS. (2017b). *Farm Sector Income Forecast*.

USDA-ERS. (2019a). *Feedgrains Sector at a Glance*. https://www.ers.usda.gov/topics/crops/corn-and-other-feedgrains/feedgrains-sector-at-a-glance/

USDA-ERS. (2019b). *USDA ERS - Ag and Food Sectors and the Economy*. United States Department of Agriculture-Economic Research Service. https://www.ers.usda.gov/data-products/ag-and-food-statistics-charting-the-essentials/ag-and-food-sectors-and-the-economy/

USDA-NASS. (2014). *Farms and Farmland Numbers, Acreage, Ownership and Use*. https://www.nass.usda.gov/Publications/Highlights/2014/Highlights_Farms_and_Farmland.pdf

USDA-WASDE. (2019). *Grain Supply and Demand*. https://www.agmanager.info/grain-marketing/grain-supply-and-demand-wasde/us-corn-supply

USDA. (2017). *USDA Agricultural Projections to 2026*. https://www.ers.usda.gov/publications/pub-details/?pubid=37818

USDA. (2019). *World Agricultural Supply and Demand Estimates*.

Vedaldi, A., & Fulkerson, B. (2008). *VLFeat: An Open and Portable Library of Computer Vision Algorithms*. http://www.vlfeat.org/index.html

Velandia, M., Buschermohle, M., Larson, J. A., Thompson, N. M., & Jernigan, B. M. (2013). The economics of automatic section control technology for planters: A case study of middle and west tennessee farms. *Computers and Electronics in Agriculture*. https://doi.org/10.1016/j.compag.2013.03.006

Weirich Neto, P. H., & Lopes, A. R. C. (2012). *Emergence of Corn According To the Sowing Depth of the Seed and*. 326–332.

Wiatrak, P., Khalilian, A., Muleller, J., & Henderson, W. (2009). Applications of soil electrical conductivity in roduction agriculture. *Better Crops*, *93*(2), 16–17.

Zhai, C., Long, J., Taylor, R., Weckler, P., & Wang, N. (2019). Field scale row unit vibration affecting planting quality. *Precision Agriculture*, *0123456789*. https://doi.org/10.1007/s11119-019-09684-4

Appendix A - Corn grain yield differences between fixed and active downforce systems

A.1. Introduction

Planting accuracy and efficiency to maximize yield potential can be attained through optimization of field management practices and adoption of latest equipment technology. Right conditions at planting can highly influence how the plant progress for the rest of the growing season. Soil temperature level and moisture determines the proper seeding depth for optimum growth and development of corn. Thus, weather conditions during the planting season, as well as the timeliness of planting, impacts the yield outcome. In northeast Kansas, optimum planting window for corn ranges from April 15 to May 10 where the ideal soil temperature of 55 degrees Fahrenheit at a 2-inch depth is reached for favorable planting operations (Roozeboom et al., 2007). Planting within ideal planting dates have shown to affect potential yield (Lauer et al., 1999; Nielsen, 1995). However, frequency of extreme precipitation events that may be due to climate change (Urban et al., 2015) resulting to fields becoming too wet restricting access for planting machinery potentially reducing the planting window (Urban et al., 2015). Moreover, seeds on wet soil may be exposed to very low or fluctuating soil temperatures affecting germination and seedling emergence (Abendroth et al., 2017). Thus, farmers adopt several management practices to compensate for reduced planting days through selection of suitable tillage systems (Long et al., 2017), longer or shorter maturity hybrids when planting early or late, or planting with higher ground speed to cover more acres.

In the context of advanced planting machinery, manufacturers have developed technologies to continuously improve planter performance in the field. Among them is how to consistently plant at the target seeding depth by effectively selecting and implementing the ideal downforce on planter row units. Downforce is the amount of load applied on the

row unit to achieve the desired seeding depth. This load is distributed to the opening disc for soil penetration at the desired seeding depth and the excess load is taken up by the gauge wheel. The gauge wheel load can be used anytime by the opening disc when additional load is required for soil penetration usually at heavier textured soil (clay). As such, it is important to always maintain an optimum level of load on the gauge wheel to prevent shallow planting. More often, downforce requirement varies across the field due to inherent spatial field variability which can significantly influence the selection of row unit downforce applied during planting (Badua et al., 2018). Soil moisture, texture and crop residue are several field conditions that affects openings discs ability for proper soil penetration which could result in shallow seeding depth or sidewall compaction. Insufficient load on the row unit could cause too much row unit bounce which could result in uncertain seeding depth and non-uniform seed spacing. Thus, proper downforce selection is critical to achieve desired seed placement consistency. Badua et al., (2018) reported that proper selection of planter downforce setting could potentially result in uniform seed placement even at faster planting speed. Therefore, this study aims to assess the grain yield difference when implementing different levels of downforce settings for two different downforce systems.

A.2. Methodology

A.2.1 Planter set up

A row-crop planter planter (Maestro 30 SW, Horsch Maschinen GmbH, Schwandorf, Germany) with 12 row units spaced at 762 mm apart operated by a John Deere 8250R tractor was used in planting corn (Figure A.1). The planter was programmed to implement fixed and active downforce system.

Figure A.1. The row crop planter used in the study

Each row was equipped with a load cell (Model 6784, Horsch Maschinen GmbH, Schwandorf, Germany) to measure the real-time gauge wheel load (GWL) applied during planting. Row units are grouped into control sections where pressure transducers (HAD 844L-A-0250-161, Hydac, Glendale Heights, IL, USA and Model KM41, Ashcroft Inc., Stratford, CT, USA) were installed on each section to measure the real-time hydraulic oil pressure applied. Oil pressure readings will indicate the hydraulic system applying pressure on row units to implement desired downforce setting during planting. The planting unit utilizes an electronic drive pneumatic seed meter equipped with 21 slot seed plate for medium round corn seed. Providing feedback on seed singulation was a seed sensor (Hy Rate Plus, Dickey-John Corp., Auburn, IL, U.S.A.) placed along the seed tube on each row unit. Four accelerometers (Model 3741E1210G, PCB piezotronics, Depew, NY, USA) were mounted on selected row units (rows 1, 5 7, and 12) to record row unit vibration during planting and a potentiometer (Model 424A11A090B, Elabou sensor Technology Inc., Waukegan, IL, USA) mounted on one row unit was used to measure toolbar operating position. Location and travel speed was measured using a sub-inch accuracy GPS unit (GR5, Topcon Positioning Systems, Inc., Livermore, CA, USA). Load cells, pressure

transducers, accelerometers, potentiometer and GPS signals were recorded using laptop computer (Latitude 14 3470, Dell, Round Rock, TX, USA) and a NI cRIO chassis via C Series modules (National Instruments, Ausin, TX, USA) at 10 Hz sampling frequency.

A.2.2 Field and experimental layout

Research was conducted in 2017 in a production field located at Blaine, KS (39.358068, -97.160018) (Figure A.2). The field adopt a no-till management practice with moderate amount of crop residue. Using the USDA Web soil survey, field has silty loam soil type and well-drained soil property. Volumetric soil moisture content at planting ranges from 25.4% to 40.3% with an average of 30.6% measured at 15.2 cm depth using a digital moisture meter (Hydrosense II, Campbell Scientific, Logan, UT). Experimental plots for fixed and active downforce study were placed side by side in the test area.

Figure A.2. The aerial image of the study area showing location of experimental plots

The field layout was arranged in a one factorial Randomized complete Block Design (RCBD) structure with three replicates. The treatment factor was downforce system with two levels selected to implement low and high downforce. Farm owners/collaborators were consulted on their previous target gauge wheel load (GWL) implemented when

planting and decided to select 620 N (140 lb) to implement a low downforce, referred herein as “low setting” and set the GWL at 980 N (220 lb) for high downforce implementation, referred herein as “high setting”. Such values where almost like load ranges implemented by Hanna et al. (2010). Two downforce systems were utilized to implement both settings. Fixed downforce system is characterized by setting up the planter to apply a fixed GWL level necessary to place the seed at the desired depth. The planter will then apply this constant load throughout the field during planting operations. However, varying field conditions may alter gauge wheel load requirement (Badua et al., 2018) for proper seed placement. As a result, seeding depth may have been compromised due to inconsistent load application as fixed systems are unable to compenstate for varying conditions across the field during planting. Active downforce system is capable of adjusting load application in order to maintain the target GWL set on the planter. The system utilizes hydraulic cylinders to increase and decrease GWL based on field conditions during planting. Thus, the system can apply uniform load which could result in a consistent seed placement.

Each plot corresponds to one whole width the planter consisting of 12 rows. The experimental unit consists of one row randomly selected among the 12 rows where a 0.6 m (17.5 ft) long strip was staked. This row length is equivalent to 1/1000th acre for a row width of 30 inches which is recommended to achieve an adequate sample that would represent the rest of the field (Benson, 1990). A seeding rate of 84,000 seeds/ha (34,000 seeds/acre) was applied and target seeding depth was set at 5.1 cm (2 in) for all the treatments.

A.2.3 Grain yield calculation

Measuring yield was performed by manually harvesting the corn ears of all the plants along the experimental unit which ranges from 28 to 32 ears per treatment. After removing the husks, corn ears were weighed using a digital weighing scale (Scout II, Ohaus Corp., Florham Park, NJ) (Figure A.3a) before the ears were individually shelled using an electric driven corn sheller (Black Beauty, Durbin Durco, Inc., St. Louis, MO) (Figure A.3b) located at the North Agronomy Farm at Kansas State University.

a **b** **c**

Figure A.3. Weighing of corn ear (a), shelling to collect grain and (b) and moisture tester for grain moisture measurement

After shelling, corn cob was weighed using the digital scale. Weight of the cob was subtracted to the weight of the ear to determine the weight of the grain. Shelled grain were collected and measured for grain moisture using a grain moisture tester (Dickey-John GAC 2000, Auburn, IL, USA) (Figure A.3c). Corn yield were calculated following the procedure described by Lauer (2002).

A.2.4 Data analysis

Analysis of variance (ANOVA) were performed using the MIXED procedure in SAS University Edition (2017 version, SAS Institute Inc, Cary, NC, USA). The CORR

procedure was used to perform a correlation analysis between the main effects. Comparison among means were done using Fishers protected (Least significant difference) LSD test. Unless otherwise indicated, effects were considered statistically significant at the 0.05 level of probability.

A.3 Results and Discussion

Results indicate that implementing an active downforce system could result in higher corn grain yield compared to fixed system (Figure A.4). Results show that grain yield difference was 817.6 kg/ha between active and fixed downforce systems. Yield can be influenced by many factors including machine, field and weather conditions. However, on a machine standpoint, planter equipped with an active downforce system can provide the optimum loading across all row units for proper soil penetration regardless of field and soil conditions which could result in a uniform seeding depth and spacing of plants. Uniformity of seed placement have been reported to result in maximum yield potential in corn. Such result indicates the potential advantage of an active downforce system over fixed systems. Fixed downforce may not be able to maintain the desired load for all row units as different soil textures may require varying loading levels to overcome soil resistance in creating seed furrow at the desired depth. Thus, this highlights the importance of selecting the proper downforce system or downforce setting to implement the required down pressure in achieving the desired seed placement consistency on the field which may maximize grain yield.

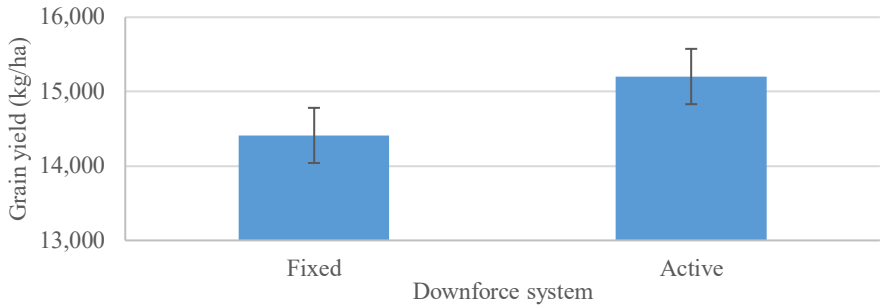

Figure A.4. Grain yield difference between fixed and active downforce systems. Error bars represent the 95% confidence interval for the means.

A.4 Conclusion

This study examined how grain yield of corn respond to varying downforce setting and system of a row crop planter. Results indicated that grain yield is affected by the downforce system. On average, grain yield difference was 817.6 kg/ha between active and fixed downforce system. It is suggested that selection of an active downforce setting for the field conditions under study could result in achieving desired seed placement resulting in higher yield compared to a fixed downforce system.

Appendix B - Field tests equipment specifications

B.1 Horsch row-crop planter

Model	**Maestro 12 30 W**
Transport width (ft)	12
Transport height (ft)	13
Length (ft)	31
Weight empty (lb)	15,300
Downpressure (lb)	125-300
Tire size	20.8 R42, 520/85 R38
Number of rows	12
Row spacing (in)	30
Seed hopper capacity (bu)	140
Fertilizer hopper capacity (gal)	1000
Drilling depth (in)	0.5-3.5
Recommended tractor power (hp)	180
Hydraulic control units (hp)	3
Case drain	1
Oil quanity	
Fertilizer pump (gpm)	6
Fan SOD (gpm)	6
Fan vacuum (gpm)	7
Required current (A)	50

B.2 John Deere Tractor

Model	**8270 R**
Tractor Power (PTO)	261 HP
Engine	Variable geometry turbocharged diesel
Manufacturer	John Deere
Fuel (gal)	180
Cylinders	6-cylinder 24-valve
Displacement (L)	9
Rated engine operating rpm	1,500 – 2,100
Cooling system	Liquid
Coolant capacity (L)	40
Engine oil capacity (L)	25
Hydraulic oil capacity (L)	40
Hydraulic type	Closed center, pressure and flow compensated
Hydraulic flowrate (lpm)	166.5
Transmission	John Deere PowerShift
Type	Full power shift
Mechanical	
Chassis	4x4 MFWD 4WD
Steering	Hydrostatic power
Dimension	
Wheelbase (in)	120.1

B.3 John Deere Field computer

Model	GreenStar-3 2630
Manufacturer	John Deere
Dimension (mm)	9.2 x 21.7
Display size (in)	10.4
Internal hard drive (MB)	800
Mounting bracket	
USB connectivity	2.0
Input voltage (V_{dc})	13.6
Software version	GS3

B.4 Load cell

Model	6784
Manufacturer	Horsch Maschinen GmbH
Measuring range (kg)	0 - 1000
Output (mA)	4 - 20
Input voltage (V_{dc})	12

B.5 Pressure transducer/ Hydraulic sensor

Model	KM41 Pressure transducer
Measuring range (psi)	0 – 7,500
Voltage output (V_{dc})	0.5 – 4.5
Current output (mA)	4 - 20
Supply current (mA)	5
Supply voltage (V_{dc})	10 - 30
Housing	Stainless steel
Weight (g)	90
Cable	Shielded Cable, 3´ standard, 24 AWG, PVC Jacket

B.6 Ground speed radar

Model	Radar III
Manufacturer	DICKEY-john
Velocity range (kph)	0.53 – 70.8
Mounting angle (deg)	35 +/- 5
Mounting height (in)	18 - 48
Power requirements (Vdc)	9 -16
Weight (kg)	0.5
Dimension (in)	4 x 3.4 x 3.1
Output signal (Vdc)	0.7 – 1.5
Connector	Amp 206429-1(Mating Connector AMP 206430-2) • Pin 1 Ground - Black • Pin 2 Signal Out - Green • 0 - 12 VDC • Symmetrical Squarewave • Pin 3 +12 VDC - Red • Pin 4 Radar Presence

B.7 Seed tube sensor

Model	**Hy Rate Plus**
Manufacturer	DICKEY-john
Dimension	
Photo detector module (in)	5.6 x 1.1 x 0.65
LED Module (in)	2.37 x 1.16 x 0.49
Operating voltage (Vdc)	7.5 – 8.75
Operating current (mA)	75
Connector	3-pin weather pack • Pin A – Green Wire – Signal • Pin B – Black Wire – Ground • Pin C – Red Wire – Supply Voltage

B.8 Potentiometer

Model	**424A11A090B**
Manufacturer	Elobau Sensor Technology, Inc
Bearing type	Ball
Central position (mA)	12
Operating temperature (deg C)	- 40 to + 85
Input current (mA)	18
Input voltage (Vdc)	12
Output signal (mA)	4 - 20
Connector	3 pin AMP Superseal 1,5

B.9 Soil EC mapper

Model	**MSP 3**
Manufacturer	Veris Technologies
Dimension (in)	90 x 72 x 108 (3-point); 174 (pull-type)
Weight (kg)	635
Minimum power required (hp)	30
Coulter-electrode blade diameter (in)	17; thickness 4mm; with tapered roller bearings and cast iron hubs ; Rock guards for hub and cap protection
Hitch	2” ball coupler and safety chain with 7,000 lb rating (3173 kg)
Maximum field speed (kph)	25
Maximum transport speed (kph)	50
EC surveyor instrument	
Dimensions (in)	2 1/16 x 9 x 7.5
Power (Vdc)	10 - 15
Input	GPS and EC signal cable
GPS requirement	NMEA 0183 protocol; input from GGA and VTG or RMC strings at a 1 Hz rate (4800-8-N-1); serial connection with DB9 connector, female sockets; GPS signal on pin 2, ground on pin 5; no signal or power on other pins
Output	serial port to computer, recording device or Data-Logger; ASCII tab delimited EC and GPS text
Mapping software	Compatible with Windows XP Displays EC data real-time for coverage verification and visual review of map quality Records geo-referenced EC data to computer

B.10 Soil sampler

Model	**Model L**
Manufacturer	Oakland Apparatus
Total length (in)	36
Soil tube length (in)	12 inches soil tube and a replaceable, screw-on S-2 Regular Soil Tip
Handle length (in)	8
Outer probe diameter (in)	15/16
Soil sample dimension (in)	9 x 3/4
Material	High-grade nickel chrome plated steel

B.11 Soil moisture sensor

Model	**Hydrosense II**
Manufacturer	Campbell Scientific
Measurements	Volumetric water content of porous media (such as soil)
Sensors	Interchangeable sensors; can swap the 12 cm and 20 cm sensors with the reader.
Power supply (Vdc)	6 (4 AA batteries)
Dimension (in)	7.9 x 3.9 x 2.3
Weight (g)	340
Water content accuracy	3% typical (Accuracy assumes solution EC of < 6.5 dS/m when using the CS659 12-cm probe.)
Volumetric water content resolution (%)	< 0.05
Volumetric water content range (%)	0 - 50
Cable length (in)	98
Rod diameter (in)	0.14

B.12 DC Response Accelerometer

Model	3741E1210G
Manufacturer	PCB Piezometrics
Sensitivity (mV/g)	400 +/- 3%
Measurement range (g)	+/- 10
Supply voltage (Vdc)	6 - 30
Housing material	Anodized aluminum
Weight (g)	9.92
Cable length (ft)	10 ft

B.13 RTK-GPS Unit

Model	GR-5
Manufacturer	TOPCON Positioning Systems, Inc.
Serial number	800-20765 (base) 800-20792 (rover)
GNSS	
GPS	L1 C/A, L1C, L2P, L2C
GLONASS	L1 C/A, L1P, L2 C/A, L2P
Galileo	E1, E5a, E5b, AltBOC
BeiDuo	B1, B2
SBAS	L1 C/A WAAS/MSAS/EGNOS
QZSS	L1 C/A, L1C, L2C
Number of channels	226-Channel Vanguard Technology with Universal Tracking Channels
Antenna type	Integrated Fence Antenna with Ground Plane
Accuracy (RMS)	
RTK	H: 10 mm + 1.0 ppm V: 15 mm + 1.0 ppm
Static	H: 3.0 mm + 0.1 ppm V: 3.5 mm + 0.4 ppm
Memory	Removable SD/SDHC Card
ASCII Output	NMEA 0183 version 2.x and 3.0
Enclosure	Magnesium I-Beam Housing
Operating temperature (deg C)	-40 to 158
Dust/Water protection	IP66

B.14 RTK-GPS Unit Field Controller

Model	FC-5000
Manufacturer	Topcon Positioning Systems, Inc.
Serial number	199536
Display size	7 inch touch display
Processor	Intel Atom Z3745
Operating system	Windows 10 imbedded
Camera	8 MP (rear), 2 MP (front)
RAM	4GB LPDDR3 (Low Power Double Data Rate memory)
Storage	Optional 64GB or 128 GB eMMC (embedded Multi-Media Controller)
Bluetooth	Yes
WiFi connectivity	Yes
USB Port	1
Battery life	10 hrs

B.15 High speed camera

Model	acA640-750uc
Manufacturer	Basler
Serial number	21722791
Dimension (mm)	29.3 x 29 x 29
Sensor	PHYTON 300
Sensor type	CMOS
Sensor size (mm)	3.1 x 2.3
Resolution (pixel)	640 x 480
Resolution	VGA
Frame rate (fps)	751
Mono/Color	Color
Interface	USB 3.0
Exposure control	Programmable via the camera API; hardware trigger
Power requirements	Via USB 3.0 interface
Digital input	1
Digital output	1
General purpose I/O	2
Lens mount	C-mount
Weigth (g)	80

B.16 Camera lens

Model	C125-0418-5M F1.8 f4mm
Manufacturer	Basler
Serial number	1GB00245
Focal length (mm)	4.0
Aperture range	F1.8 – F22.0
Iris type	Manual
Maximum image circle (in)	1/25
Working distance (mm)	100
Resolution	5 MP
Lens mount	C-mount

B.17 Light section sensor

Model	PosCon OXH7-11159406
Manufacturer	Baumer
Serial no.	700001666909
Type	Height
Measuring range (width) (mm)	48 - 72
Measuring range (distance) (mm)	100 - 150
Measuring frequency (Hz)	570
Light source	Pulsed red laser diode
Adjustment	RS485
Connection type	Connector M 12 8 pin
Voltage supply (Vdc)	15 - 28
Output signal (mA/Vdc)	4-20/0-10
Weight (g)	130

Appendix C - Data acquisition equipment specifications

C.1 CompactRIO controller

Model	**cRIO-9024**
Manufacturer	National Instrument
Part Number	193965H-01L
Serial number	18F5971
Operating system	Real-time
CPU clock frequency (MHz)	800
Memory (MB)	512
Ethernet port	2
Ethernet port type	10BaseT, 100BaseTX, 1000BaseTX Ethernet
Serial RS232 port	1
USB port	1
Power requirement (Vdc)	9 - 35

C.2 CompactRIO chassis

Model	cRIO-9114
Manufacturer	National Instrument
Part number	96604B-04L
Serial Number	18CD172
Operating system/target	Real-time
Reconfigurable FPGA	Virtex-5 LX30
Number of slot	8
Total chassis power consumption (W)	3.3
Operating temperature range (deg C)	-40 to 70
Weigth (g)	880

C.3 National Instrument 9205 C series analog module

Measurement type	Voltage
Manufacturer	National Instruments
Form factor	CompactDAQ, CompactRIO
Part number	190315J-01
Serial number	19E8326
Operating system/target	Real-time
Isolation type	Ch-Earth ground isolation
Analog input	
Differential Channels	16
Single-ended channels	32
Resolution (bits)	16
Sample rate (kS/s)	250
Maximum voltage (Vdc)	+/- 30

C.4 National Instrument 9265 C series analog module

Measurement type	Current
Manufacturer	National Instruments
Form factor	CompactDAQ, CompactRIO
Part number	198845A-01L
Serial Number	1BFCD13
Operating system/target	Real-time
Isolation type	Ch-Earth ground isolation
Analog output	
Channels	4
Output range (mA)	0 - 20
Resolution (bits)	16
Sample rate (kS/s)	100
Power supply voltage range (Vdc)	9 - 36

C.5 National Instrument 9203 C series analog module

Measurement type	Current
Manufacturer	National Instruments
Form factor	CompactDAQ, CompactRIO
Part number	198861A-01L
Serial number	19A9696
Operating system/target	Real-time
Isolation type	Ch-Earth ground isolation
Analog input	
Channels	8
Input range (mA)	0 - 20
Resolution (bits)	16
Sample rate (kS/s)	200
Maximum voltage (Vdc)	+/- 30

C.6 National Instrument 9476 C series digital output module

Measurement type	Digital
Manufacturer	National Instruments
Form factor	CompactDAQ, CompactRIO
Part number	199018B-02L
Serial number	18B45ED
Operating system/target	Real-time
Isolation type	Ch-Earth ground isolation
Digital output	
Channels (output only)	32
Single ended channels	
Update rate (µs)	500
Continuous current (mA/channel)	250
Maximum output voltage (Vdc)	60
Maximum supply voltage range (Vdc)	6 - 36

C.7 National Instrument 9221 C series analog module

Measurement type	Voltage
Manufacturer	National Instruments
Form factor	CompactDAQ, CompactRIO
Part number	194934D-01L
Serial number	1DFA230
Operating system/target	Real-time
Isolation type	Ch-Earth ground isolation
Analog input	
Single ended channels	8
Resolution (bits)	12
Sample rate (kS/s)	800
Maximum input voltage range (V)	+/- 60

C.8 National Instrument 9870 RS232 serial interface module

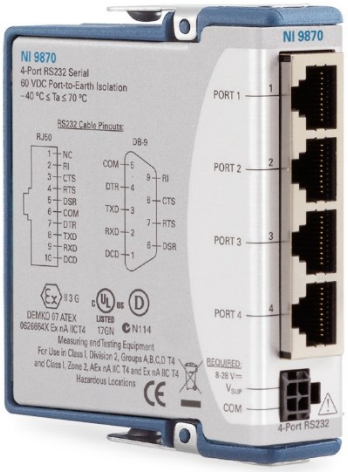

Measurement type	
Manufacturer	National Instruments
Form factor	CompactRIO
Part number	198850E-01L
Serial number	1DEC4EE
Operating system/target	FPGA
Voltage (V_{RMS})	5
Serial standard compatibility	RS232
Number of ports	4
External supply voltage range (Vdc)	8 - 28

C.9 Control computer

Model	Latitude 14-3470
Manufacturer	Dell
Operating system	Windows 7
Processor	Intel Core i7-6500U
Base clock speed	2.5 GHz
RAM	8 GB
Graphics card	Nvidia GeForce 920 GPU
Hard Disk	128GB SSD
Ethernet port	1
HDMI Output	Yes
VGA Output	Yes
SD Card slot	Yes
USB 3.0 Port	2
USB 2.0 Port	1

C.10 DC Power Supply

Model	E3630A
Manufacturer	Agilent
Dimension (in)	3.5 x 8.4 x 12.5
No. of outputs	3
DC output rating	+/- 20 V, 0.5 A
Meter resolution	
Voltage	10 mV
Current	10 mA

Appendix D - LabVIEW Program

D.1 The user interface of the LabVIEW program

D.2 LabVIEW program

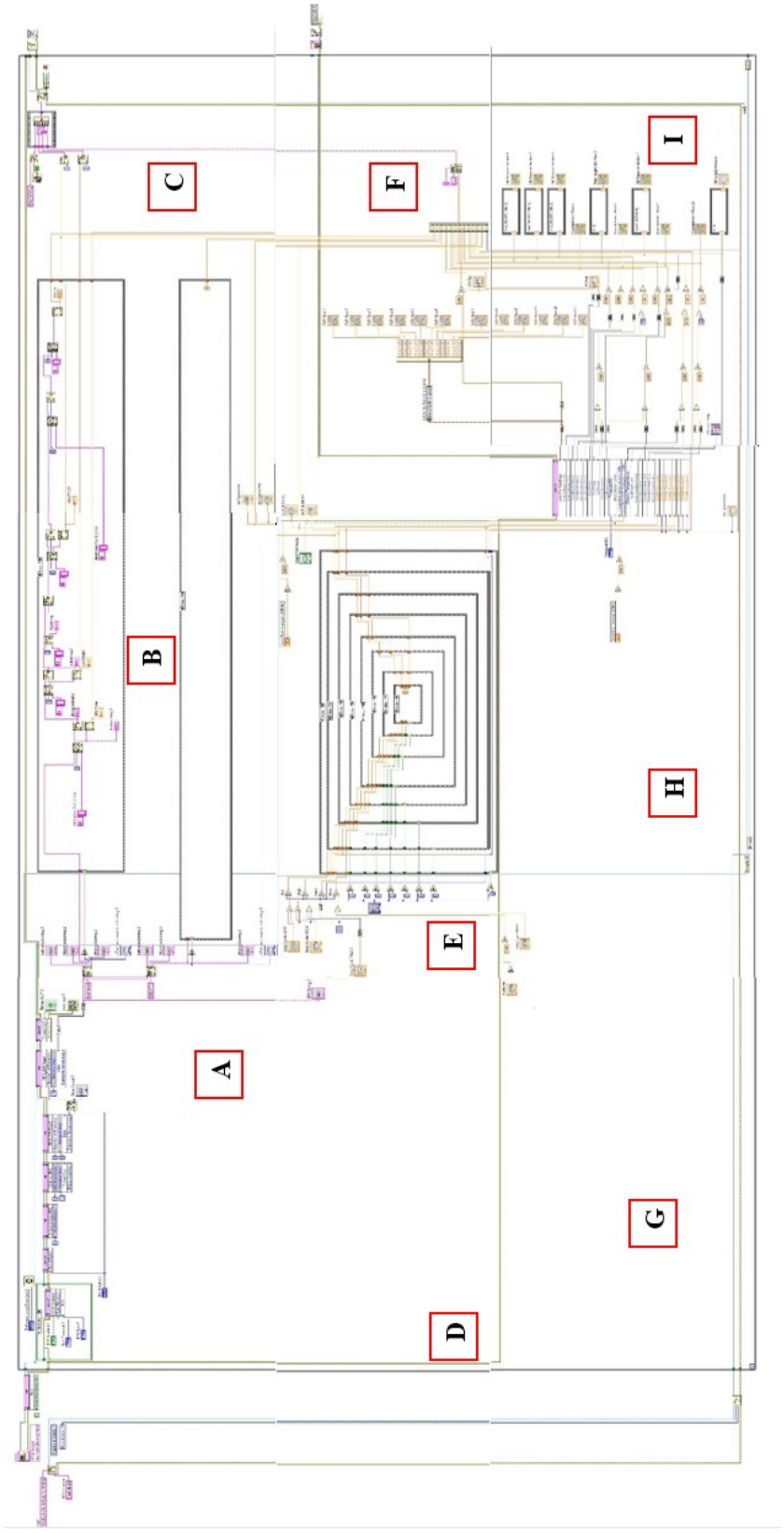

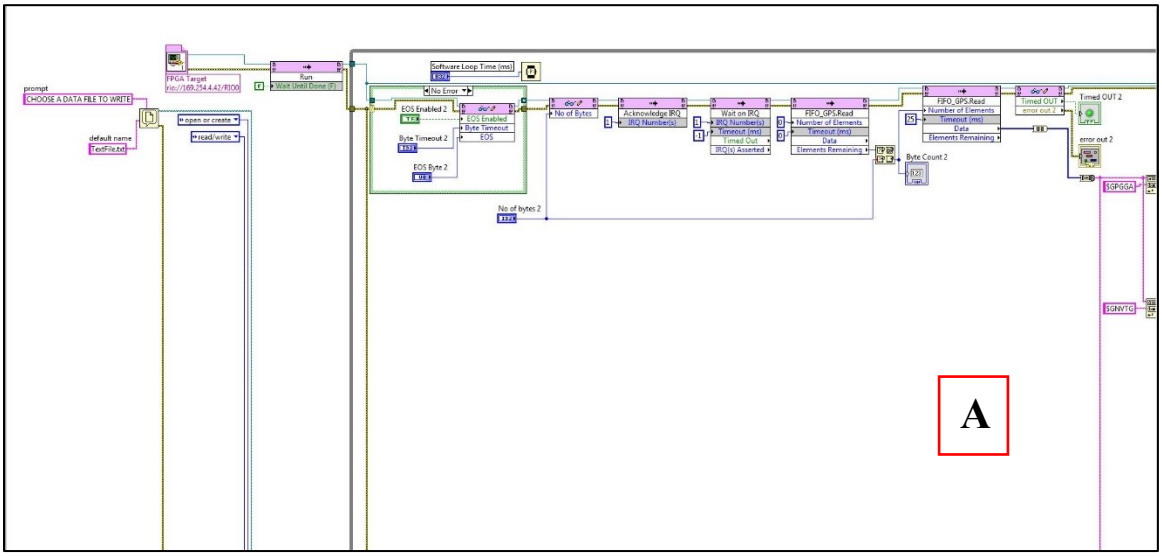
prompt
CHOOSE A DATA FILE TO WRITE
default name
TextFile.txt
FPGA Target
rio://169.254.4.42/RIO0
Run
Wait Until Done (F)
Software Loop Time (ms)
No Error
EOS Enabled 2
Byte Timeout 2
EOS Byte 2
No of bytes 2
Acknowledge IRQ
Wait on IRQ
FIFO_GPS.Read
Byte Count 2
Timed OUT 2
error out 2
$GPGGA
$GNVTG
A

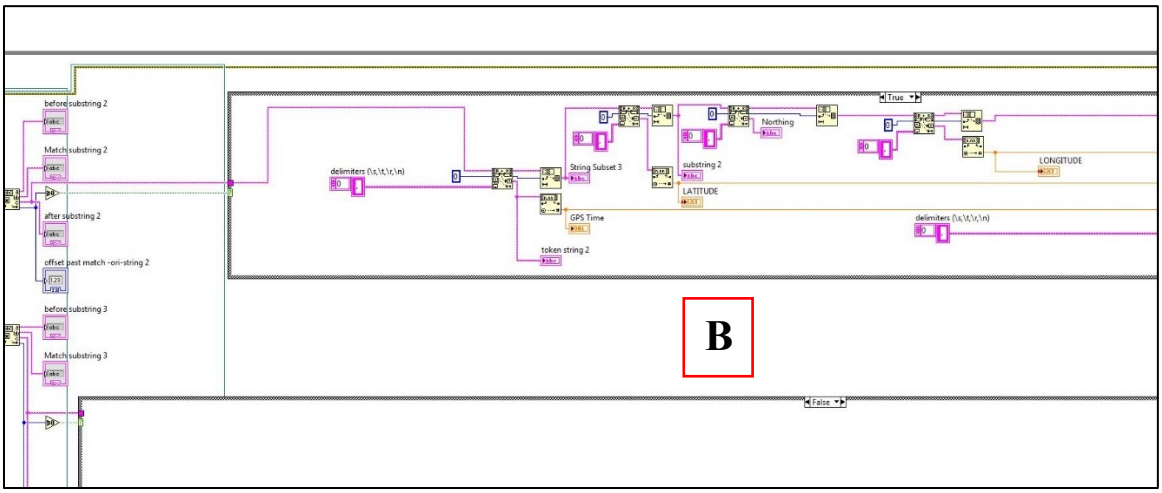
before substring 2
Match substring 2
after substring 2
offset past match -ori-string 2
before substring 3
Match substring 3
delimiters (\s,\t,\r,\n)
String Subset 3
GPS Time
token string 2
Northing
substring 2
LATITUDE
LONGITUDE
True
False
B

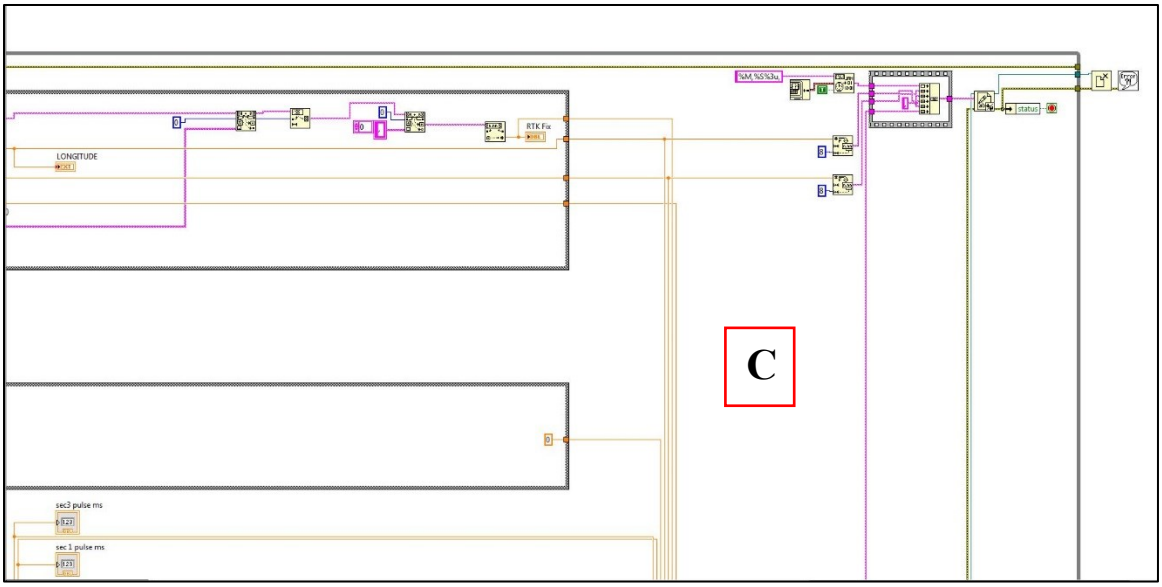
LONGITUDE
RTK Fix
status
sec3 pulse ms
sec 1 pulse ms
C

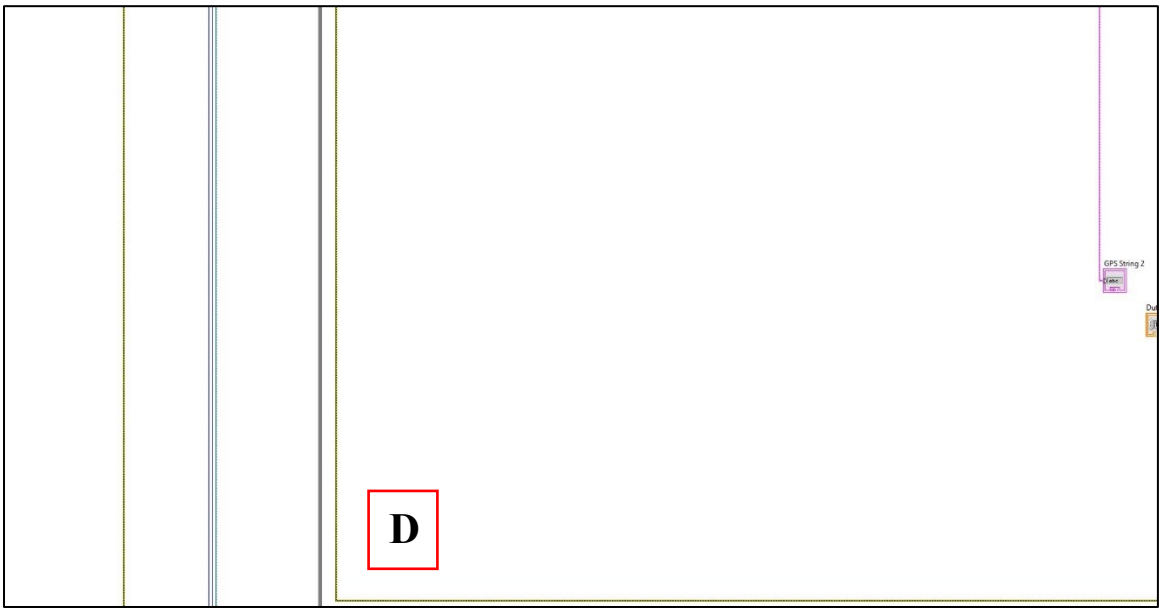
GPS String 2
D

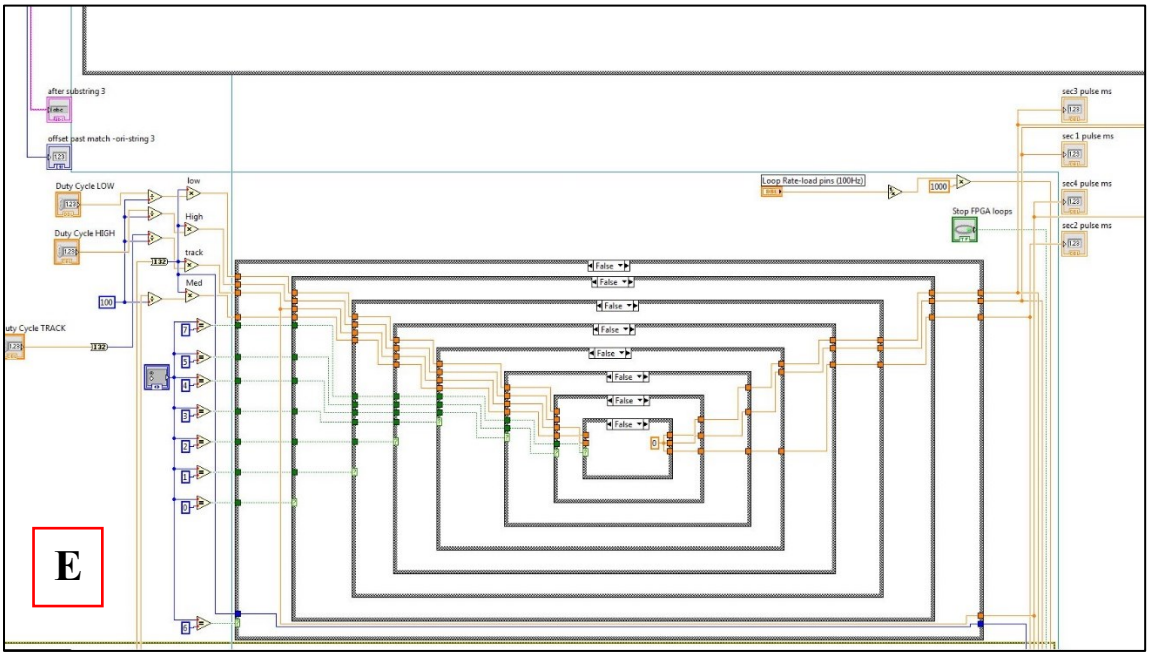
after substring 3
offset past match -or-string 3
Duty Cycle LOW
Duty Cycle HIGH
low
High
track
Med
100
Loop Rate-load pins (100Hz)
1000
Stop FPGA loops
sec3 pulse ms
sec 1 pulse ms
sec4 pulse ms
sec2 pulse ms
False
E

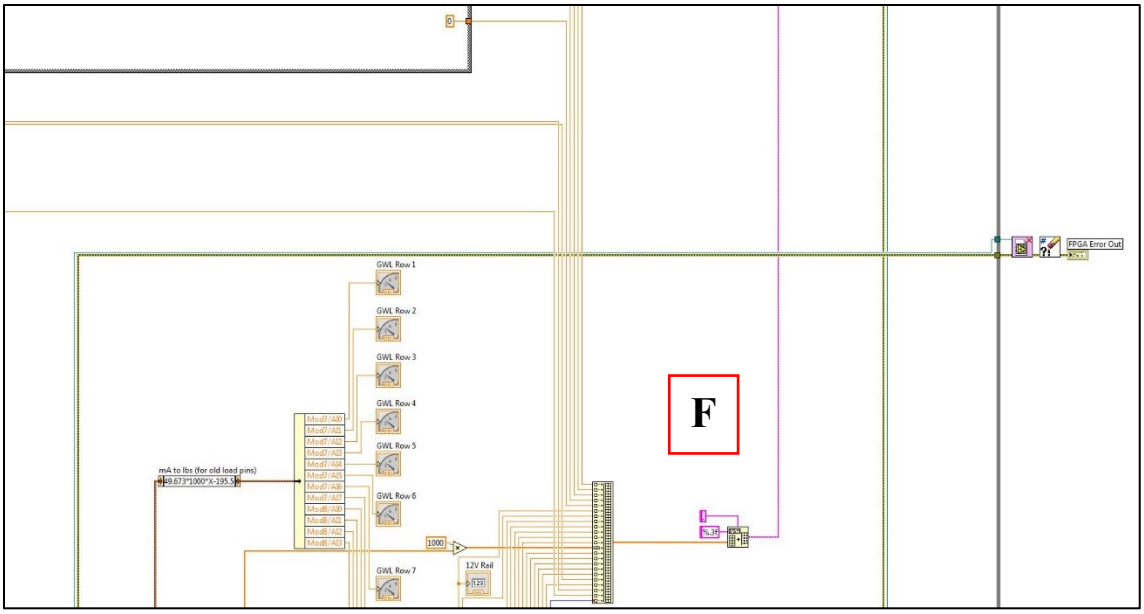
0
GWL Row 1
GWL Row 2
GWL Row 3
GWL Row 4
GWL Row 5
GWL Row 6
GWL Row 7
mA to lbs (for old load pins)
1000
12V Rail
FPGA Error Out
F

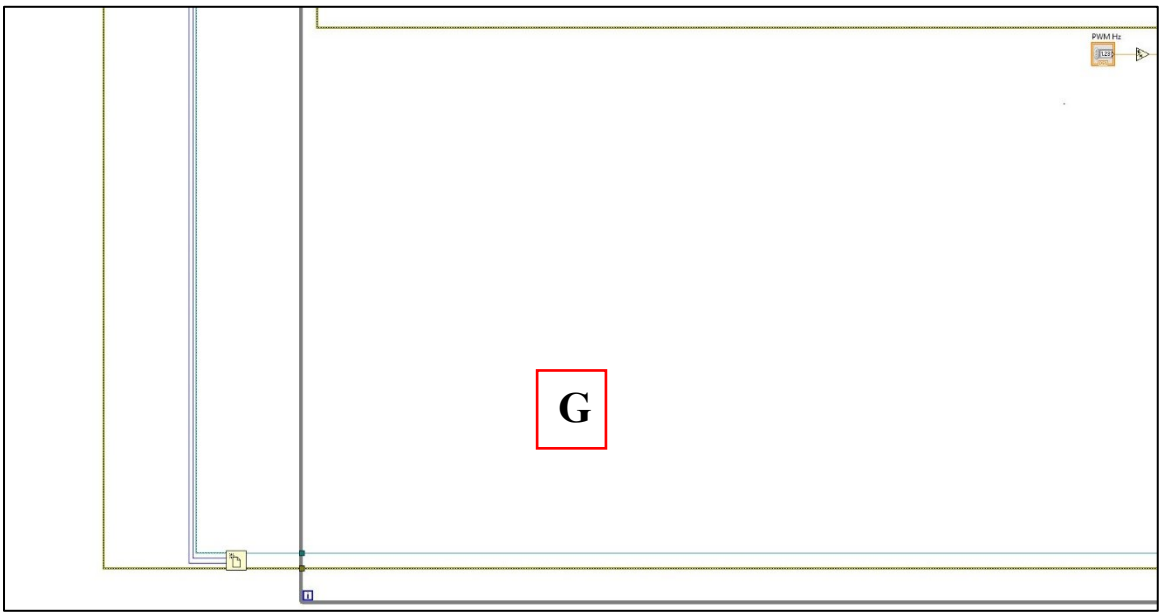
PWM Hz
G

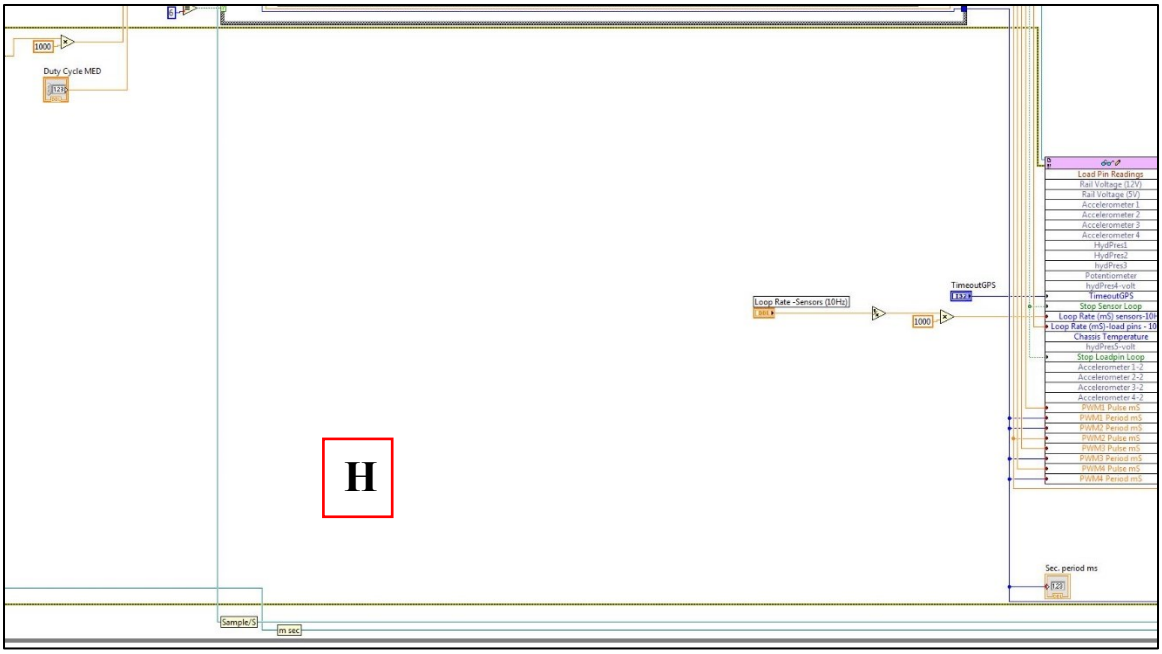
1000
Duty Cycle MED
H
Loop Rate -Sensors (10Hz)
1000
TimeoutGPS
Load Pin Readings
Rail Voltage (12V)
Rail Voltage (5V)
Accelerometer 1
Accelerometer 2
Accelerometer 3
Accelerometer 4
HydPres1
HydPres2
hydPres3
Potentiometer
hydPres4-volt
TimeoutGPS
Stop Sensor Loop
Chassis Temperature
hydPres5-volt
Stop Loadpin Loop
Accelerometer 1-2
Accelerometer 2-2
Accelerometer 3-2
Accelerometer 4-2
PWM1 Pulse mS
PWM1 Period mS
PWM2 Period mS
PWM2 Pulse mS
PWM3 Pulse mS
PWM3 Period mS
PWM4 Pulse mS
PWM4 Period mS
Sec. period ms
Sample/S
m sec

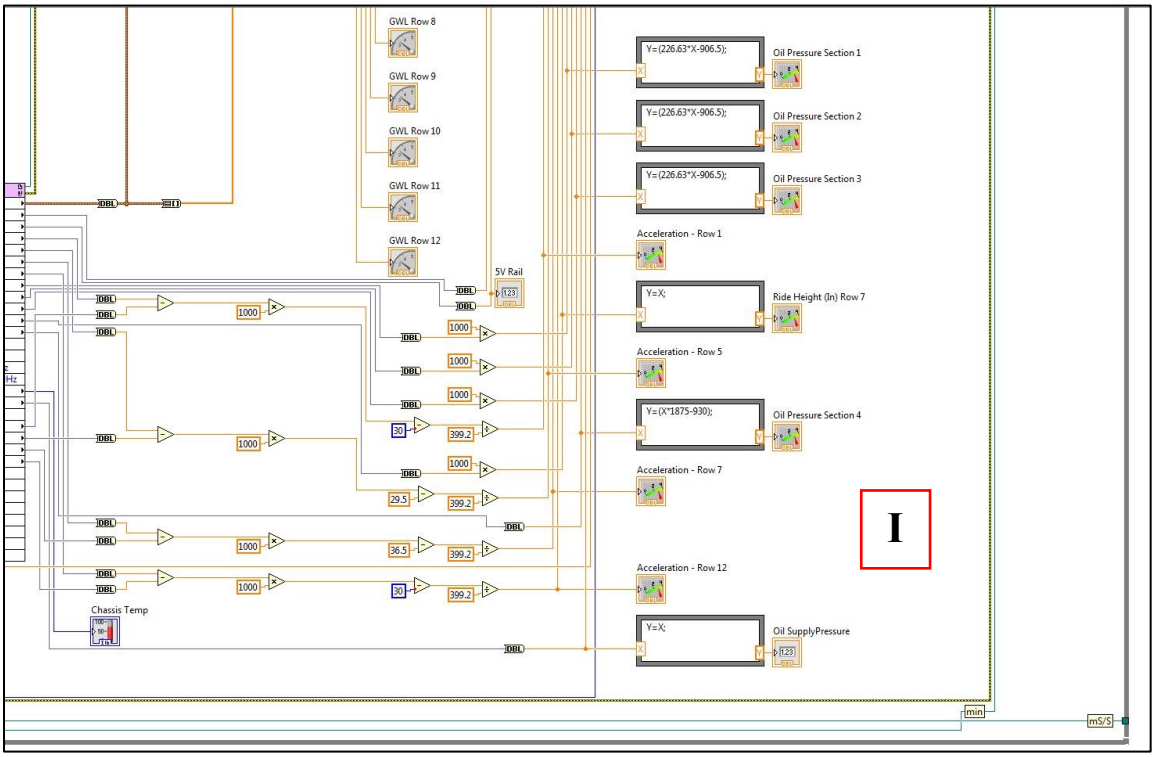
GWL Row 8
GWL Row 9
GWL Row 10
GWL Row 11
GWL Row 12
5V Rail
Chassis Temp
Y=(226.63*X-906.5);
Oil Pressure Section 1
Y=(226.63*X-906.5);
Oil Pressure Section 2
Y=(226.63*X-906.5);
Oil Pressure Section 3
Acceleration - Row 1
Y=X;
Ride Height (In) Row 7
Acceleration - Row 5
Y=(X*1875-930);
Oil Pressure Section 4
Acceleration - Row 7
Acceleration - Row 12
Y=X;
Oil SupplyPressure
I
min
mS/S